博士論文

Study on Nanoparticles-based Neutron Capture Therapy

(ナノ粒子を用いた中性子捕捉療法の研究)

Novriana Dewi
ノフリアナ　デウィ

A thesis submitted in partial fullfilment for the degree of

Doctor of Philosophy in Engineering

in the

School of Engineering
Department of Nuclear Engineering and Management

2015

For my parents and my family, who have never failed to give me support, and offered encouragement whenever it was needed.

Acknowledgements

I would like to express my grateful to my supervisor Professor Hiroyuki Takahashi, not only for welcoming me into his research group, but also for his guidance and continuous support throughout my stay in Japan. For every advice and research input from him during my study in The University of Tokyo. I also would like to express my gratitude especially to Professor Hironobu Yanagie, for all the support and the extraordinary technical guidance he has given. For all the discussion and advice througout my experiment as well as the manuscript preparation. This work will also not be possible without the guidance from Professor Kenichi Ishikawa, who has been helping me a lot in performing the simulation part of this research, which I was not familiar with at the beginning. His suggestion and comment even until the very last minute means a lot to me. Their dedication, passion and integrity will always inspire me.

I would also like to acknowledge Professor Atsuko Shinohara and Assistant Professor Takehisa Matsukawa from Juntendo University, who have been assisting me a lot during the quantitative analysis of the samples from the *in vivo* experiment. I would also like to thanks all the collaborators from Kyoto University Research Reactor Institute, Profesor Minoru Suzuki, Associate Professor Yoshinori Sakurai, Associate Professor Hiroki Tanaka, and everyone else including the technician who have been a big help for me during the irradiation and every other experiment at the reactor facility. To Mrs. Yuriko Sakurai and Mrs. Morishita, who have been helping a lot in every experiment especially the histological analysis part of this work.

It has been a pleasure to work in Takahashi's lab that I cannot mention all the lab members one by one I want to thank to. But surely, this work may not be completed yet without their support thoroughout my academic years in The University of Tokyo. I would like to thanks our Lab's secretaries, especially Ms. Ayako Watanabe who has been helping me with every administrative things even before I came to Japan.

To the very kind and friendly Ms. Yoshiko Shiraishi from International Office in School of Engineering, who has been the first person who sent me notification of acceptance for Research Student in The University of Tokyo, who has been helping me to apply for a scholarship after my Master study finished, and all the kindness that she had offered. To all the staff at Nuclear Engineering and Management Department, who have been helping a lot during my academic life in The University of Tokyo. All of Indonesian friends in The University of Tokyo, who have been with me all these years, struggling together with all the hospitality and enjoyment.

I also would like to thank Hashiya Scholarship Foundation, for the chance that has been given to me to pursue my study with their support. Not to mention the financial support, but also their dedication, motivation, and hospitality during my scholars period.

I would like to deeply thank my parents and my whole family for their love, patience and support, especially to my husband who has been supporting and encouraging me all the time until I could finish this thesis.

And finally, I would like to thank God for all the blessings He has given to me until the end of this PhD journey.

Abstract

Neutron capture therapy (NCT) is a form of cancer treatment that combines neutron irradiation and the preferential loading of high concentration of neutron absorber (generally stable isotope), where the secondary particles produced after neutron capture reaction deposit most of their dose locally in target cancer cells, sparing the surrounding normal tissues.

Boron and gadolinium are two of few elements taken into consideration as NCT agent due to their high neutron cross section and the characteristics of secondary particles they produce after neutron capture reaction. Even though currently used compound in clinical trials is boron-based compound, investigations of gadolinium as NCT agent have been carried out by many researchers interested in several advantages that gadolinium offers.

Current clinical trials and experimental investigation of boron and gadolinium as NCT agent have shown promising results for the application of this therapy modality in cancer treatment. On top of that, recent development of accelerator-based neutron source for a more hospital-friendly installment has been encouraging more researchers to work on the optimization of NCT treatment toward a wider application in radiotherapy.

In this thesis we evaluated the feasibility of gadolinium-based nanoparticles for as agent by performing neutron irradiation to colon-26 tumor-bearing mouse injected intravenously by gadolinium-based compound as an effort to investigate the effectivity of cancer cells killing after NCT treatment. Significant tumor growth suppression was observed for mice group after neutron irradiation, indicating its effectivity in treating surface-tumor. However, we observed significant toxicity in irradiated gadolinium-platinum nanomicelles-injected group, suggesting that further investigation might be necessary to obtain the feasible optimization on combined effect of radiochemotherapy.

Early stage of dose deposition investigation was also performed in this study, aimed as an early stage before going into real calculation of dose deposition for both boron and gadolinium based NCT. Investigation of possible neutron depression effect was also preformed by setting up high neutron agent concentration on simple cylindrical phantom as well as the assessment of combined effect feasibility evaluation was also carried out for the two compounds. Nevertheless, since the result of dose calculation in current study is still a preliminary investigation, we can not come into conclusion yet before performing further advanced calculation especially the necessary to perform microdosimetry of dose deposition from very short range secondary particles such as Auger and Coster-Kronig electrons produced after GdNCR.

Contents

List of Figures

List of Tables

Chapter 1

Introduction

1.1 Research Background and Motivation

Glioblastoma multiforme is one type of brain cancer, which is the most aggressive diffuse glioma of astrocytic lineage and is classified into grade 4 based on WHO classification [1, 2]. With the average incidence rate of 3.19/100,000 population, median survival of 15 months, and median age of diagnosis is 64 years, GBM remains an incurable disease [3]. The incidence and mortality are almost equal, indicating the fatal outcome of this brain malignancy, and the need for new therapeutic approaches. Although molecular biology-based therapeutic approaches are the major focus of current clinical research efforts, a more immediate impact might be obtained by developing a safe radiation dose-escalation strategy [4], and NCT represents such a novel approach.

Neutron capture therapy is a form of cancer treatment that combines neutron irradiation and the preferential loading of target tissues or cells with particular compounds [5]. In NCT, neutron beam is applied to the region of interest where the target tissue contains a relatively high concentration of neutron absorber (generally stable isotope) compounds compared to the surrounding normal tissues. Reaction between these compounds with neutron creates secondary products that deposit most of their dose locally, sparing the surrounding normal tissues as illustrated in Fig 1.1.

Thermal neutrons are preferable in NCT treatment, considering that slow neutrons generally spend more time around a nucleus and are more likely to be captured. To ensure maximum cell damage on target tissue, the neutron absorber nuclides used as NCT agent need to have very high abilities to absorb thermal neutron (e.g. boron and gadolinium) compared to other elements present in bulk of biological tissues shown Table 1.1 to compensate the high percentage of those elements in tissue.

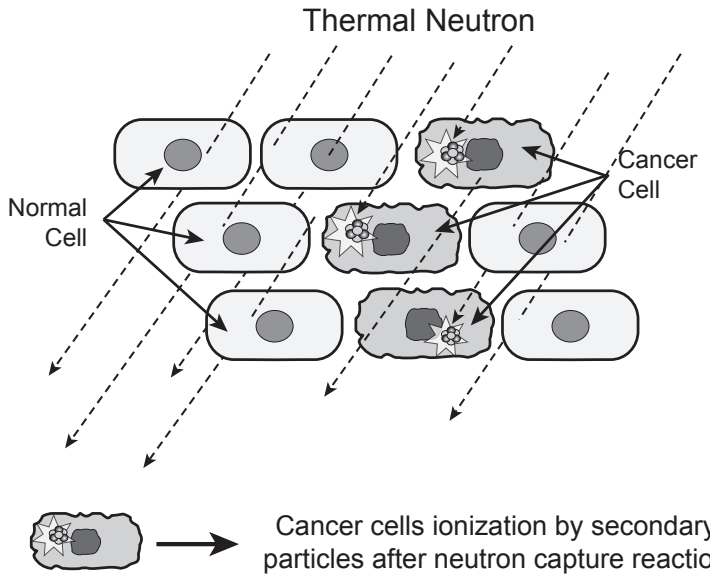

Figure 1.1: Illustration of cancer cells killing by neutron capture threrapy

Table 1.1: Thermal neutron cross section (σ_{th})of the elements commonly present in biological tissues [6]

Isotope	σ_{th} (barn)	Weight (%) in biological tissues
^{1}H	0.333	10.00
^{12}C	0.0035	18.00
^{14}N	1.83	3.00
^{16}O	0.00019	65.00
^{23}Na	0.43	0.11
^{24}Mg	0.0053	0.04
^{31}P	0.18	1.16
^{32}S	0.53	0.20
^{35}Cl	32.68	0.16
^{39}K	2.1	0.20
^{40}Ca	0.4	2.01
^{56}Fe	2.57	0.01

Note. 1 barn = 10^{-24}cm^2.

Commonly used NCT agent in clinical trials is the isotope ^{10}B, which splits into high linear energy transfer α particle and ^{7}Li nucleus upon neutron absorption. Alpha particle and lithium ion emitted by the boron neutron capture reaction (BNCR) have combined path length of approximately one cell diameter i.e. about 12 microns, which theoretically limiting the radziation effect to those tumour cells that have taken up a sufficient amount of ^{10}B. However, this short flight range of alpha particles and recoil lithium released after BNCR might also bring an inherent problem that it is necessary to deposit boron homogenously intracellularly to destroy the cell.

Gadolinium-157 is another isotope under investigation as an alternative or complimentary to boron in NCT. The use of gadolinium as NCT agent has been getting attention because of its highest neutron cross section (255,000 barns) which is around 66 times larger compared to boron-10 thermal neutron cross section. The advantage of gadolinium's higher neutron cross section is that the same number of neutron capture reactions with ^{10}B, can be produced with lower neutron fluence. Gadolinium neutron capture reaction (GdNCR) also produces γ-rays, internal conversion electrons, X-rays and Auger electrons with total kinetic energy about 3 times of that produced by boron in BNCR. Gadolinium neutron capture reaction results in release of gamma rays which is considered as a drawback as well as favorable characteristic, because it might cause ionizing effect to outer normal tissue while at the same time providing the advantage that the location of the element is not critical with regard to target cell due to their longer flight ranges. Gadolinium neutron capture reaction also produces a series of low-energy conversion and Auger electrons, which are high linear energy transfer (LET) secondary particles effective in breaking DNA double strand.

Besides boron and gadolinium, some other nuclides besides boron with high neutron cross section, such as ^{6}Li and ^{235}U were initially also considered as NCT agent (Table 1.2) [7, 8, 9]. However, ionic Li^{+} is mentioned to be easily dispersed thoroghout the body, while ^{235}U has its inherent toxicity and radioactivity that finally they were not further investigated. Nevertheless, NCT has been showing encouraging results on several clinical trials and animal experiments, not only on the glioblastoma multiforme, as its first main target cancer type, but also on different types of cancer, which has motivated a lot of research groups in working on the optimization of this therapy modality.

Table 1.2: Thermal neutron cross section (σ_{th}) of several nuclides considered to be NCT agent [7, 8, 9]

Isotope	Neutron capture reaction	σ_{th} (barn)
^{3}H	(n,p)	5333
^{6}Li	(n,α)	941
^{10}B	(n,α)	3838
^{113}Cd	(n,γ)	20600
^{135}Xe*	(n,γ)	2720000
^{147}Sm	(n,γ)	40140
^{151}Eu	(n,γ)	9200
^{155}Gd	(n,γ)	60900
^{157}Gd	(n,γ)	255000
^{174}Hf	(n,γ)	561
^{199}Hg	(n,γ)	2150
^{235}U*	(n,f)	681
^{241}Pu*	(n,f)	1380
^{242}Am*	(n,f)	8000

Note: 1 barn = 10^{-24}cm^2. * Radioactive.

1.2 Objective and Contributions of Thesis

The main purpose of this thesis is to carry out a thorough study of nanoparticles-based neutron capture therapy, covering *in vivo* evaluation of two nanoparticles-based gadolinium compounds as NCT agent, as well as an early stage calculation of dose deposition to compare both boron neutron capture therapy (BNCT) and gadolinium neutron capture therapy (GdNCT) and to evaluate the possibility of combining the two compounds in NCT treatment.

In this work, *in vivo* evaluation for GdNCT was performed on colon-26 tumor-bearing mice irradiated at nuclear reactor facility of Kyoto University Research Reactor Institute. Biodistribution of gadolinium-based drug compounds were observed to decide the optimum time after compound administration to perform neutron irradiation of NCT procedures and antitumor effectivity was evaluated within one month after NCT treatment. Preliminary investigation of NCT dose calculation was performed by using PHITS (Particle and Heavy Ion Transport code System) calculation method, as an independet approach for evaluating energy deposition for each of BNCT and GdNCT as well as their combined effect.

1.3 Outline of Thesis

Chapter 1 in this thesis gives brief introduction of NCT as the research backround and motivation, then outline the contributions of current works.

Chapter 2 will cover the basic principles of neutron capture therapy, starting from the history of NCT itself; describe the current status of research fields in NCT, which includes description of the mechanism for both BNCT and GdNCT; mention several previous clinical trials and experimental results during long history of NCT; present current development on neutron source and treatment planning for NCT; and finally, discuss NCT prospects in the future will to give broader view of what lies ahead in this field.

Chapter 3 will discuss about drug delivery system (DDS) in general, as well as its important role in neutron capture therapy. Introductory description on the application of nanoparticles as drug carrier in NCT, which is the main target of this work, will also be given in more detail, together with several related works for both BNCT

and GdNCT.

Chapter 4 will give the description of The Heavy Water Neutron Irradiation Facility of the Kyoto University Research Reactor (KUR-HWNIF) as neutron source for GdNCT trial in current work. The characteristics of this reactor, which has been used for many cases of NCT clinical trials, will also be outlined to give a brief overview of the facility.

Chapter 5 will describe about the continued work of gadolinium-platinum nanomicelles evaluation compound as NCT agent. Nanomicelles preparation as well as experimental methodology will be elaborated in more detail, and the results of antitumor effectivity evaluation will be discussed in this chapter.

Chapter 6 will cover detail explanation of experimental results on evaluation of Gd-DTPA/CaP nanoparticles as NCT agent. Advantages of calcium phosphate nanoparticles itself will first be presented as the background of drug carrier choice. Single and multiple injections of drug compund were performed for this gadolinium drug carrier to investigate the effect of GdNCT on tumor site with different concentration of gadolinium. The results will be presented and discussed as the evaluation of its feasibility as GdNCT agent.

Chapter 7 will be the part in which preliminary study of dose deposition calculation in NCT will be presented. This chapter will give description about the simulation system used for the calculation, simple phantoms designed in the calculation, as well as description for the calculation setup. Simulation results will be discussed to obtain preliminary understanding on energy deposition for both BNCT and GdNCT.

Chapter 8 will finally give concluding remarks about current research and suggestions for future work.

Chapter 2

General Introduction of Neutron Capture Therapy

Neutron capture therapy (NCT) is one non-invasive cancer therapy approach, where secondary particles produced after neutron capture reaction are utilized to ionize and kill the cancer cells. In NCT, a stable, non-toxic, and non-radioactive nuclide is first delivered and preferably accumulated into tumor cells, and then a neutron beam is narrowly exposed to the target site. Based on the interaction of the nuclide and the neutron beam, localized cytotoxic radiations are emitted to kill the tumor cells [10].

2.1 History of Neutron Capture Therapy

Soon after the discovery of neutron by Chadwick in 1932, the basic idea of binary concept for cancer treatment with neutron capture therapy was introduced by Gordon L. Locher in 1936 [5] : "In particular, there exist the possibility of introducing small quantities of a strong neutron absorber into the regions where it is desired to liberate ionization energy (a simple illustration would be the injection of a soluble, non-toxic compound of boron, lithium, gadolinium or gold into a superficial cancer, followed by bombardment with slow neutrons)". Since then, NCT has been through continuous advancement in different fields of study including dedicated neutron beam facilities, intense drug development, detection and imaging, computer-assisted dosimetry as well as treatment planning software, as well as radiation oncology field.

The first experiment on boron neutron capture therapy (BNCT) was reported by Kruger in 1940 [11], where he performed *in vitro* experiment with boric acid followed by neutron irradiation and reported observation of lower transplantation efficiency compared to controls. This was then followed by an *in vivo* experiment of NCT

efficiency evaluation with the injection of boric acid on mouse sarcoma reported by Zahl et al., [12]. After these reports, the treatment of brain tumors by NCT was then proposed [13], in which the work also considered lithium together with boron as NCT agent, as well as description on various agencies for localizing both compounds.

Following this result, the first clinical application of BNCT in human was performed on 1951 in USA, where 10 patients with malignant glioma were treated at the Brookhaven Graphite Research Reactor [14, 15, 16, 17]. It was reported that a short-time improvement of the clinical situation was observed in nine of the ten cases. The median survival of the patients in this first series was comparable to standard therapy. However, improvement of clinical situation was short and all patients died of their progressive disease. Unfortunately, significant survival prolongation could not be achieved on several BNCT trials after this first clinical application. Some severe side effects such as acute brain edema and perivascular fibrosis but especially the appearance of brain necroses were even observed within a few months on the patients treated at the reactor of the Massachusetts Institute of Technology after injection of ^{10}B-enriched 4-carboxlyphenyl boronic acid [18, 19]. The unfavorable results of these BNCT trials lead to discontinuation of NCT research in the USA for three decades. The poor localization of boronated compound in tumor site was mentioned be one of the possible causes of these discouraging results. Underestimation of dose contribution from fast neutron and photon contamination is also one of the aspects need to be considered carefully.

Hiroshi Hatanaka brought NCT to Japan after his 2-year fellowship in Sweet's laboratory at the Massachusetts General Hospital, where the group there were working with BSH, which had been developed as a boron delivery agent by Soloway at the Massachusetts General Hospital [20]. Hatanaka then resumed the BNCT clinical trials in Japan, with the procedures of prior tumor excision as an intraoperative radiotherapy before BSH injection and neutron irradiation. He reported encouraging results, where 58% of a small group with selected patients suffering from malignant glioma grades 3 and 4 achieved 5 years survival rate [21]. These promising results presented by Hatanaka had then stimulated new efforts on BNCT clinical trials worldwide.

As also described in previous chapter, some other nuclides with high neutron cross section were initially also considered as NCT agent. However, few of the unfavorable inherent characteristics from those elements have halted further investigation of their feasibility. Even gadolinium was at first precluded from the use for NCT because of the high toxicity of its non-complexed inorganic salts. GdNCT itself was then revisited

around late 1980s after the development of gadolinium-labeled MRI contrast agents [22, 23].

2.2 Current Status of Neutron Capture Therapy

2.2.1 Boron Neutron Capture Therapy (BNCT)

Theoretically, BNCT provides a way to selectively destroy malignant cells and spare normal cells. It is based on the nuclear capture and fission reactions that occur when boron-10 (^{10}B), which is a nonradioactive isotope of natural elemental boron, is irradiated with low energy thermal neutrons to yield high linear energy transfer (LET) alpha particles (^{4}He) and recoiling lithium-7 (^{7}Li) nuclei, with combined path length of about one cell diameter, making it possible to optimize localization of cells killing effect.

2.2.1.1 Properties of Boron as NCT Agent

Natural boron has two stable isotopes, which are ^{10}B and ^{11}B, with a natural abundance of about 20 and 80%, respectively. Impure form of boron was first isolated by Davy, Gay-Lussac, and Thénard in 1808 accomplished through the reaction of boric acid with potassium. However, only in 1892 that a quite pure form of boron was obtained by Moissan, who prepared elemental boron by the reduction of B_2O_3 with Mg. In the past century, high purity boron was finally obtained. Boron has many similarities with carbon and silicon. The main features that influence the chemical behavior of boron are its small size, high ionization energy, and electronegativity that is close to that of C and H (and Si), leading to an unusual ability to form covalent bonds [24]. This feature affect its chemistry and is the main reason for the choice of boron in medicinal chemistry, together with its large cross-section for neutron capture. It is also possible to easily incorporate boron atoms in organic compounds.

The boron neutron capture reaction, ^{10}B(n,α)^{7}Li, was first characterized in 1935 and can be described by two parallel nuclear fission processes that take place upon absorption of a thermalized neutron [25]. The excited ^{11}B nucleus splits and produces two high energy ions, $^{4}He^{2+}$ and $^{7}Li^{3+}$ as described in Fig. 2.1, with the range of approximately 9 and 5 μm respectively. Combined path length of these particles is about the same size of one cell diameter, which makes it possible to localize irradiation effect into target cells where boron compound is accumulated. Both of $^{4}He^{2+}$ and $^{7}Li^{3+}$ are high linear energy transfer (LET) particles; 1.47 for alpha particle and 0.84

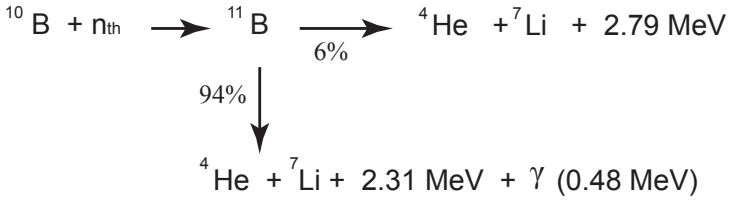

Figure 2.1: Schematic drawing for thermal neutron capture reaction of ^{10}B(n,α)^{7}Li (adapted from [6]).

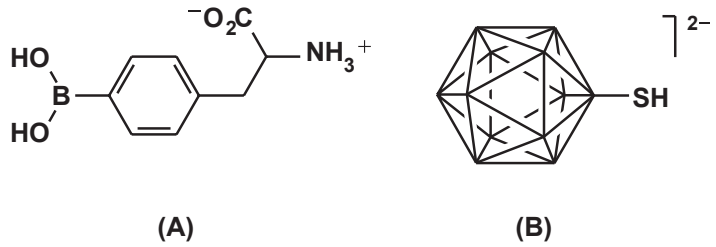

Figure 2.2: Chemical structure of currently used BNCT agents: (A) Boronophenylalanine (BPA). (B) Mercaptoundecahydrododecaborate (BSH). [6]

MeV for lithium recoil, making them efficient at localizing the cancer cell killing in which the neutron capture reaction took place. However, the short range of these secondary particles may not reach the nuclei of some nearby cells, which might increase the possibility of cancer recurrent [26]. Therefore, compared to secondary particles with lower LET, the celullar range of alpha and lithium particles makes it necessary to achieve homogenous delivery of ^{10}B atom to every tumor cell nucleus to ensure the desired therapeutic effect of BNCT.

2.2.1.2 Boron Delivery Agents

The only two BNCT agents currently in use for clinical trials are dihydroxyboryl derivative of phenylalanine, referred to as boronophenylalanine or "BPA", and mercaptoundecahydrododecaborate or "BSH" ($Na_2[B_{12}H_{11}SH]$), with the chemical structure as shown in Fig. 2.2. BSH was used in the 1960s by Hiroshi Hatanaka as BNCT agent for high grade gliomas [27], while BPA was first clinically used in 1988 by Mishima on BNCT treatment of patients with cutaneous malignant melanomas [28].

BSH has the characteristics that it cannot pass through the BBB (Blood Brain Barrier) effect. Since BBB of tumor cells are damaged, BSH is able to accumulate in tumor cells without being taken up into normal brain cells. BSH also has poor membrane permeability and low accumulation in tumor cells. Furthermore, because

of its dependency on selective barrier such as the BBB in brain, it serves benefit quite limited to malignant glioma [29, 30]. While the other boron delivery agent, BPA, is capable of accumulating selectively in malignant melanoma because of its chemical structure, which resembles tyrosine and DOPA (dihydroxy-phenylalanine), the precursor of melanin metabolism. Moreover, BPA is also an amino acid analogue hence it is taken up by the cells that amino acid metabolism is active and may pass through the BBB. BPA is by character difficult to be dissolved in saline, but by complexation with fructose it is possible to increase its solubility, which makes it soluble at neutral pH. Therefore, BPA-fructose has become more commonly used as BNCT agent for tumors. However, if compared to BSH, the BPA's characteristics of being capable on passing through BBB makes it unfavorable for treating brain tumor, since BPA has the possibility to also accumulate into normal brain tissue. Nevertheless, several results have been reported that boron accumulation in brain tumor cells could be enhanced by combining each advantageous characteristics of BPA and BSH [31].

Derivatives of BSH and BPA, other boron-containing amino acids, and boron clusters have been synthesized in order to develop new low and high molecular boron agent. One of the reason amino acids are employed for boron carrier is because they have the tendency of selective accumulation in tumor cells due to increased amino acid transport across plasma membranes on rapidly growing malignant cells, where amino acids could be used for protein synthesis. Tumor cells might also overexpress to specific peptide receptors, therefore, utilization of corresponding amino acids might increase the possibilty of boron compound accumulation in tumor site [32]. Some results on boronated amino acids reported recently, containing one or more boron clustres in order to deliver higher concentration of boron to target tumor. Unnatural boronated cyclic amino acids have also shown promising results as BNCT agent [33, 34] because of its higher metabolic stability compared with the natural ones. Recent results reported by Kabalka et al., [35] have shown superior tumor selectivity of boronated amino acids for both *in vitro* and *in vivo*.

Besides independet application of BPA and BSH, clinical trial on combined use of these two BNCT agents has been reported by Miyatake for the case of GBM by utilizing characteristic of each compound and expected different subpopulations in tumor cells [36]. This combined use of two boron compounds was performed based on experimental data showing different uptake characteristics of tumor cells depending on the cell-cycle.

In general, boron carriers has been through development in two directions: small boron molecules and boron-conjugated biological complexes. Eventhough there have been several studies reporting on the development of new boron compounds or carriers of old compounds, the difficulty of translating many this experimental data into clinical trial has been one of the reasons of the lack improvement in this part of BNCT aspect. Because of the long and costly procedure necessary for the certification of a new boron compounds to be achieved, boron-conjugated biological complexes approach has become one of the recent trends to achieve high accumulation of ^{10}B in tumor tissues [37].

2.2.1.3 Clinical Trials of BNCT

Previously described two ^{10}B-based compounds (BSH and BPA) have been used for clinical trial in several NCT facilities in the world and has been showing promising therapy results for patient with difficult to treat cancer type [38]. It was at first aimed to treat brain cancer such as glioblastoma multiforme [39, 40, 41], but also is currently being extended to the treatment of head and neck cancer [42, 43, 44], liver [45, 46] and also melanoma [47, 48].

The first BNCT clinical trials in United States were performed using sodiom tetraborate (borax), sodium pentaborate, *p*-carboxyphenylboronic acid, or sodium decahydrodecaborate ($Na_2[B_{12}H_{11}SH]$) utilizing thermal neutron source as its neutron beam (cari reference nya). Later on 1990s, clinical trials in United States were it was then resumed with BPA as its main boron delivery agent [41, 49, 50, 51], and the patients were irradiated with higher enery epithermal neutron beam after consideration of its deeper tissue-penetrating properties.

Hatanaka and Nakagawa in Japan performed pioneering BNCT trials using BSH as the boron delivery agent with thermal range neutron beam [52, 53]. Afterward, several clinical teams in Japan have carried out BNCT studies by using either BPA alone or in combination with BSH, mainly on patients with glioblastoma [54, 55, 56, 57]. Later in 2001, Kato and his co-workers iniatiated BNCT trials on patients with recurrent head and neck cancers. These patients had failed all other treatments before finally treated with BNCT at Kyoto University Research Reactor Institute (KURRI) [58]. Promising results were reported on 5 out of 6 cases of recurrent head and neck cancers treated in the trials, even for a huge or far advanced head and neck malignancies (HNM). A total of 42 times BNCT treatment for 26 patients have been performed since then by the group reporting 1-72 months (mean 13.6 months) survival periods after BNCT. They are capbale of ascertaining the effectiveness of BNCT for 22 out of 26 patients

with advanced or recurrent HNM for which there were no other treatment options [59, 60]. A more detail review on current status of BNCT of high grade gliomas and head and neck cancer has been recently reported by Barth and co-workers [61].

Many research groups in Europe have also been working thoroughly on NCT, with the group in Finland has carried one of the most intensive BNCT clinical trials. BNCT research in Finland has been actively performed since 1992 [40, 62, 44]. FiR1 research reactor was constructed between 1993 to 1997 as treatment facility and started to use for clinical trials on 1999 [63], and the facility was mentioned to be capable of treating patient regularly on a weekly basis [64]. Several developments on optimization of neutron source, dose calculation and treatment planning, boron imaging up into molecular level, as well as diffusion imaging to detect BNCT effect in patients were performed by BNCT group in Finland to promote full potential of BNCT [65]. Unfortunately, the treatments in FiR1 facility was unavoidably terminated in 2012.

Some other clinical trials in Europe is the one conducted in Petten (performed by European Organization for Research and Treatment of Cancer) and Czech Republic, using BSH either alone or in combination with BPA on patients with GBM to investigate the toxicity of i.v. administration on BSH and the maximum tolarated radiation dose [66, 67, 68]. Clinical studies were also performed in Sweden with higher total amount of BPA infused for over 6 hours to the patient undertaking the treatment [69]. This higher dose and longer infusion time was reported to be tolerated by 29 patients enrolled in the study [39, 70].

Besides those clinical trials in US, Japan, and Europe, BNCT group in Taiwan has also presented their preliminary clinical trial results on patients with locally recurrent head and neck cancer, where they observed shrinkage of tumor with tolerable early toxicities after treatment [71].

2.2.2 Gadolinium Neutron Capture Therapy (GdNCT)

Celullar range of alpha and lithium particles produced after BNCR as described at the beginning section of this chapter, makes it necessary to achieve homogenous and intracellular delivery of ^{10}B atom to every tumor cell nucleus to ensure killing effect and minimize possibility of recurrence. Gadolinium as an alternative of boron for NCT agent is considered to be capable of compensating the difficulty on homogenous element distribution with its longer range secondary particles produced after neutron capture reaction.

GdNCT was first formulated in the in the 1980s [72, 73]. However, its development has suffered due to lack of appropriate Gd-containing tumor-selective agents [74]. Its clinical application has been rather limited because of the difficulty in retaining a sufficient amount of Gd in tumors (50-200 μg of Gd/g wet tumor tissues) during the neutron irradiation [26].

The use of gadolinium as NCT agent has been getting attention because of its highest neutron cross section (255,000 barns) which is around 66 times larger compared to boron thermal neutron cross section. The advantage of gadolinium higher neutron cross section is that the same number of neutron capture reactions with ^{10}B, can be produced with significantly lower neutron fluence. Thus, it is possible to reduce neutron dose received by surrounding normal tissue by using ^{157}Gd compound. The spectrum of the secondary particles emitted by gadolinium is complex, and spreads out a broad region of dose delivery, thus limiting the selectivity of the therapy. The photons emitted in the (n,γ) reactions interact with the tissues but deposit energy over a longer path length than the boron reaction products. This is the main drawback of GdNCT. However, if ^{157}Gd uptake is limited to tumor bulk, having a size of the order of some cm^3 by volume, then an additional effect, in the increasing of tumor dose in the attenuation of the capture photon yield, will be added [75]. These properties of GdNCT can also increase the possibility of killing tumor cells even when Gd is outside the tumor cells, thus eliminating the requirement of intracellular delivery of gadolinium [76].

GdNCT is recently rekindled mainly based on the action of its high linear energy transfer (LET) Auger and IC electrons generated by ^{157}Gd after neutron capture. Dose contribution of gadolinium neutron capture reaction (GdNCR) short-range products such as Auger electro emission has often been neglected because it was assumed that Gd compounds remained extracellular and could not reach the cell nucleus. However, De Stasio et al., [76] showed that Gd-DTPA not only penetrates the plasma membrane of the cells but accumulates at higher concentration in the nucleus than in the cytoplasm.

2.2.2.1 Properties of Gadolinium as NCT Agent

Gadolinium, a rare earth lanthanide, was discovered in 1886 by Charles Marignac, who named it after the Finnish chemist, Johan Gadolin. The 40^{th} most abundant element in the earth's crust, gadolinium is a bright, silver, ferromagnetic metal, and is usually found in the mineral monazite [77]. Investigations of the nuclear properties of gadolinium began shortly after the discovery of the neutron. In fact, ^{157}Gd has the

Table 2.1: Stable gadolinium isotopes. The natural abundance and neutron cross sections of gadolinium isotopes with atomic weights from 152 to 160 [77].

Stable Isotope	^{152}Gd	^{154}Gd	^{155}Gd	^{156}Gd	^{157}Gd	^{158}Gd	^{160}Gd
Natural abundance (%)	0.20	2.18	14.80	20.47	15.65	24.84	21.86
Thermal neutron absorption, σ_{th} (barns)	700	60	61000	2	255000	2.4	1

highest thermal neutron cross section of any isotope of any element. This high cross section is the reason why gadolinium has been investigated for many nuclear physics applications, ranging from nuclear control rod absorbing material to the medical neutron capture therapy research.

There are seven stable isotopes of gadolinium and eight radioisotopes with half-lives longer than one day. Table 2.1. lists the gadolinium isotopes with atomic weight from 152 to 160, their natural abundance and neutron cross section [77]. Of these stable gadolinium isotopes, the candidates for NCT are those with very high neutron capture cross sections. It is shown that ^{157}Gd has the highest neutron cross section and significant natural abundance compared to the other isotopes. This high neutron cross property of gadolinium, which is approximately 66 times that of ^{10}B, can help to shorten the irradiation time and is expected to improve patient's quality of life after NCT treatment.

Schematic drawing of a thermal neutron capture reaction of ^{157}Gd is shown in Fig. 2.3. ^{157}Gd atom, which has 15.65% natural abundant ratio, releases Auger electron, internal conversion (IC) electron, γ rays and X rays by a thermal neutron capture reaction. Among these, the most biologically relevant for cancer cells killing are the high LET Auger and IC electrons with an average LET of 0.3 MeV/μm. By comparison, in boron neutron capture therapy the average LET is 0.2 MeV/μm for both Li and alpha particles [4].

Mass-and charge-carrying Auger electrons are highly ionizing over a short range. The longest radiation length is on the order of tens of nanometers for most energetic electrons. Most favorably for GdNCT, Auger electrons may induce double-strand damage if gadolinium is in the proximity of DNA [73]; which requires gadolinium compound to be accumulated intranuclearly to ensure dose enhancement due to double-strand damage inside cell nucleus. When Auger Coster-Kronig electron is emitted, it most likely will interact with a water molecule within radius of a few nanometers producing hydroxyl radical, which in turn locally propagates the oxidativfe damage [72],

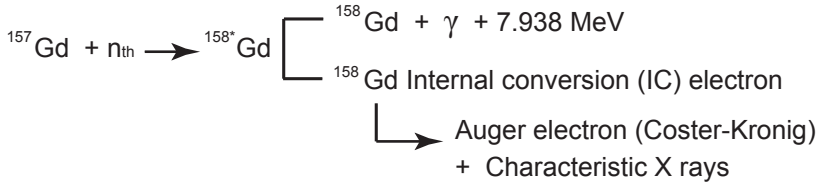

Figure 2.3: Schematic drawing for thermal neutron capture reaction of ^{157}Gd(n,γ)^{158}Gd (adapted from [6]).

and it has been reported that lethal double-strand DNA breaks occur in proportion to the extent of the radiation-induced oxidative damage [4].

Several gadolinium-based compound are already commonly used as MRI contrast agent, which makes it possible to integrate radiotherapy and MRI diagnosis. This would permit the simultaneous dynamic MRI monitoring of the gadolinium distribution levels prior to and during neutron irradiation for better treatment results. The possibility of real-time observation of drug distribution will eventually increase the accuracy of the treatment and enable to feedback the therapeutic efficacy at the earlier stage and promptly adjust the treatment strategy [78]. Several Gd compounds are known to target brain gliomas because of the BBB disruption in these tumors. They are in fact used as tumor contrast-enhancing agents for MRI, a result of the large magnetic moment of the Gd^{3+} ion.

2.2.2.2 Gadolinium Delivery Agents

Gadolinium ion (Gd^{3+}) is known to be toxic and must be chemically stabilized by chelation. Therefore, standard ^{157}Gd-containing MRI contrast agents should be considered as the most realistic option for GdNCT agent. Their pharmacology has been extensively studied and has already been approved for clinical use. The optimal ^{157}Gd concentration in tumors for GdNCT was reported to be 50-200 μg/g tumor tissues, and less than 1,000 ppm since neutron fluence rapidly decrease in the deeply seated tumor due to high absorption of neutron by Gd atoms [79]. Several MRI contrast agent such as Gd-DTPA, Gd-DOTA, Gd-BOPTA, Gadoteridol and Gadobutrol have been reported to be evaluated as the feasible GdNCT agents (described in the following subsection). Motexafin gadolinium, a redox-active tumor selective agent, has also been considered to be utilized as GdNCT because of its characteristics of being capable in accumulating gadolinium into brain tumor and mostly to cell nuclei [80, 81].

In the past GdNCT trials, several MRI contrast agents were evaluated as gadolinium compound for NCT, but it was a major problem that a sufficient quantity of gadolinium could not be retained in tumor tissue during neutron irradiation after compound injection [82] and most of gadolinium-based MRI contrast agents are reported to have short blood circulation time and low specificity in tissue accumulation [22]. Thus, effective drug delivery systems are needed in order to deliver sufficient amount of Gd into tumors for the optimization of GdNCT. This has been more focused on for the optimization of GdNCT compared to the development of the new gadoliniium-based compound besides the established MRI contrast agent.

2.2.2.3 Status of GdNCT Feasibility Evaluation

Studies on GdNCT have been limited to *in vitro* and *in vivo* experiments due to the lack of efficient drug delivery system of gadolinium compound, and also because of the longer range gamma rays it produces after neutron capture reaction. Nevertheless, quite a lot of reports have been presented suggesting promising applicatin of gadolinium as NCT agent.

De Stasio and co-workers [4] have reported the promising results of Gd-DTPA and Gd-DOTA accumulation by performing *in vitro* experiment using human glioblastoma cell lines, as well as *in vivo* studies on C6 glioblastoma-bearing rats. It was found that gadolinium is present in 54 and 85% of cell nuclei after single and double Gd-DOTA injection, respectively. They also performed GBM resection on six GBM patients, who had agreed for injection of Gd-DTPA 1-2 hours before tumor excision. The results have shown that only 6.1% of cell nuclei contain Gd pixels detected by MEPHISTO spectromicroscope [83] after single injection of Gd-DTPA. However, the extrapolated experimental results of *in vitro-in vivo* correspondance indicated the possibility of achieving 84% of gadolinium accumulation in tumor cell nuclei after 72-hour continuous infusion. Theoritically, multiple administration and longer exposure of Gd compound might lead to higher accumulation and prolonged retention of gadolinium in target cells.

Our previous work on colon-26 tumor-bearing mice injected with gadoteridol-encapsulated liposome has also shown significant tumor growth suppression of GdNCT treated group compared to the non-treated group suggesting the effectivity of gadolinium as NCT agent [84]. *In vitro* and *In vivo* evaluation results reported by Hofmann and co-workers [85] have shown that the use of Gadobutrol MRI contrast agent revealed therapeutic benefit with the neutral Gd complex after GdNCT treatment on

melanoma cells and solid tumor. Khokhlov and co-workers have also presented encouraging results on *in vivo* experiment application of gadopentetate dimeglumine as GdNCT agent on tumor-bearing rats [86]. Yasui and co-workers [87] have also reported the effectivity of gadolinium neutron capture therapy in vitro on glioblastoma multiforme cells, where they observed significant enhancement of cell killing on cells preloaded with Gd-DTPA and treated with neutron irradiation. Following observation of no necrosis with high cancer cells killing effectivity after GdNCT was reported in their experiment compared to other mice group treated with gamma, fast neutrons, and modified enhanced thermal neutron beam [88].

Even though most of current evaluations on GdNCT is still limited to *in vivo* and *in vitro* experiments, many types of cancer have been evaluated worldwide and the results have been showing encouraging and promising therapy effectivitiy that this investigation is worth to be advanced for optimization of NCT in the future, either as an alternative to boron, or as a complimentary in the development of NCT agent.

2.2.3 Neutron Sources for NCT

The concept of NCT itself was actually formulated long before the establishment of appropriate neutron sources. Early clinical trials for the treatment of high grade gliomas in Brookhaven National Laboratory (BNL) and the Massachusetts Institute of Technology (MIT) were conducted with beams of thermal neutrons and have actually revealed NCT effectivity in cance cells killing [14, 15, 17]. However, because of the poor tissue penetration of thermal neutrons, clinical team in MIT/Harvard had then performed open cranium irradiation to enhance neutron penetration and reduce unwanted dose to the scalp. Since then, epithermal neutron beam has been more preferable as neutron source for NCT especially to treat deep-seated tumor.

2.2.3.1 Reactor-based Neutron Source

Currently, neutron sources for NCT are still limited to nuclear reactors. Neutrons derived from reactors are commonly classified according to their energies as thermal (En $<$ 0.5 eV), epithermal (0.5 eV $<$ En $<$ 10 *k*eV), or fast (En $>$10 *k*eV). The neutrons, and gammas, emanating from the reactor, need to be moderated, filtered and/or attenuated, such that the required beam intensity and average neutron energy are within the requirements, which themselves can vary depending on the type of tumours to be treated. However, because thermal neutrons have a limited depth of penetration, it is recommended that an epithermal neutron beam is the most desirable

beam with respect to having the greatest potential for the treatment of many tumour types, sespecially deep-seated ones, because it loses energy and fall into the thermal range as they penetrate tissue.

Several reactors with very good neutron beam quality have been developed and used clinically for NCT trials. These include (a) MITR; (b) the clinical reactor at Studsvik Medical AB in Sweden; (c) the FiR1 clinical reactor in Helsinki, Finland; (d) R2-0 High Flux Reactor at Petten in the Netherlands; (e) LVR-15 reactor at the Nuclear Research Institute in Rez, Czech Republic; (f) Kyoto University Research reactor in Kumatori, Japan; (g) JRR4 at the Japan Atomic Energy Research Institute; and (h) the RA-6 CNEA reactor in Bariloche, Argentina; (i) National Tshing Hua University reactor (THOR) in Taiwan; (j) Low power reactor in a suburb of Beijing in China [90, 91]. Unfortunately, some of these reactors are no longer open to treat patients or under threat of closure

Two approaches have been used for the design of epithermal neutron irradiation facilities at fission reactors. Major approach are direct use of core neutrons, where more of such facility have been constructed for clinical use in America, Europe and Asia. Another approach is the use of sub-critical array of fuel called fission converter, initially proposed by Rief and co-workers [92], where fission neutrons are produced oustide the reactore core from thermalised neutrons emanating from the reactor. However, it is quite impossible to build a new reactor in the near future, especially near medical facilities, due to recent environmental concern about nuclear activities after the accident in Fukushima, Japan.

A total number of more than 1,000 BNCT clinical trials have been performed worldwide. Looking at the encouraging results of BCNT clinical trials in several nuclear reactor facilities (as described in previous subsection), it is expected that an efficient and optimized neutron source incorporated with hospitals could be developed in the near future in order to restart BNCT treatments in several countries where the trials are currently being halted and to obtain further positive clinical trial results for NCT to be approved and applied as common therapy modality.

2.2.3.2 Accelerator-based Neutron Source

Accelerator-based neutron source (ABNS) is a more attractive option for a compact neutron source to be to be sited in hospitals, allowing for more effective but technically more complicated procedures to carry out NCT. Many efforts are currently being performed to optimize neutron beam produced by ABNS. However, it is still a

challenge to construct ABNS with a beam quality comparable with that of the nuclear reactor, that provides a current of sufficient magnitude for clinical trials.

ABNS generally produce low intensity neutron fluxes compared to reactor sources and this has been a problem for its implementation. An increase in neutron beam intensity is crucial if ABNS are to be competitive with nuclear reactor sources for clinical NCT. In those ABNSs developed for NCT treatment currently being developed in some countries as an alternative of neutron sources for NCT, neutron is produced from nuclear reaction induced by charged particles. Lithium and beryllium are two of the elements to be considered as target material to be bombarded by charged particles in ABNS system for NCT. Among various reactions to produce accelerator-based neutrons, bombarding a ^{7}Li target with protons is one of the efficient method because high neutron yield in relatively low energy ranges. A sufficiently low accelerator current (10 mA) is required for producing a high intensity of reasonably low energetic neutrons with the average energy of 0.4 MeV and maximum energy of 0.8 MeV [90, 65]. Such neutron beams with functional lithium targets and beam shaping assemblies have been studied and developed at the University of Birmingham in the UK [93], the Institute for Physics and Power Engineering in Obninsk Russia [94] and the Atomic Energy Commission of Argentina in Buenos Aires [95], as well as the group in Korea [96, 97, 98].

Due to lower and less widely distributed neutron source energies; ABNS potentially can produce neutron beams with an energy distribution that is equal to or better than that of a reactor. However, reactor derived neutrons can be well collimated, while in contrast it might be difficult to achieve good collimation of ABNS neutrons at reasonable proton beam currents. The necessity of good collimation for the effective NCT treatment is another important and tough issue that may affect usefulness of ABNS for NCT. Furthermore, since the beam position in ABNS system is stationary, the patient needs to be directed and rotated in the treatment fields, which have become one of the issue to be handled in optimizing the use of ABNS in NCT treatment [99, 100]. Development of the ABNS for NCT is still facing few challenging tasks; the necessity of high power accelerator to producing high-current particle beam, the threshold and compensation in choosing appropriate target with efficient heat removal system, and an optimized beam shaping assembly (BSA) to reduce initial neutron energy produced by the system down to the optimal range for NCT treatment [101].

The most recent ABNS facilities are those in Japan, especially the facility at Kyoto University Research Institute, which has obtained approval by the Pharmaceutical

and Medical Safety Bureau of the Japanese Ministry of Health, Labour, and Welfare. They have started the clinical trial with the system constructed by Sumitomo Heavy Industries [102]. In this ABNS facility, neutrons are produced by hitting beryllium plate with proton beam from a 30 MeV cyclotron. Emitted neutrons are moderated by lead, iron, aluminium and calcium fluoride. Peak neutron fluxes of 1.8×10^9 n/cm^2/s at 20 mm from the surface with 1 mA proton beam have been measured in phantoms.

Another recent project on ABNS in Japan is being developed by a group in Ibaraki Prefecture, Japan. This project is a collaboration between University of Tsukuba, High Energy Accelerator Research Organization (KEK), JAEA, Hokkaido University, Ibaraki Prefecture and Mitsubishi Heavy Industry Co. (MHI). Different from the ABNS system in KURRI, this team has selected beryllium as target material with incident particel of 8 MeV proton beam. Calculation results have been reported to achieve the goals of epithermal neutron flux ($>2.0 \times 10^9$ n/cm^2/s) at the beam port, when average proton current is set to 10 mA. Accelerator facility has been installed and a new Monte-Carlo based system treatment planning is currently under development [103]. Few other projects of ABNS in Japan such as the one in Southern Tohoku Research Institute for Neuroscience in collaboration with the facility in KURRI, and also the project at National Cancer Center, which are providing promising future wider application of NCT in patient treatment.

A more detail discussion on possible charged-particle-induced nuclear reactions is presented by Kreiner [104], covering the characteristics of produced neutron beam along with development of ABNS facilities worldwide, as well as several advatages that ABNS offer compared to currently employed nuclear reactor [105, 91]. The optimization of ABNS for NCT treatment would eventually give a big impact into the socialization and familiarization of this therapy modality for a more patient-friendly facility in the future.

2.2.4 Other Developments

Besides those aspcets, which have been previously discussed about the developments of drug delivery and neutron source, other development such as detection and imaging as well as dosimetry and treatment planning for NCT also play important role in the optimization of NCT effectivity.

2.2.4.1 Detection and Imaging

As also mentioned in the subsection of Drug Delivery System, high tumor accumulation of boron or gadolinium along with high concentration ratio compared to blood and normal tissue, is necessary to ensure localization of radiation effect into tumor target. Therefore, detection of boron or gadolinium compound during NCT treatment is a crucial factor in order to fully comprehend cancer cells killing effect during treatment. It is necessary to determine biodistribution of administrated drug compound in tumor site or normal tissue of patient's body up to the subcellular level, its molecular accumulation as well as the transport and circulation of drug compound in the body.

Detection and imaging methods for NCT should be capable of quantifying bulk concentration of NCT agent as well as its spatial distribution at macroscopic and microscopic level. Non-invasive methods are preferable to allow for *in vivo* measurement, especially those with the capability to be performed during neutron irradiation, has quick response and are capable of visualizing an online detection analysis of drug distribution. However, most methods that have been developed up until now are invasive and still face the difficulty for an online detection.

Prompt gamma-ray analysis (PGRA) is one of the fast method that is capable of measuring the average concentration of element in samples and has been used for many years in BNCT trials [106, 107, 108, 109]. Khokhlov and co-workers [110] have reported the application of PGRA on both of boron and gadolinium in their MEPhI neutron facility for pharmacokinetic studies and has proven that the system is capable of measuring concentration of boron and gadolinium with satisfying detection limit required for NCT treatment. Several reports on the development of detecting system were also presented by several groups, especially those who work on semiconductor detector for the application of BNCT SPECT [111, 112, 113, 114, 115, 116]. These works are mostly focusing on the detection of 478 keV gamma ray produced after BNCR (as shown in decay scheme of ^{11}B in Fig. 2.4).

Development of detecting system for clarification of intra tumor distribution for boron and gadolinium with micro-particle induced X-ray emission (PIXE) analysis was also conducted by Endo and co-workers [117], followed by the work of Yamamoto and co-workers [118] in which they demonstrated intra tumor visualization of gadolinium distribution after administration of gadolinium containing fullerene, indicating the feasibility of Micro-PIXE as imaging technique for NCT. Detection of characteristic X-ray emission after GdNCR was also considered to be feasible method of quantifying gadolinium biodistribution as continous work of the group from Canada

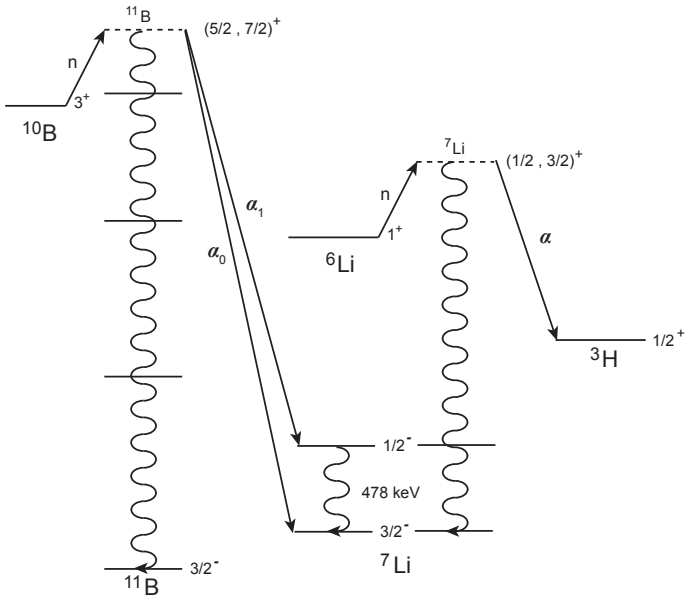

Figure 2.4: Decay scheme of ^{11}B after neutron capture reaction by ^{10}B(adapted from [124])

[119, 120, 121] by emphasizing on the detection of characteristics X-ray of energy as shown in gadolinium decay scheme shown in Fig. 2.5. The detection limit was reported to be better by around 30% compared to analysis without incorporating X-ray signal.

Inductively Coupled Plasma-Atomic Emission Spectroscopy (ICP-AES) together with ICP-MS (Inductively Coupled Plasma Mass Spectrometry) are two methods of quantitative analysis in measuring element concentration in samples. ICP-MS is often preferable over ICP-OES in determining boron concentration in samples because it has higher sensitivity and lower detection limits. Compared to other methods, ICP-MS is also capable of measuring isotopes of ^{10}B and ^{11}B simultaneously in one sample [123]. A more detail review on boron analysis and imaging has been reported elsewhere, where it also includes autoradiography methods, laser post-ionization secondary neutral mass spectrometry (laser-SNMS), ion trap mas spectrometry, as well ass nuclear magnetic resonance (NMR), magnetic resonance imaging (MRI) and positron emission tomography (PET) [124].

2.2.4.2 Dosimetry and Treatment Planning System

Dosimetry and treatment planning for NCT demands a high technical quality of the involved dose contributing components. The physical parameters involved are well

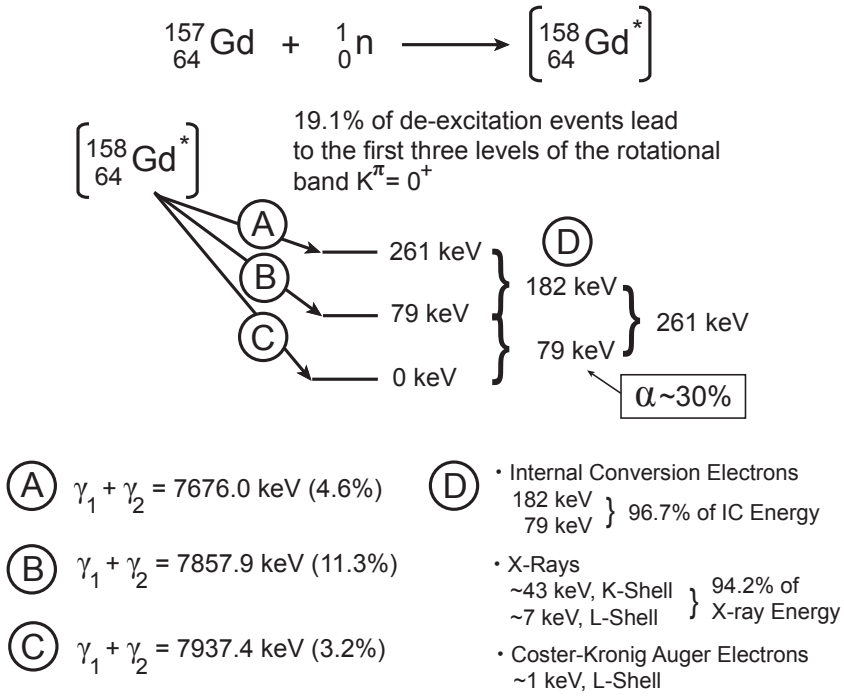

Figure 2.5: Summary of ^{158}Gd decay scheme following neutron capture reaction by ^{157}Gd(adapted from [122])

known but interact in a rather complex way, requiring specialized software for the dose estimation. calculation of the absorbed dose in a target organ is determined by the sum of the doses of neutrons and secondary gamma, and the dose of primary photons of the beam.

Compared to conventional radiotherapy, where usually only a single low-LET dose component must be computed, the radiation field in NCT is a complex mixture of high- and low-LET dose components with varying biological effectiveness that depends on both the tissue and the chemical form of the neutron capture agent. The spatial distribution of each dose component is different and depends on the tissue composition as well as the neutron and photon fluence spectra.

Treatment planning system for NCT mostly rely on Monte Carlo simulations because of the complex neutron transport. Dose calculation is conducted by integrating neutron and photon flux against energy-dependent kerma coefficients during neutron irradiation [49, 125]. In some planning systems, doses are computed on an element-wise basis, while in others doses are calculated using kerma factors precomputed depends on the tissue composition. A more detail summary on NCT treatment planning system is recently reported by Kumada and Kiger [126].

A lot of efforts have been carried out for the optimization of NCT dosimetry involving both boron and gadolinium. A more established dosimetry and treatment planning systems are currently available for BNCT compared to those for GdNCT. However, the optimization and the attempt to perform an international dosimetry exchange for BNCT has been conducted to enable future combination of clinical data from different centers conducting BNCT trials [127, 128]. Several studies on microdosimetry calculation have also been reported as an effort to optimize the estimation of delivered dose during NCT treatment [129, 130, 131, 132]. Estimation of neutron kerma in biological tissue containing boron and gadolinium was also reported by Sheino and co-workers [133], where they performed calculation of neutron and photon kerma during NCT and also presented comparison of calculated parameters of electron and photon spectra after GdNCR between several previous reports [134, 135, 136]. A more recent dosimetry calculation was reported by Enger and co-workers [137], where they performed Monte Carlo simulation for neutron and photon absorbed dose on a cell model with three scenarios of gadolinium accumulation.

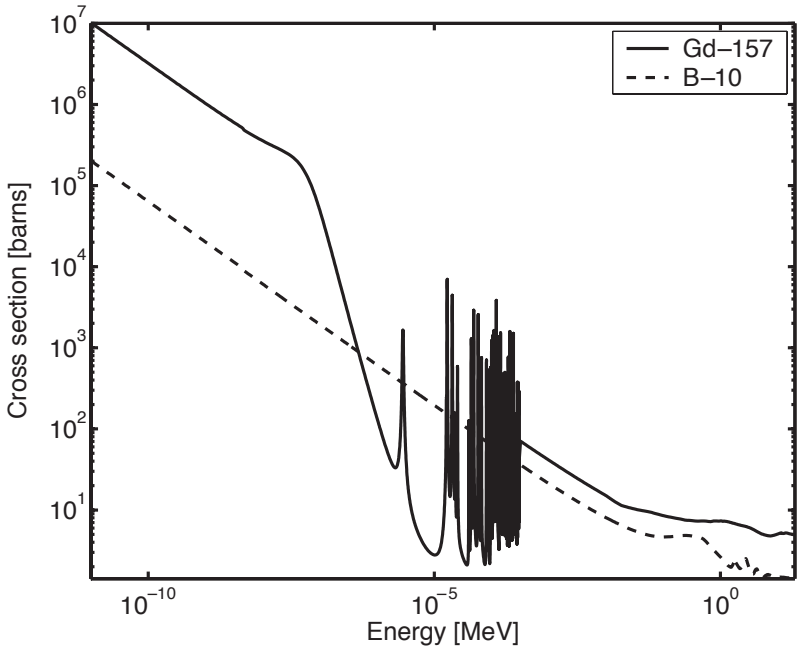

Figure 2.6: Comparison of neutron cross section between ^{10}B and ^{157}Gd [138, 139]

2.3 Comparison of BNCT and GdNCT

The neutron interaction characteristics are generally similar between ^{10}B and ^{157}Gd, as shown by the comparsion of their total cross sections in Fig 2.6. As previously mentioned, the higher neutron cross section of gadolinium bring about the advantage that the same number of neutron capture reactions with ^{10}B, can be produced with significantly lower neutron fluence. Thus, it is theoritically possible to reduce neutron dose received by surrounding normal tissue by using ^{157}Gd compound. However, the secondary particles it produces after capturing neutron are a mixture of prompt and cascade-induced photons and electrons, which reduce the localization effect of cancer cells kiling. GdNCR produces longer range gamma rays as plotted in Fig. 2.7. Referring to the interaction range of photons in water as described in Table 2.2, it is evident that the secondary particles of GdNCR (especially its gamma rays) might deposit its energy up to few centimeters range and might affect surrounding normal tissue, which is not desirable in cancer therapy. Nevertheless, there are positive aspects associated with a lack of dose localization when considering non-uniform drug uptake in the advanced and diverse tumor targeted with BNCT. If the uptake of ^{157}Gd is isolated to a bulk tumor cluster in the order of few cm^3, then an additional effect will supplement the attenuation of the capture photons.

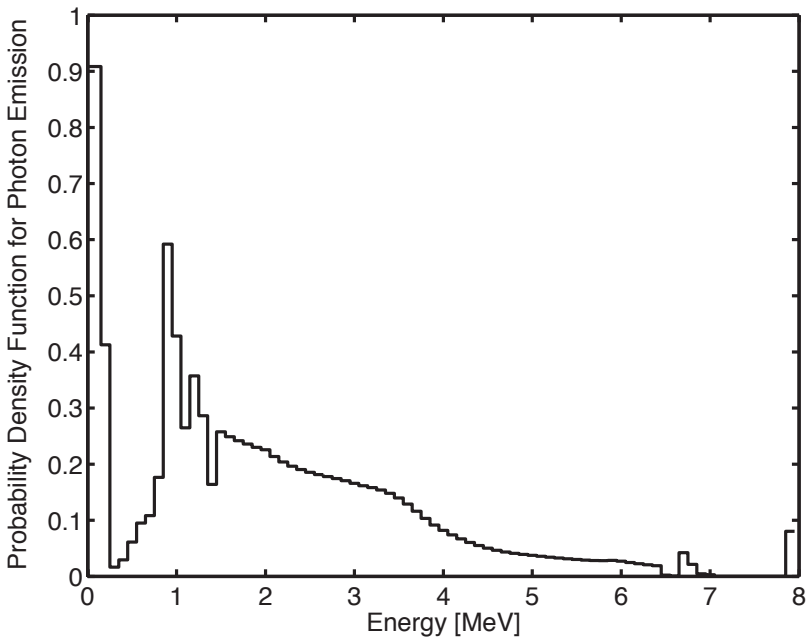

Figure 2.7: Library representation of MCNP MISC5XS1 for spectrum of gamma radiation after thermal neutron capture reaction of ^{157}Gd [139, 141].

As illustrated in Fig. 2.8 [140], we can see the comparison of energy deposition effect between high and low LET in cell. The characteristic of high LET radiation, such as α particles, is that the ionizing effect is concentrated in a relatively small number of dense tracks of limited range. Therefore, if the doses given is low, it is quite a problem to ensure the effectivens of cell killing by ionization due to this single track. While for low LET ionizing radiation, such as gamma rays or X-rays, the energy deposited on cells is sparse and more distributed. For that reason, even low doses of low LET might still result in cell killing effect although the dose is reduced.

Furthermore, by looking at the decay scheme of ^{158}Gd in Fig. 2.5, there is also the possibility of cancer cells killing effect from the DNA strand break caused by the short range Auger and Koster-Cronig electrons as illustrated in Fig. 2.9. The most commonly emitted electron energies after GdNCR have ranges that are many times the dimensions of the average 10 μm of cell diameter. In water, 50 keV electrons have a range of 42 μm and 100 keV electrons have a range of 140 μm [142, 143], which would also add into the effectivity of GdNCT treatment. A brief summary of comparison between BNCT and GdNCT is presented in Table 2.2.

A Feasibility evaluation of comparison and combination between gadolinium and boron for NCT has been previously reported by Tokuuye and co-workers [147] and

Table 2.2: Selected interaction range for photons in water [142]

Photon energy (keV)	$1/\mu$ (cm)
5	0.024
10	0.197
100	5.86
150	6.64
1000	14.1
2000	20.2
6000	36.2

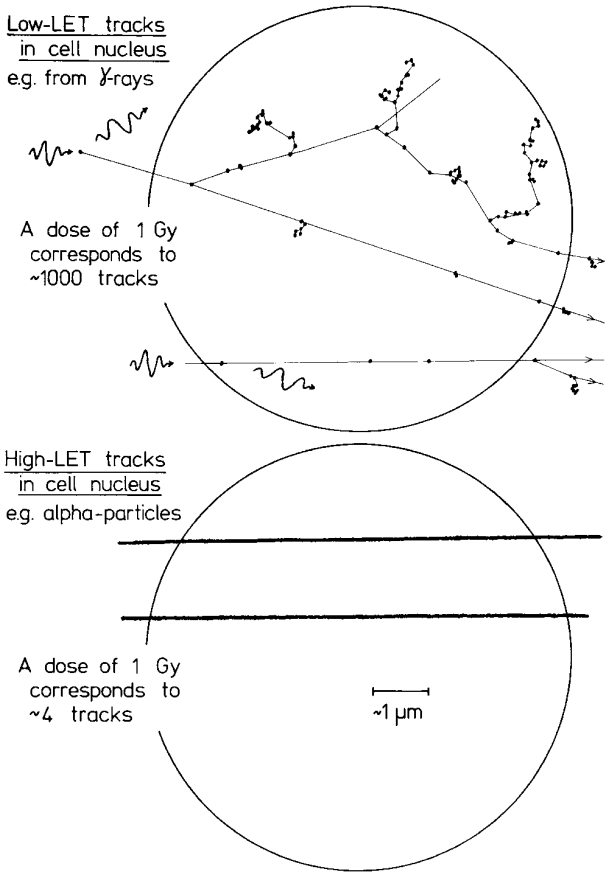

Figure 2.8: Schematic representation of a cell nucleus irradiated with two electron tracks from gamma-rays (low LET) or two α-particle tracks (high LET) [140], originally published by Goodhead [144].

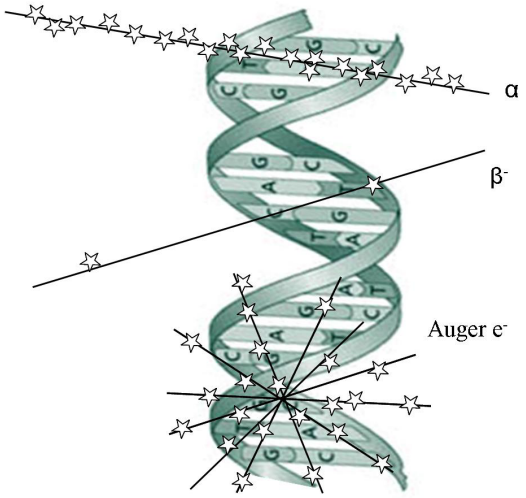

Figure 2.9: Illustration of radiation effect on DNA strand break [145].

Table 2.3: Characteristics Comparison of BNCT and GdNCT

	BNCT	GdNCT
Thermal neutron cross section	3,830 barns for ^{10}B	255,000 barns for ^{157}Gd
Average total kinetic energy (Q-value)	$\approx$ 2.33MeV	$\approx$ 7.94MeV
Secondary particles range	- 5.33 - 5.97μm for Li particle - 9.62 - 11.14μm for α particle	- 0.1 - 1μm for Auger electron - 14 - 360μm for IC electron - Up to few centimenters for long range gamma raysμm for IC electron
Approximated required neutron fluence	$\approx 10^{13}$ - 10^{14}n/cm^2	$\approx 10^{11}$ - 10^{12}n/cm^2

also by Matsumura and co-workers [146], where the results indicate varied additive effects depending on gadolinium concentration and it was suggested that achieving suitable concentrations of both gadolinium and boron in the tumor may increase their therapeutic effect, but an excessive concentration may result in a negative therapeutic effect. A computational assessment of improved cell-kill by gadolinium-supplemented on boron neutron capture therapy was also previously reported by Culbertson and Jevremovic [148], where they performed dosimetry calculation and quantified the benefits and limitations of gadolinium-supplemented BNCT. Therefore, it is necessary to carry out further investigation on combined effect of BNCT and GdNCT instead of separate use only of these radiotherapy modalities.

2.4 Neutron Capture Therapy Prospects in the Future

Collaboration between different disciplines from nuclear physics, medical doctors, chemistry, radiation oncology, mathematics to treatment management, is crucial for the success of neutron capture therapy. Interdisciplinary exchange between those scientific communities will contribute much to the development of NCT treatment. A well-developed hospital-based neutron source is also one of the important aspects to optimize the application of neutron capture therapy itself. An easy-to-understand socialization to public would also play an important role in the advancement of NCT. With many parameters and variables to be considered and taken into account, development of NCT has been quite challenging and rewarding that brings scientists and researchers from different fields together, because the improvement of one aspect could correlate to the others. A combination of boron and gadolinium in NCT as well combination of NCT with other types of radiation therapy (e.g. proton therapy, brachytherapy and synovectomy) would be more beneficial instead of exploiting each of them as a single treatment.

Chapter 3

Nanoparticles as Drug Delivery System in NCT

As also remarked previously, one of the key factors for the success in NCT is to deliver and maintain sufficient amount of NCT agent (e.g. boron and gadolinium) in tumor tissues during neutron irradiation. Therefore, an efficient drug delivery system plays a great role as a method or process of administering a pharmaceutical compound to achieve a therapeutic effect in humans or animals. With drug delivery system, it is possible to modify drug release profile, absorption, distribution, and elimination for the benefit of improving drug efficacy and safety, as well as patient convenience. This chapter will discuss in more detail about mechanism of drug delivery system and describe more about the application of nanoparticles as drug carrier.

3.1 General Introduction of Drug Delivery System

Drug delivery system is a method or process of administering a pharmaceutical compound to improve their accumulation in target site. It modifies drug release profile, absorption, distribution, and elimination for the benefit of improving drug efficacy and safety, as well as patient convenience. A drug delivery system (DDS) is most often associated with particle carriers such as emulsion, liposome, and nanoparticles, which are designed to optimize drug localization and drug-release in the target site [149]. The biodegradable drug delivery systems have received considerable attention as potent carrier for enhancing the objective effects and minimizing the side effects in various therapies.

It is important to consider several parameters such as; route administration, product stability, toxicity, and efficacy, to decide the appropriate drug delivery systems to

get an optimum drug accumulation and an improved therapeutic efficacy. An efficient drug carrier should be able to establish high tumor to normal tissue (T/N) and tumor to blood (T/B) concentration ratio in order to deliver high radiation dose to the tumor with tolerable dose to healthy tissue. Particulate carriers such as emulsion, liposome, and nanoparticles, have been of interest for drug delivery system considering that they posses the characteristics necessary to enhance drug localization and allow for a slow drug release from the delivery system in the target site [149]. A slow and limited release should also slow down the diffusion of the drug compound out of the tumors before and during the neutron irradiation. Administration route is also one of the most important factors in biodistribution and pharmacokinetics of drugs carriers. Previous study by Miyamoto and co-workers [150] had shown that intraperitoneal (i.p.) route allows the injection of relatively large amount of gadolinium compound and consequently delivers a large amount of gadolinium to the tumor via the systemic circulation. However, even with i.p. injection, many factors affect the biodistribution and pharmacokinetics of the drug carriers, including the absorption of these carriers from the abdominal cavity and the localization of these carriers in the lymph nodes, making the estimation of the in vivo fate of the drug carriers difficult [151].

3.1.1 Targeted Drug Delivery

Delivering drug into target area is generally divided into categories of "passive" and "active" targeting. Passive targeting usually occurs to most of drug carriers by taking advantage of the leaky vasculature around tumor area. It is known that the blood vessels in some diseased tissues (e.g. at tumors and inflammation sites) are not well-developed and rather leaky. Therefore, colloidal particles are able to pass those blood vessel walls and they will subsequently be retained in the tissues that they have entered. This so-called enhanced retention and permeation (EPR) effect provides some level of selectivity in drug targeting.

Since passive targeting utilize blood circulation and extravasation in drug delivery process, administrated drug usually also end up accumulated in other organs, in particular liver, spleen, kidney, and lungs. This is where an "active targeting" can help the enhancement of drug delivery through specific ligand-receptor interaction between drug carrier and target cells [152, 153, 154]. However, even though refered as "active targeting", ligand-receptor interactions are actually only possible when both are in a very close proximity. Therefore, it is necessary to combine both passive and active targeting, where drugs are being circulated by blood and extravasation

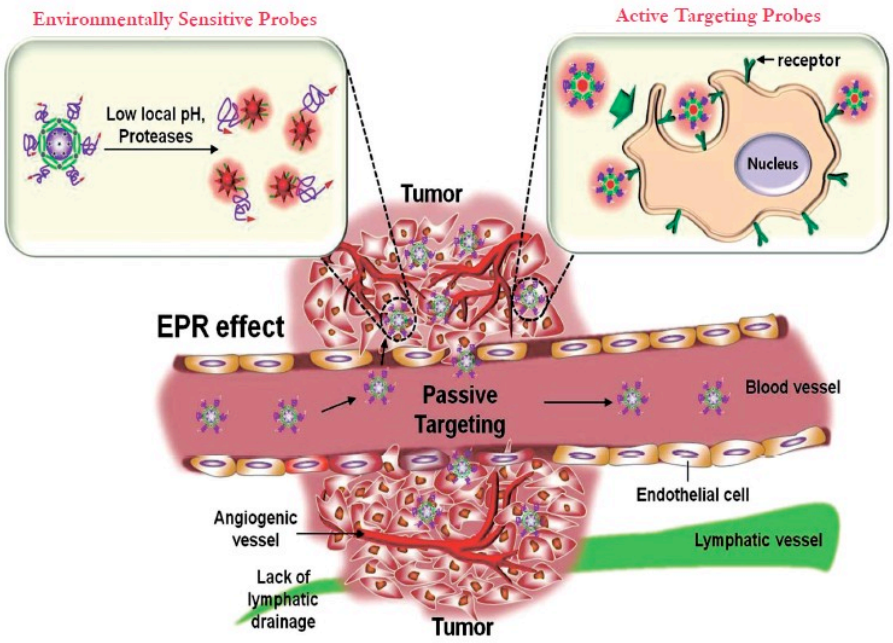

Figure 3.1: Illustration of active and passive targeting in drug delivery system [155]

before it gets close enough to target area for the active ligand-receptor interaction to happen. General illustration of active and passive targeting in drug delivery system is shown in Fig 5.1.

3.1.2 Nanocarriers as Drug Delivery System

In the past few decades, nanotechnology has been through siginificant progress on its application in medical field as the drug delivery system. Nanocarriers encompassing materials with size range of 5-200 nm for the optimum effectivity of delivering drug into target site as described in Fig 5.2 [156]. These nanocarriers are designed to improve the circulation time and enhance drug accumulation through the passive targeting.

Liposomes, which are vesicles having membranes made of double layers of phospholipids, for example, has been developed as drug delivery system because it retains, targets, and releases drug into the tumour site effectively during neutron irradiation [79]. Because of their size, hydrophobic and hydrophilic character, biocompatibility, biodegradability, low toxicity and immunogenicity, liposomes are promising systems for drug delivery. And also, by varying the type of phospholipid used to make liposomes and/or by attaching certain molecules to the surface of liposomes, they can be engineered to have many useful properties.

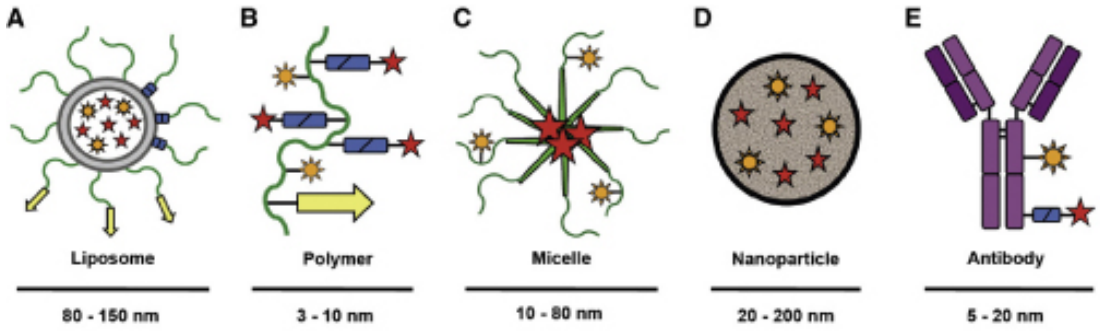

Figure 3.2: Systems and strategies used for drug targeting to tumors. A-E: Drug targeting systems. Liposomes and liposomal bilayers are depicted in gray, polymers and polymer-coatings in green, linkers allowing for drug release and for sheddable stealth coatings in blue (rectangles), targeting ligands in yellow (arrows), antibodies and antibody fragment in purple, imaging agents to monitor biodistribution and target site accumulation in orange (suns), and conjugated or entrapped (chemo-) therapeutic agents in red (stars) [156]

On the other side, micelles, are an aggregate of surfactant molecules dispersed in a liquid colloid with only tens of nanometers in diameter and are thus ideally sized for enclosing individual drug molecules. Polymeric micelles hats, made up of polymer chains, are usually spontaneously formed by self-assembly in a liquid. The main advantages of this system are the possibility to incorporate a variety of drugs including hydrophobic substances, metal complexes, and charged macromolecules such as nucleic acids as well as control their release properties by engineering and modification of the micelle-forming block copolymers [78].

Nanoparticles, especially, are getting attention as carrier device because of its capability in improving the pharmacological properties of conventional drugs due to its advantages over low molecular weight agents for example large loading capacity, capability to protect the payload from degradation, specific targeting, and controlled or sustained release [157]. Modifying the characteristic such as the nanoparticles'size, charge, and surface coating, might enhance the capability of nanoparticles in delivering drugs into target tumor [158].

Most of nano-sized agents accumulate into tumor site passively due to the EPR effect [159]. The core of nanoparticles can contain small (or bigger) molecules such as therapeutic drugs, while the shell provides interactions with the solvent and make the nanoparticles thereby stable in the liquid. For example polymeric micelles, which are either formed from block copolymers by ionic or by hydrophobic interactions, are

mentioned ot have several advantageous features over conventional surfactant micelles that make them interesting as drug delivery system. Nanomicelles made up of a well-defined core-shell architecture and the core of amphiphilic block copolymer micelles is capable to accommodate poorly water-soluble drugs that are otherwise difficult to administer to the body. The hydrophilic shell provides colloidal stability to the whole assembly [160, 161, 162].

Another key requirement for an ideal drug delivery system is that its particle size should be less than 150nm in order to efficiently target tumors [163, 164]. Small size particles (about 100 nm) were reported to be ideal to avoid uptake by liver macrophages and the reticuloendothelial system (RES) [165, 166] and to deliver molecules to specific tissues of interest [167]. Having a prolonged circulation time in blood is also critical because it has been shown that there was a strong correlation between the residence time of a drug delivery system in blood and its uptake by implanted tumors in mice [168]. A longer blood circulation time is associated with repeated passages of a high concentration of the delivery system through the tumor microvascular bed, and thus a greater efficiency of extravasations per unit volume of the transports. PEGylation is one method, which has been utilized widely to modify pharmacokinetics of nanoparticles. Several reports have mentioned that PEGylation have increased systemic circulation time of nanoparticles as drug carrier [169, 170, 171].

Stability of nanoparticles is also an important factor in optimizing blood circulation and drug accumulation in target cells. Because the critical micelle concentration (CMC) of a block copolymer can be several orders of magnitude lower than that of a 'classical' surfactant, micelles are also highly resistant against dilution that is unavoidable when administered to the patient (e.g. by injection), which increase its physical stability [160]. However, the use of nanoparticles as drug delivery system also have few drawbacks and limitations. Its small size and large surface area might cause aggregation between nanoparticles. There is also a possibility of low loading capacity and efficiency of desired drug. Technical modification is then necessary to optimize medical application of nanoparticles as drug delivery system. A detail review on targeted drug delivery is recently summarized by Bae and Park [172].

3.2 Nanoparticles as NCT Delivery Agent

The application of nanoparticles as drug delivery system in NCT has been investigated extensively by many researchers worldwide. Promising results have been presented

showing the effectivity of those systems in increasing the accumulation of NCT agent in tumor site, which is expected to enhance the effect of cancer cells killing after neutron capture reaction.

3.2.1 Drug Delivery System in BNCT

A more promising method is to introduce boron compound into nanosize dryg delivery system such as liposome and nanoparticles to enhance the uptake and retention of boron during neutron irradiation. Our group was the first to apply liposomes as boron carrier in BNCT and had shown that immunoliposome could serve as selective and efficient carriers of ^{10}B atoms to target tumor cells [173], continued with several application of drug delivery system on BNCT [174, 175, 176]. Since then, a lot of promising results of prolonged blood circulation as well as high retention of boron in tumor site, had been reported on the use of liposome and nanoparticles as boron carriers in NCT [177, 178, 179, 180]. Anti-epidermal growth factor receptor (EGFR) monoclonal antibody (mAb) is one of the promising targeting agent as reported by Yang and co-workers [181] with an extensive studies on EGFR targeting MoAb cetuximab [182]. A review on several other boron-containing nanoparticles has been reported elsewhere [183].

3.2.2 Drug Delivery System in GdNCT

Le UM [184] has previously developed improved method in the uptake and retention of gadolinium with a pegylated liposome encapsulating Gd-DTPA MRI contrast agent. It is mentioned that the liposome increase blood circulation of drug carrier and capable of accumulating gadolinium higher than 50 μg per gram tumor wet tissue. Previously, we have also performed *in vivo* experiment on tumor-bearing mice with gadolinium encapsulating liposome gadoteridol MRI contrast agent, where we could observe enhancement of gadolinium accumulation in tumor site of liposome-encapsulated gadoteridol compared to the group injected with a free gadoteridol [84].

Research group in Kobe Gakuin University, who have been working on nanoparticles as gadolinium carrier in NCT, have reported their work on chitosan nanoparticles containing gadolinium developed and synthetized for radiosensitization [185, 186]. This nanoparticles has successfully been incorporated into cells *in vitro*, with higher incorporation than molecular contrast agents. After intratumoural injection in melanoma-bearing mice, thermal neutron irradiation was applied to the tumor site, and tumor growth delay was observed indicating GdNCT effectivity [187].

Chapter 4

KURRI Nuclear Reactor Facility for NCT Treatment

4.1 General Description of The Facility

Nuclear reactor facility at Kyoto University Research Reactor Institute in Kumatori, Osaka, has been operated not only in clinical trials for treating several types of cancer, but also for the application on many research fields such as physics, engineering, agriculture, biology, etc. The Heavy Water Neutron Irradiation Facility (HWNIF) was updated in March 1996; mainly for an improvement in boron neutron capture therapy (BNCT). This facility has a heavy water tank of approximately 2 m^3 adjacent to the KUR core with the layout of KUR Advanced Clinical Irradiation System shown in Fig Fig. 4.1 including the HWNIF, and the outline of the HWNIF facility is given in Fig. 4.2.

Due to the update in March 1996, the utility and application of the facility for NCT clinical irradiation is thought to be remarkably improved. Especially in the performance, neutron irradiation with several neutron energy spectra, from almost pure thermal neutrons to epithermal neutrons, became available by the control of the heavy water thickness in the neutron energy spectrum shifter and the aperture sizes of the thermal neutron filters of cadmium and boral. The HWNIF has an irradiation field of 54 cm diameter on the bismuth layer surface, and it is available for the wide-area and uniform neutron irradiation. Also, by the installation of irradiation rail deive and remote caryying system, the irradiation utilization is more extensive for size and shape of irradiated sample [188].

A clinical irradiation for neutron capture therapy at the facility was carried out in

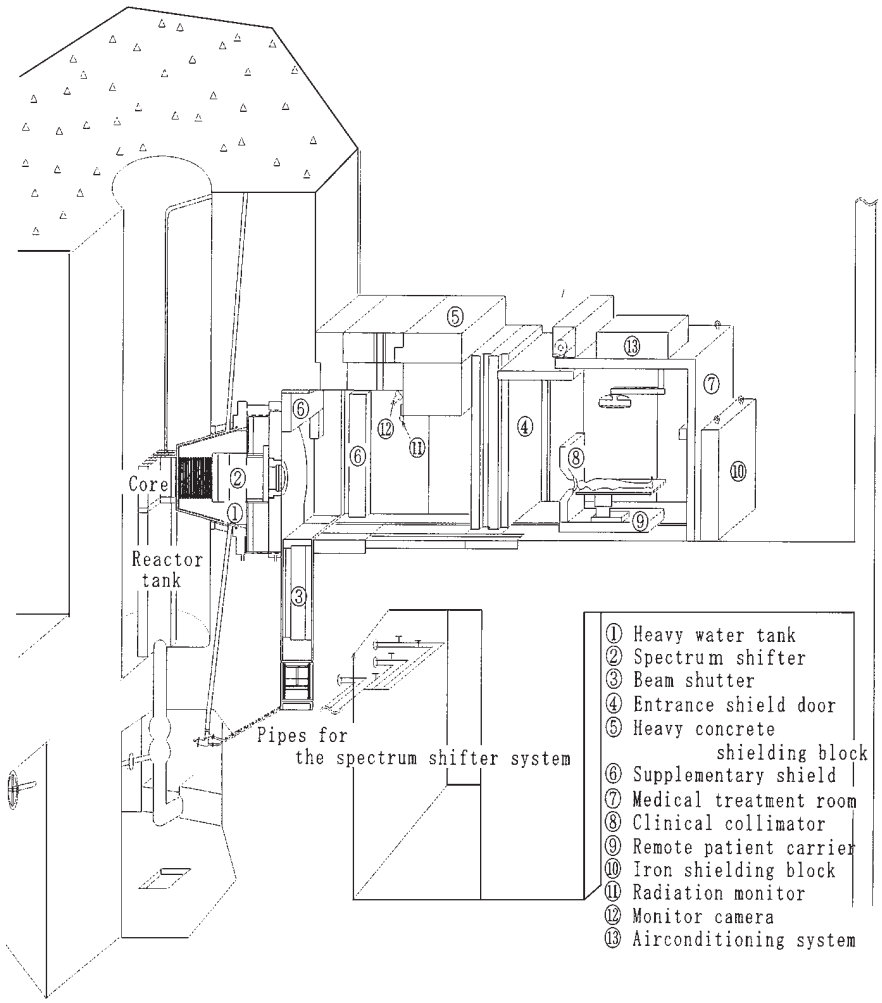

Figure 4.1: Layout of the KUR Advanced Clinical Irradiation System [188].

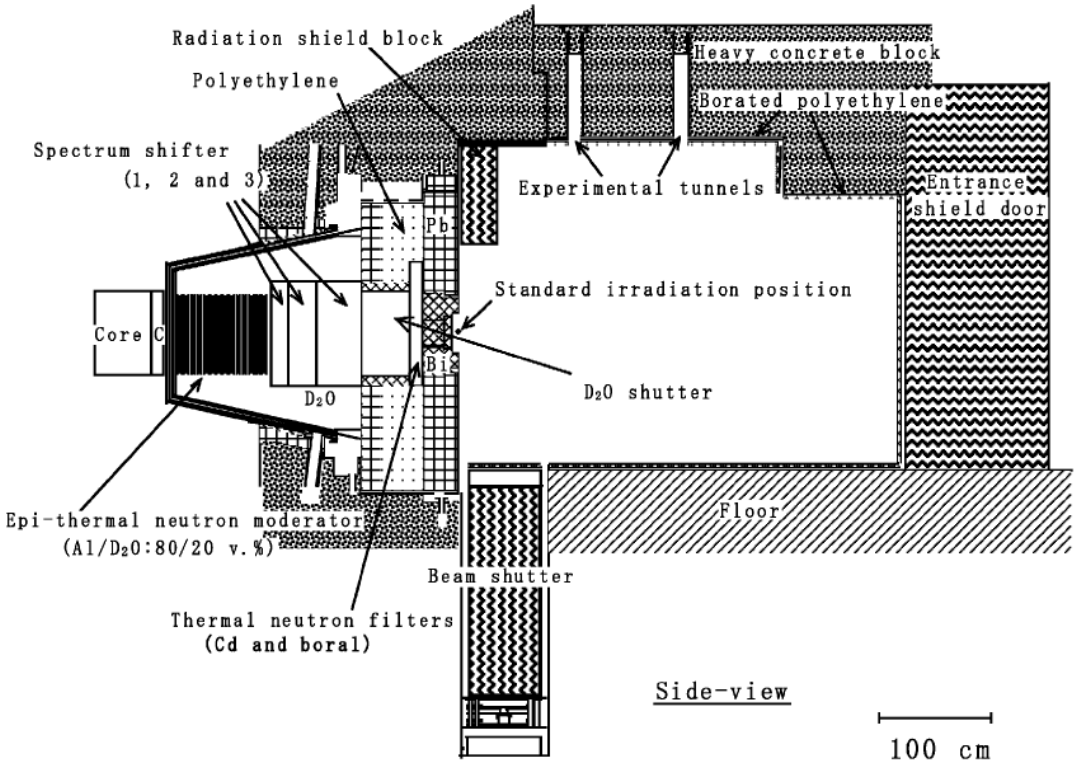

Figure 4.2: Outline of the Heavy Water Neutron Irradiation Facility of the Kyoto University Research Reactor [189].

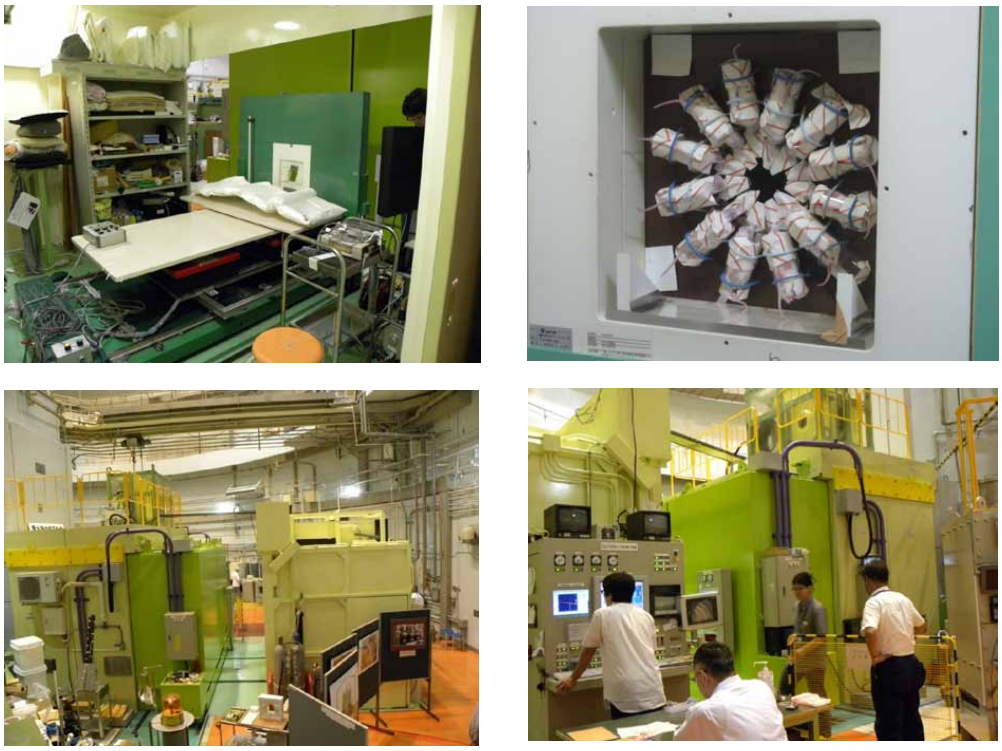

Figure 4.3: Nuclear reactor facility of Kyoto University Research Reactor Institute. Clockwise from top left: irradiation bed for patient treatment, irradiation setup for animal experiment on the neutron beam window, view of entrance door to the irradiation room, control panel and monitoring system during irradiation.

May 1974 for the first time, and it has been regularly performed since February 1990. By November 1995, just before the remodeling, 61 clinical trials were carried out for 6 yr [190]. As of the end of March 2011, 315 NCT clinical irradiations have been performed, namely, 168 for brain tumours, 105 for head and neck tumours, 22 for malignant melanomas, 7 for lung tumours, 7 for liver tumours, and 6 for tumours of the other body-parts, using the three standard irradiation modes of thermal-neutron, mixed-neutron and epi-thermal neutron. Treatment room and the control panel for patient treatment as well as the animal experiment facility can be seen in Fig. 4.3.

4.2 Neutron Spectra and Beam Characteristics of HWNIF

The calculated energy spectrum for each neutron and photon used for NCT animal experiment is given in Fig. 4.4. Here the operation mode is OO-0000-F with operating

power of 1 MW. Sakurai and Kobayashi [188] have also reported the measured data for gamma-ray dose equivalent rate on the vertical axis and the thermal neutron flux on the horizontal axis for OO-yyyy-F mode group (Fig. 4.5). Unexpectedly, the measured gamma-ray doses are not perfectly proportional to the thermal neutron flux. These relations between the gamma ray dose rate and the thermal neutron flux are thought to be dependent on the mixing ratio of the other components.

In the heavy water tank, an aluminium-heavy water mixture (Al/D_2O=80/20 in volume percent), and a neutron-energy spectrum shifter of heavy water whose thickness changed from 0 to 90 cm, are installed in order from the core side. Outside of the spectrum shifter, two thermal neutron filters of 1mm-thick cadmium plate are installed. The energy spectrum of the neutron beam can be controlled from almost pure thermal to epi-thermal within five minutes by remote control under a continuous reactor operation [189]. The overview of neutron flux and absorbed dose rate on different operation mode of KUR is given in Fig. 4.6.

The thermal neutron irradiation of HWNIF is suitable for a tumor seated near the surface such as melanoma, etc., but its application is limited for deep-seated brain tumor, etc. On the other hand, for solo irradiation of epi-thermal neutrons, its irradiation characteristic is a merit for treatment of deep-seated tumor, however, the shallow part may not be sufficiently irradiated by thermal neutrons. Application of mixed neutron irradiation has also been proposed to compensate the respective demerits of thermal and epi-thermal neutron depending on the depth of the treated tumor [188].

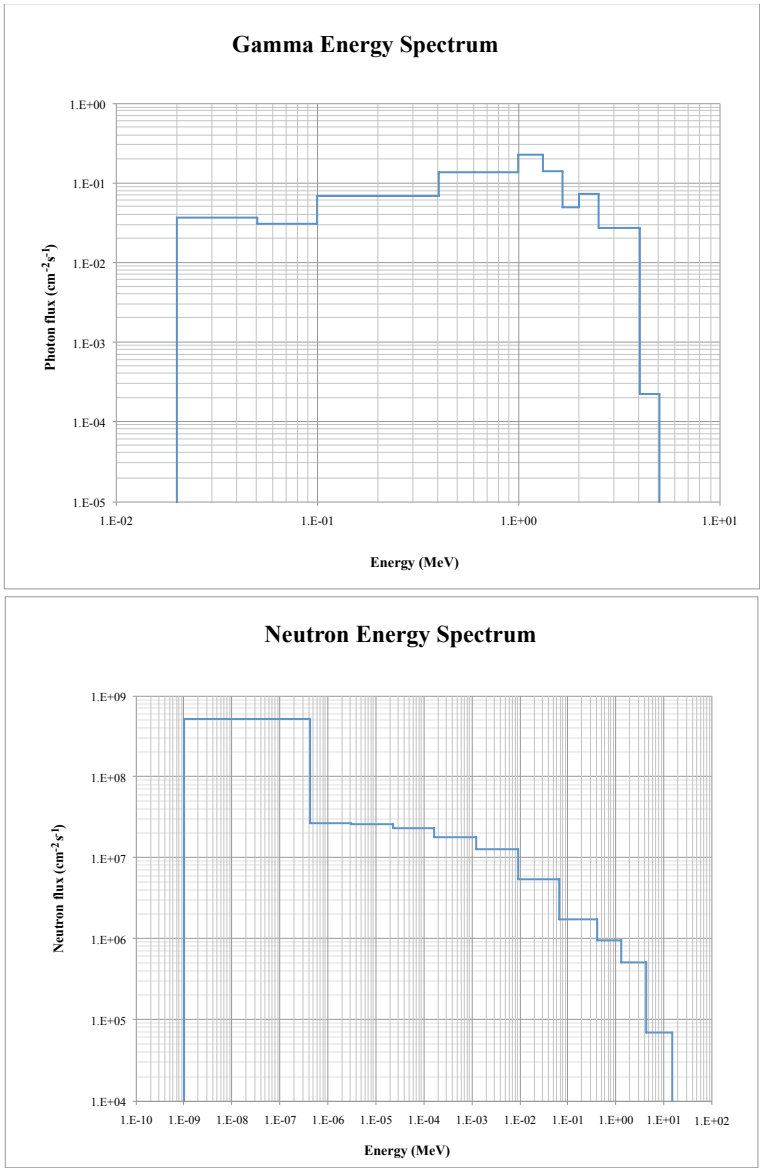

Figure 4.4: Calculated spectra of neutron and gamma source on the exit window of neutron irradiation at HWNIF of the KURRI.

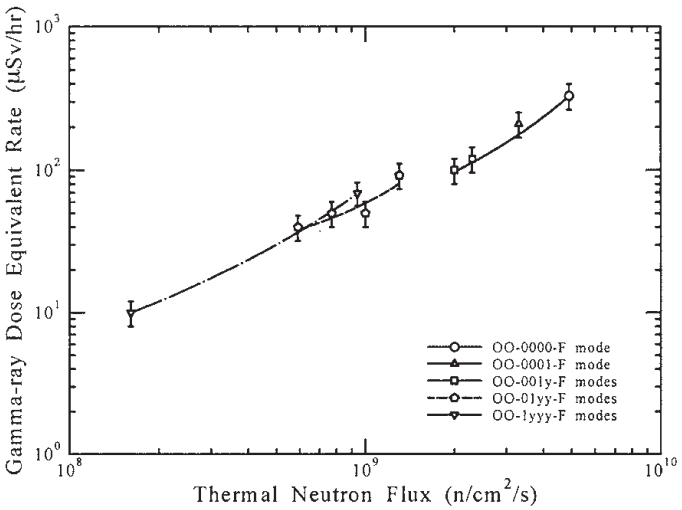

Figure 4.5: Relation between the thermal neutron flux and the gamma-ray dose equivalent rate at the normal irradiation position for the OO-yyyy-F mode group [188].

The beam parameters in free-in-air condition for the xx-0000-F mode group

Irradiation mode	Neutron flux ($cm^{-2}s^{-1}$)			Absorbed dose rate (cGy/h)			
	Thermal	Epithermal	Fast	Thermal	Epithermal	Fast	Gamma-ray
OO-0000-F	4.98E+09	7.99E+08	4.74E+07	2.42E+02	2.29E+01	1.63E+02	3.30E+02
CO-0000-F	3.04E+07	7.28E+08	4.74E+07	2.38E-01	2.24E+01	1.63E+02	6.20E+01
OB-0000-F	1.59E+07	3.88E+08	4.59E+07	5.39E-01	1.89E+01	1.60E+02	5.00E+01
CB-0000-F	4.55E+06	3.82E+08	4.60E+07	3.51E-02	1.89E+01	1.60E+02	5.00E+01

Figure 4.6: Neutron flux and absorbed dose rate for four types of KUR's operation mode [189].

Chapter 5

Evaluation of Gadolinium-Platinum Nanomicelles as NCT agent

5.1 Introduction

One of the key factors for the success in GdNCT is to deliver and maintain sufficient amount of gadolinium in tumor tissues during the neutron irradiation. Thus, effective drug delivery systems are needed in order to deliver sufficient amount of Gd into tumors for the optimization of GdNCT. Gadolinium-platinum nanomicelles compound used in this research is a continued work from previous investigation, in which we expected to combine radiotherapy effect from GdNCT with chemotherapy effect from commonly used oxaliplatin.

Combination therapy has been nowadays getting more attention because it showed improved outcome from the different mechanisms of drugs that help to attack multiple targets. Sometimes, low-dose chemotherapy and/or radiation therapy after surgery can help to destroy any remaining cancer cells. Another time, they were given before the surgery to shrink the tumors, thus providing greater ease in tumor removal. Frequently, radiation and chemotherapy or many chemotherapy agents were also incorporated together for the treatment of advanced and metastatic cancers [184]. Therefore, by combining citotoxicity effect from platinum as chemotherapy agent and the ionization from secondary particles of GdNCR, better tumor suppression from the improvement of cancer cells killing effect might be achieved. It is expected that we could shorten the irradiation time, reduce total injected drug dose, and eventually improve patient's quality of life.

The Gd-DTPA/DACHPt-loaded nanomicelles was kindly provided by Kaida and

co-workers [78] where Gd-DTPA, a widely used MRI contrast agent, is incorporated together with DACHPt in micelles core. The polymeric micelles was developed as a self-assembly of amphiphilic block copolymers consisting of hydrophobic segments forming the drug-loaded core and water-soluble segments forming the biocompatible shell. The main advantages of this system are the possibility of incorporating a variety of drugs as well as controlling their release properties by engineering and modifying the micelle-forming block copolymers. Moreover, polymeric micelles can be designed to be responsive to environmental changes and capable of target recognition [78]. It is also mentioned that some clinical studies have revealed that polymeric micelles showed reduced side effects and high effectiveness to various intractable tumors.

Radiosensitizing possibility of platinum-based drugs in combined modality treatment has actually been studied intensively in medical field. Cisplatin for example, is widely accepted as potentially radiosensitizing and combined modality treatment, including radiotherapy and cisplatin, is now frequently and successfully used in the treatment of lung cancer and cervical cancer [191]. Nevertheless, increased acute and late toxicity effects have been reported in several cases that stirred the resistance of this combined modality. Therefore, it is necessary to perform thorough research for combined radiochemotherapy with superior efficacy and less toxicity.

5.2 Materials and Methods

5.2.1 Nanomicelles Preparation

The micelles was developed as a theranostic core-shell polymeric micelles based on the self-assembly of block copolymers with both a magnetic resonance imaging (MRI) function and cancer therapeutic capacity. It incorporates gadolinium-diethyl enetriaminepentaacetic acid (Gd-DTPA), a widely used T_1-weighted MRI contrast agent, and (1,2-diaminocyclohexane)platinum(II) (DACHPt), the parent complex of the potent anticancer drug oxaliplatin, in their core by reversible complexation between DACHPt, Gd-DTPA, and poly(ethylene glycol)-b-poly(glutamic acid) [PEG-b-P(Glu)] as illustrated in Fig. 5.1. Briefly, Gd-DTPA was converted to sodium salt by adjusting the pH to 7 with NaOH, and it was lyophilized. A 5 mmol/L solution of bis(nitrato) (trans-l-1,2-diaminocyclohexane) platinum(II) [DACHPt$(NO_3)_2$; W.C. Heraeus GmbH & Co. KG] in water was mixed with the sodium salt of Gd-DTPA (5 mmol/L), and the solution was maintained for 24 hours at 37 Â°C. Then, PEG-b-P(Glu) ([Glu] = 5 mmol/L) was added to this solution ([DACHPt]/[Glu] = 1.0) and

reacted for 120 hours at 37 Â°C to prepare Gd-DTPA/DACHPt-loaded micelles. The resulting micelles were 33 nm in diameter, which is considered to be small enough to pass through the leaky vasculature of solid tumors and attain deep tumor penetration. Accordingly, both the DACHPt and Gd-DTPA complexes, which can be excreted from the kidney, thus avoiding toxicity from long-term accumulation inside the body, are released from the micelles in a sustained manner under physiologic conditions [78].

It had been shown that the incorporation of Gd-DTPA into the micelles did not influence the anticancer effect of the oxaliplatin in the micelles. Additionally, it is reported that the micelles have continuous and strong anticancer effect and enhance the MRI contrast of the tumor region in an orthotopic human pancreatic cancer xenograft model much more intensely than Gd-DTPA alone, although the diagnosis and treatment of pancreatic cancer has been considered to be the most difficult among digestive cancers. Thus, the Gd-DTPA/DACHPt-loaded micelles are expected not only to improve the effectiveness and safety of the incorporated drugs but also to assist in the real-time monitoring of the drug distribution and tumor accumulation, suggesting the great potential of visible DDS [78].

5.2.2 Cancer cells Line and Mice Preparation

In current study, we used colon-26 tumor cells injected subcutaneously into tumor bearing mice. Mouse colon carcinoma cell line Col 26 was obtained from Dainihon Seiyaku Co. Ltd. (Osaka, Japan). Colon-26 was maintained in RPMI 1640 medium (Hazleton Biologics, INC, Kansas, USA) supplemented with 10% fetal calf serum (Cell Culture Laboratories, Ohio, USA) and 100 mg/ml 1 kanamycin. All cultures were incubated in high moisture air with 5% CO_2 at 37 C. The medium was changed routinely three times a week.

Male BALB/c mice were obtained from Nihon SLC (Shizuoka, Japan) and used at 6-7 weeks of age. In each experiment, mice of similar age and weight were selected. Mice were housed in plastic cages and maintained in an air-conditioned room. Tumor models were prepared by subcutaneous injection of 1×10^5 of Col-26 cells into right femoral of the mice. The tumor was let to grow for two weeks until the average volume reached 100 mm^3. The procedures for tumor implantation and sacrifice of the animals were performed with permission of the Animal Ethics Committee of The University of Tokyo in accordance with the Declaration of Helsinki.

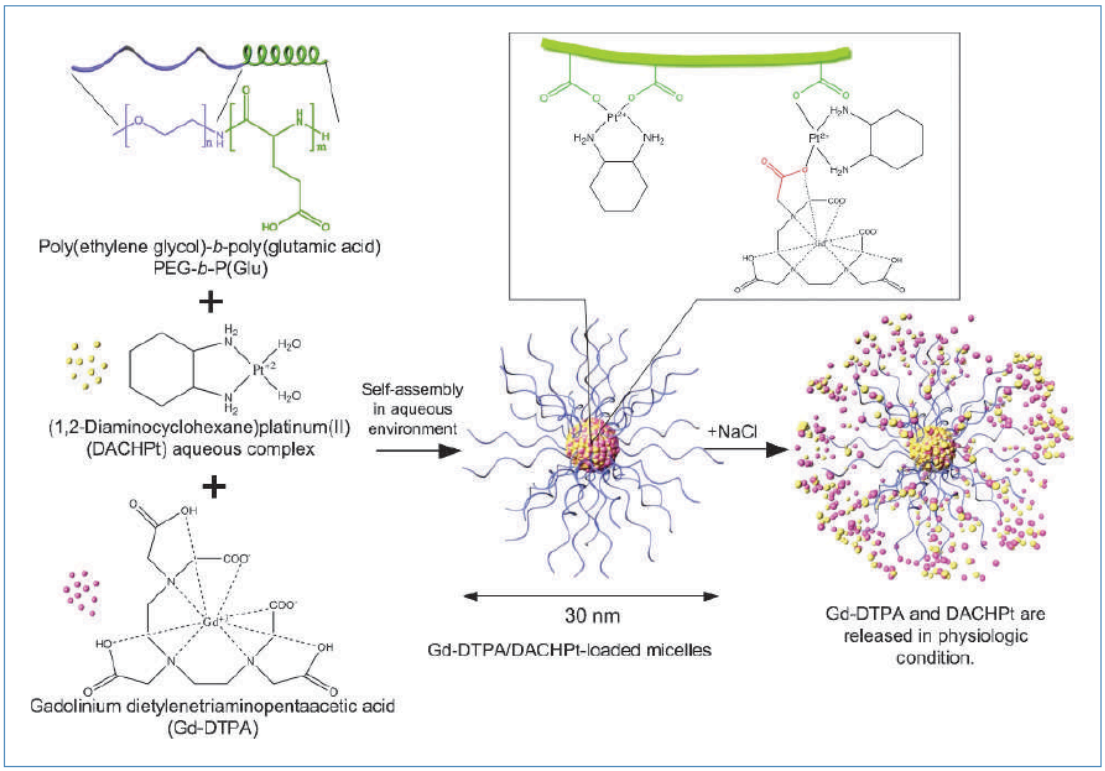

Figure 5.1: The schematic diagram of self-assembly Gd-DTPA/DACHPt-loaded nanomicelles and the release of platinum and gadolinium complexes from the micelles in chloride-containing medium [78].

5.2.3 Biodistribution Analysis

In this experiment, MRI image acquisition was performed to take cross section image of each mouse using the MRI facility in Kashiwa campus The University of Tokyo. An MRI machine uses a powerful magnetic field to align the magnetization of some atomic nuclei in the body, and radio frequency fields to systematically alter the alignment of this magnetization. This causes the nuclei to produce a rotating magnetic field detectable by the scanner and this information is recorded to construct an image of the scanned area of the body [192]. Gradients in magnetic field cause nuclei at different locations to rotate at different speeds. By using gradients in different directions 2D images or 3D volumes can be obtained in any arbitrary orientation.

MRI provides good contrast between the different soft tissues of the body, which makes it especially useful in imaging the brain, muscles, the heart, and cancers compared with other medical imaging techniques such as computed tomography (CT) or X-rays. Unlike CT scans or traditional X-rays, MRI does not use ionizing radiation which is one of the most important aspects to be considered when we apply treatment or diagnosis to the patient.

When a person is inside the powerful magnetic field of the scanner, the average magnetic moment of those protons inside human body becomes aligned with the same direction as of the magnetic field. When a radio frequency transmitter with just the right frequency is applied, it is then being absorbed and flips the spin of the protons in the magnetic field. After the electromagnetic field is turned off, the spins of the protons return to thermodynamic equilibrium and the bulk magnetization becomes re-aligned with the static magnetic field. During this relaxation, a radio frequency signal is generated, which can be measured and give information of the scanned object. Different tissue variables, including spin density, T_1 and T_2 relaxation times and flow and spectral shifts can be used to construct images. By changing the settings on the scanner, this effect is used to create contrast between different types of body tissue or between other properties, as in fMRI and diffusion MRI [193].

To enhance contrast appearance of blood vessels, tumor, or inflammation, a contrast agent is usually utilized by injecting certain elements, which has the capability of shortening the T_1 relaxation time of protons during imagin acquisition process. And the most commonly used compounds for contrast enhancement in MRI are gadolinium-based compound including the two gadolinium-based compound that we use in current study. Gadolinium has the ability of altering the relaxation times of tissues and body cavities where they are being accumulated. Therefore, it enhances

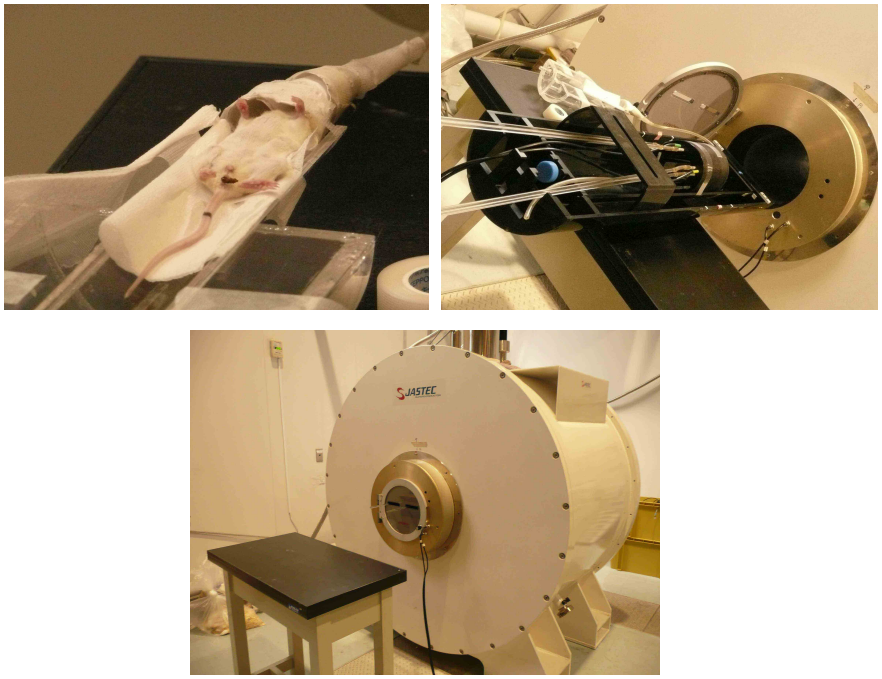

Figure 5.2: Experimental set-up for MRI image acquisition.

brightness contrast of tumor site, which normally appears darker and might not show good matter contrast.

For the MRI image acquisition, mice were injected with Gd-DTPA/DACHPt-loaded micelles intravenously and fixed in the custom-made cradle with nylon tape. The mice were anesthetized with 5% isoflurane at the beginning and maintained with 1.5% isoflurane during the MRI image acquisition. MRI images were obtained using a 4.7 Tesla superconductive magnet unit interfaced to a Varian (UNITY INOVA, Varian Inc., Palo Alto, CA) with 60mm diameter birdcage RF coil and maximum imaging gradient of 6.0 Gauss/cm. For the T_1-weighted MR imaging of live mice, the following parameter were adopted: spin-echo method, the repetition time (TR) = 300 ms, the echo time (TE) = 15 ms, the field of view (FOV) = 40 $\times$ 40 mm^2 for axial direction and equals 50 $\times$ 50 mm^2 for coronal and sagittal direction, matrix size = 128 $\times$ 128 and the slice thickness = 2 mm. Fig 5.2 shows the experimental setup for MRI image acquisition.

For the quantitative analysis, ICP-MS measurement was performed to evaluate total gadolinium and platinum concentration in tumor-bearing mice organs. For the *in vivo* experiments, injected-mice were sacrificed at 2, 12, and 24 hours after gadolinium compound injection then tumor and several vital organs such as blood, liver, kidney, spleen, heart and lungs were excised. Volume of each organ sample was

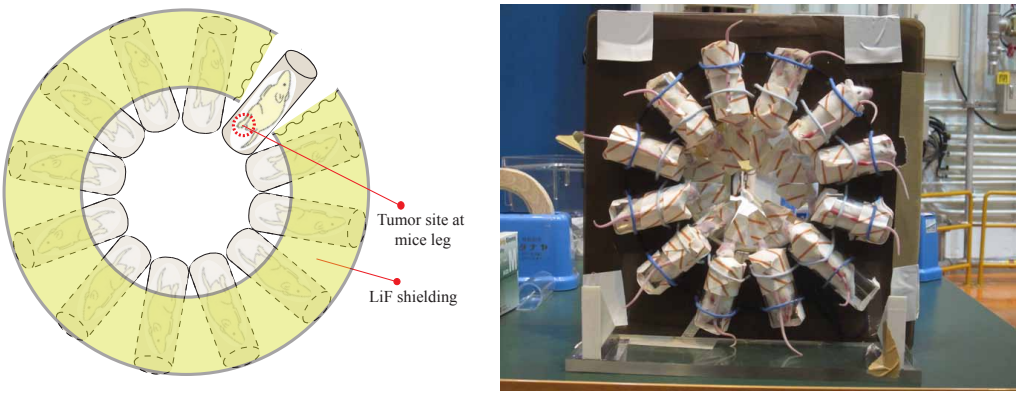

Figure 5.3: Neutron irradiation setup at KUR facility. Mice were held within acrylic tube and neutron beam was collimated to tumor site on the leg using LiF shielding.

measured, followed by digestion in HNO_3 left overnight. Samples were then digested in microwave oven to ensure that all of the sample material is dissolved. The total amount of gadolinium was measured using ICP-MS and the results were normalized to the tissue volume.

5.2.4 Neutron Irradiation

Neutron irradiation for Gd-DTPA/DACHPt-loaded nanomicelles-injected group was performed at Heavy Water Neutron Irradiation Facility (HWNIF), Kyoto University Research Reactor Institute in Kumatori, Osaka. Operation mode for this irradiation is OO-0000-F with operating power of 1 MW. Rectangular tiles made of ^{6}LiF were chosen as the collimator material to shield all mice body but the tumor area from thermal neutrons. Irradiated mice were held within acrylic tube designed specifically for collimated neutron irradiation as illustrated in Fig. 5.3, where neutron beam direction is into the page. Neutron fluence for this experiment was measured by gold foil on the surface of the tube where mice were placed for the irradiation, while gamma-ray dose component was monitored by using TLD placed at the same point as gold foils.

In previous work, we performed whole body irradiation at JRR-4 nuclear reactor facility and observed high toxicity for Gd-DTPA/DACHPt-loaded nanomicelles-injected irradiated at two hours after drug administration. Therefore, the experiment was then previously continued with neutron irradiation at 24 hours after Gd-Pt compound injection where gadolinium concentration in blood plasma has already decreased significantly, to minimize ionizing effect to normal tissues. For this second

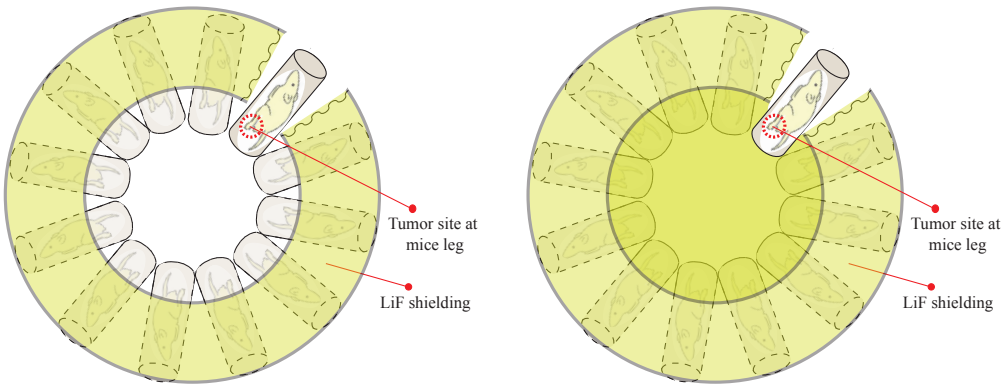

(a) (b)

Figure 5.4: a. Irradiation set-up for collimated neutron using LiF sheet with 2×10^{12}, 1×10^{12}, and 0.5×10^{12} n/cm^2 neutron fluence. b. Experimental set-up for whole-body-neutron-shielded irradiation. Neutron irradiation was exposed perpendicular to LiF sheet.

experimental procedure, we performed neutron irradiation with the setup as shown in Fig. 5.4(a) and Fig. 5.4(b) within these conditions:

- Collimated irradiation onto tumor site of the mice using LiF shielding with three different neutron fluence to evaluate the effect from various neutron irradiation doses. The thermal neutron fluence for the experiment were approximately 2×10^{12} n/cm^2 (35 minutes irradiation time), 1×10^{12} n/cm^2 (17.5 minutes irradiation time), and 0.5×10^{12}n/cm^2 (9 minutes irradiation time).

- Whole body neutron-shielded irradiation using LiF sheet to check the possibility of radiation effect from gamma contamination in the neutron beam,

Following this experiment, we also then performed neutron irradiation on mice group injected with Gd-DTPA/DACHPt-loaded nanomicelles and oxaliplatin-loaded nanomicelles only (without Gd-DTPA), to confirm the possibility of platinum photoactivation toxicity of Gd-DTPA/DACHPt-loaded nanomicelles after neutron irradiation. Neutron irradiation was carried out for injected mice group both at 12 hours and 24 hours after injection. Considering that platinum accumulation in blood at 12 hours is still quite high, and it decreases significantly at 24 hours after injection, it is expected that we could investigate whether the cause of high toxicity observed for this nanoparticles in previous experiments is associated with the irradiation of platinum only.

5.2.5 Evaluation of Antitumor Effectivity

To evaluate antitumour effectivity after neutron irradiation, tumor growth suppression needs to be monitored periodically altogether with the weight. Tumour size of each mouse was measured every two or three days until about one month from the first day of neutron irradiation. Tumor volume calculation was carried out using the formula:

$$V = a \times \frac{b^2}{2} \tag{5.1}$$

where a and b are the major and minor axes of the tumour measured by a caliper, respectively. Mice body weight was also monitored simultaneously as a parameter of systemic toxicity. The antitumor effect was evaluated on the basis of the change in tumor growth and survival rate of the mice. We also evaluated survival rate for experiment and plotted the Kaplan-Meier to estimate survival fraction of treated mice on the experiment with various neutron fluence until about 36 days after neutron irradiation.

5.3 Results and Discussions

5.3.1 Biodistribution Analysis

Coronal MRI image of tumor-bearing mice was taken after administation of 0.2 ml Gd-DTPA/DACHPt-loaded nanomicelles to observe macroscopic distribution of gadolinium. Unfortunately, on the MRI image acquisition time, we could not provide free Gd-DTPA for comparison of image enhancement, so we used MRI image data of gadoteridol-solution from previous investigated gadolinium-encapuslating liposome [84].

Contrast signal in gadolinium-platinum compound shown in Fig. 5.5 was not that much different compared to the MRI image of the gadoteridol-solution, even though the initial amount of gadolinium contained in 0.2 ml of gadoteridol-solution was actually almost 1000 times higher compared to those contained in 0.2 ml of Gd-DTPA/DACHPt-loaded nanomicelles. Therefore, toretically we can say that Gd-DTPA/DACHPt-loaded nanomicelles could accumulate much larger amount of gadolinium into the tumor site compared to free gadoteridol-solution. Better contrast enhancement of Gd-Pt nanomicelles compared to free Gd-DTPA is given in Fig. 5.6 from Kaida and co-workers' work [78], where the injected Gd-DTPA dose is in-

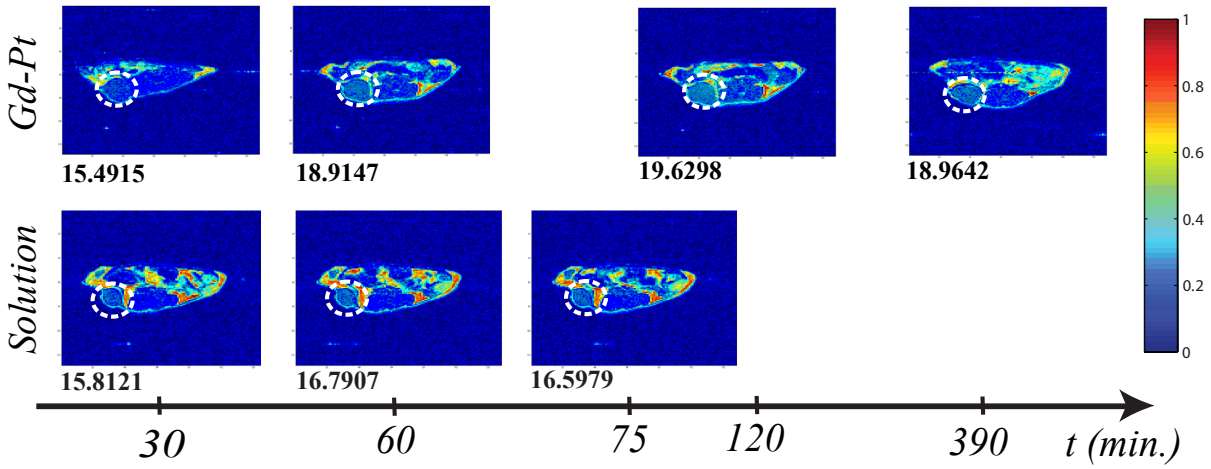

Figure 5.5: Transversal cross section MRI image comparison between Gd-Pt nanomicelles and gadoteridol-solution. Tumor site is shown by white dash circle and the number under each MRI image indicates the approximation of total signals for tumor site area.

creased up to 2.5 times higher compared to the injected dose we used to acquire MRI image in Fig. 5.5.

The result of ICP-MS measurement is presented in Fig. 5.7, which shows significant decreasing tendency of gadolinium and platinum concentration in blood, and increasing accumulation of platinum in tumor site, which agrees with the characteristics reported by Kaida and co-workers [78]. Gadolinium accumulation in tumor site is increasing at 24 hours after injection, which is also in agreement with the result presented in their paper [78].

5.3.2 Neutron Irradiation

Average neutron fluence measured by gold foil for the 60 minutes irradiation is 2.7 $\times$ 10^{12} n/cm^2 for thermal neutron range and 4.75 $\times$ 10^{11} n/cm^2 for epithermal neutron range. Physical dose from the measurement during neutron irradiation are shown in Table 5. 1. It is defined that thermal neutron region is below 0.5 keV, the epithermal neutron region is 0.5 keV-10 keV and the fast neutron region is over 10 keV. These results are also comparable to physical dose meausured in the GdNCT experiment performed by other researchers at the same reactor facility in KUR [187].

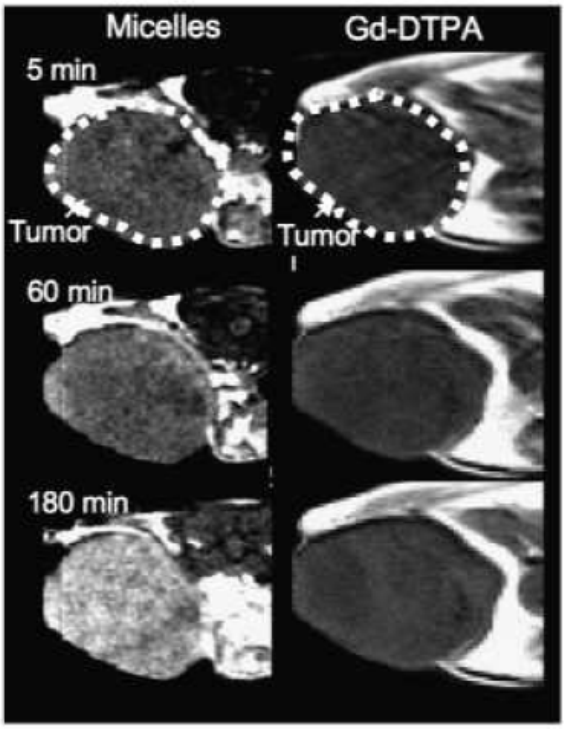

Figure 5.6: *In vivo* MRI images of T_1-weighted transaxial slices of C-26 subcutaneous tumor after i.v. injection of Gd-DTPA/DACHPt-loaded micelles compared to bare Gd-DTPA at 5 μmol/kg Gd-DTPA [78]).

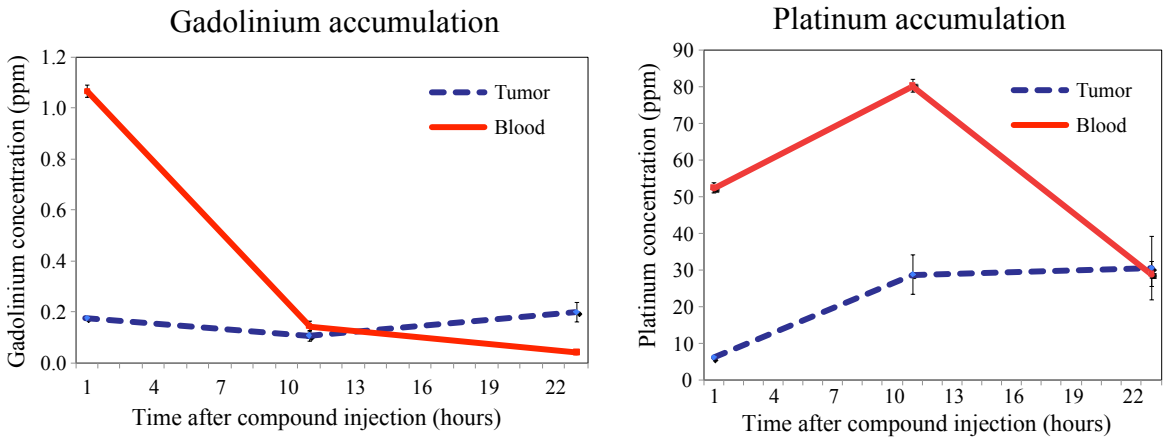

Figure 5.7: ICP-MS measurement results of gadolinium and platinum concentration accumulated in tumor site and plasma blood. Error bar indicates the uncertainty of ICP-MS and variance of samples.

Table 5.1: Average physical dose from the measurement during neutron irradiation

	Physical dose (Gy)
Thermal neutron (∼0.5eV)	3.6×10^{-1}
Epithermal neutron (0.5eV∼10keV)	3.85×10^{-2}
Fast neutron (10keV∼)	2.65×10^{-1}
Gamma ray	4.35×10^{-1}
Total	1.1
Natural gadolinium (1ppm)	3.55×10^{-3}
Gadolinium-157 (1ppm)	1.85×10^{-2}

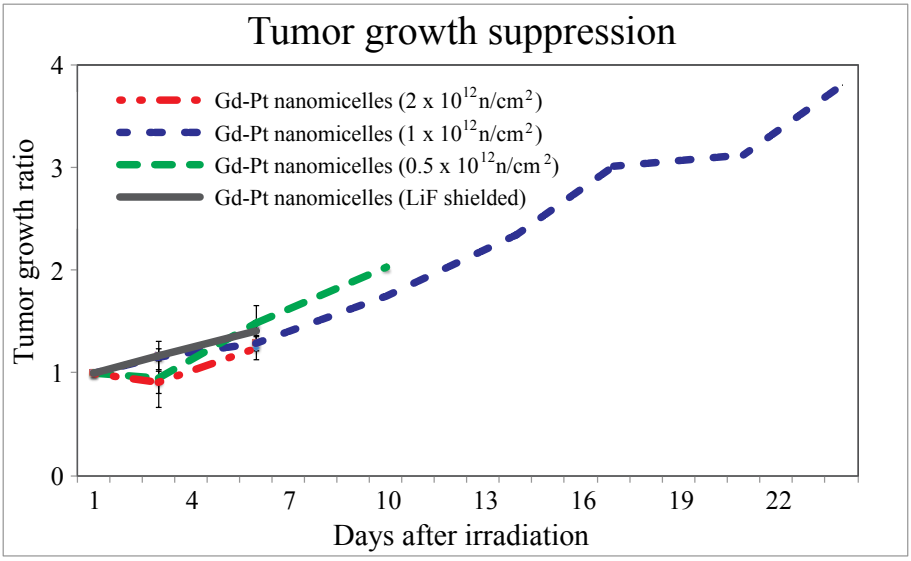

Figure 5.8: Tumor growth suppression after neutron irradiation of various fluence for Gd-Pt nanomparticles injected group. Data shown is average tumor growth ratio from 4-5 mice on each group with error bar indicating variance of measured data.

5.3.3 Evaluation of Antitumor Effectivity

Evaluation of antitumor effect was performed in the same procedure with the previous experiment on gadolinium-entrapped lipoosme for GdNCT [84]. For each treatment condition, we included at least 3 control mice (for non-injected and gadolinium-solution injected group) as a standard for comparison of the antitumor effect evaluation. Tumor sizes were measured until 24 days after neutron irradiation and the result for the experiment with various neutron fluence is shown in Fig. 5.8. Non-treated group is not shown in this graph, but the tumor growth suppression was observed to be around 5 times higher compared to the control (non-treated) non-irradiated group.

Unfortunately, even for this experimental set-up, almost all irradiated mice, which

were injected with Gd-DTPA/DACHPt nanomicelles died within 10 days after irradiation. Only two mice from group irradiated with 1×10^{12} n/cm^2 neutron fluence survived until 24 days of evaluation (as described in the Kaplan Meier plot in Fig. 5.9). We can see that mice received no treatment mostly survived until more than 20 days after neutron irradiation. Some non-treated mice even survived until 33 days after irradiation. Gd-DTPA/DACHPt nanomicelles-injected group in this experiment still showed quite high toxicity and low survival rate. Significant prolongation of survival rate for Gd-DTPA/DACHPt nanomicelles-injected mice was observed on group irradiated with 1×10^{12} n/cm^2 neutron fluence, even though only 60% survived until 27 days after neutron irradiation, the same as non-treated mice for 1×10^{12} n/cm^2 neutron fluence.

Even though we have performed collimated irradiation so that neutron will be restricted into tumor site only for this second experiment, the toxicity still seemed to be quite severe and caused death to most of the tumor-bearing mice within 9 days after thermal neutron irradiation. Irradiation with neutron-shielded experiment also showed 100% mice death within 9 days after irradiation. This shows higher possibility that gamma dose from neutron beam of the reactor facility have caused photoactivation of platinum and might as well gadolinium which also accumulated at several organs of the mice and deposit quite significant ionizing radiation dose.

Since current irradiation was performed with the standard clinical trial neutron fluence, our previous assumption is that platinum photoactivation occurs during irradiation that increases the compound toxicity. Thermal neutron cross section for natural platinum is very small (0.96 barns), therefore it is unlikely that platinum neutron capture reaction caused the high toxicity of this compound after neutron irradiation. However, since platinum K-edge shell is 78.39 keV, while gamma contamination in neutron beam have energy range above that K-edge shell energy, platinum photoactivation is very likely to occur and increase the toxicity of platinum element in mouse body.

Gd-DTPA/DACHPt-loaded nanomicelles-injected mouse were actually showing enhancement of tumor growth suppression compared to control group. Slight difference of tumor growth suppression effect was also observed compared to bare platinum irradiated group, indicating GdNCT effect even with low gadolinium concentration (below 1 ppm) in tumor site.

For the following experiment of neutron irradiation for mice group injected with both Gd-DTPA/DACHPt-loaded nanomicelles and oxaliplatin-loaded nanomicelles only, tumor growth suppresion graph after GdNCT treatment is given in Fig. 5.10.

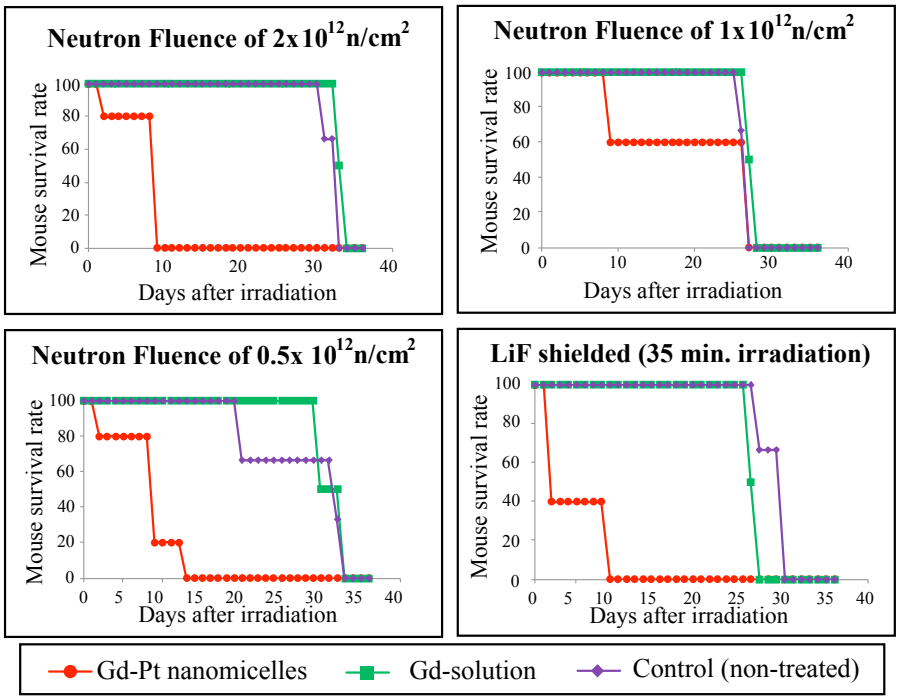

Figure 5.9: Kaplan Meier plot for experiment of neutron irradiation with different fluence on mice injected with Gd-DTPA/DACHPt-loaded nanomicelles

We still observed severe toxicity on the irradiated group for both nanomicelles-injected mice, where both nanomicelles-injected and irradiated mice group died within 10 days after neutron irradiation. Mice weight by time is also presented in Fig. 5.11, where we could observe that the weight loss for almost all group have the similar tendency until around 9 days after irradiation. However, all irradiated mice did not recover (while the non-irradiated group did) and died within 10 days after irradiation.

Previous study by [194] presented on (Tabel 5.2.) summarizes six *in vitro* studies analyzing the radiosensitizing potential of oxaliplatin. The results showed that an enhanced cytotoxic effect was obtained when the two treatments (oxaliplatin and high LET radiation) were combined taking either cell proliferation or clonogenic survival as an endpoint. This means that the effects of a combined radiation and oxaliplatin treatment are greater than the sum of the respective single responses, irrespective of being termed additive, supra additive or synergistic.

Up to date, the mechanisms causing radiosensitizing properties of oxaliplatin have not been studied in detail. Like cisplatin, oxaliplatin acts as an alkylating agent on DNA, but differences in their DNA-adducts and mechanisms of DNA-repair may be related to their specific activity profiles. Oxaliplatin forms DACH-platinum adducts which are more bulky and hydrophobic and possibly more effective in inhibiting

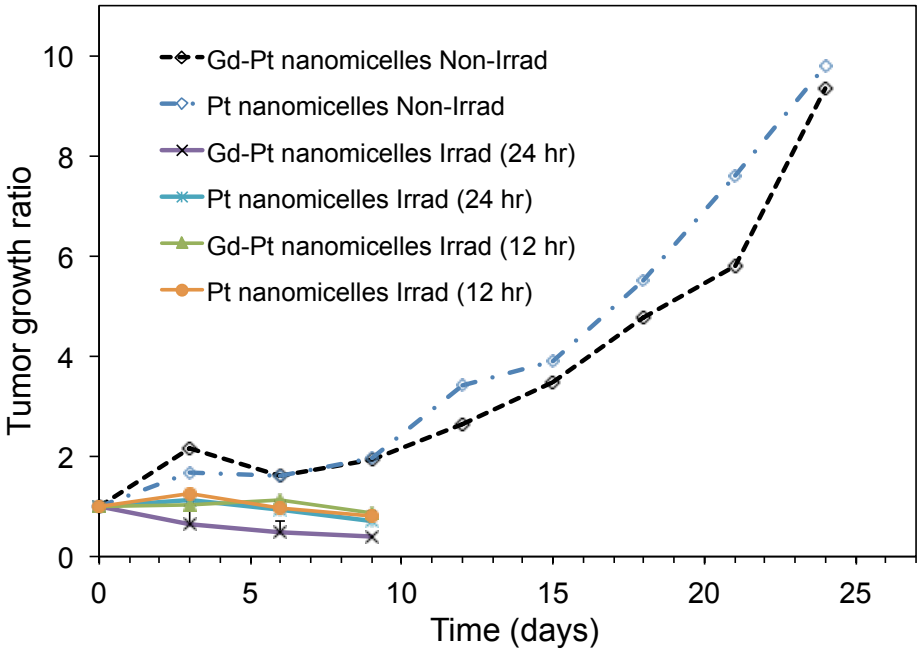

Figure 5.10: Tumor growth suppression for Gd-DTPA/DACHPt-loaded nanomicelles compared to DACHPt-nanomicelles injected group irradiated at 12 hours and 24 hours after compound injection, compared to the non-irradiated group. Data shown is average tumor growth ratio from 4-5 mice on each group with error bar indicating variance of measurement.

Table 5.2: Summary of published studies of in vitro experiment analyzing radiosensitizing potential of oxaliplatin [194]

Study	Tumor entity	Cells treated/transplanted	Treatment Oxaliplatin + radiation (IR)	Endpoint	Result
Koivusalo et al. [195]	Cervical cancer	SiHa (± p53 activity), UT-DEC-1, HeLa, CaSki	0.1-300μM+ 5Gy 6-h-incubation	Clonogenic survival Apoptosis	Oxaliplatin-induced radiosensitization Increased apoptosis Resistance through functional p53
Magne et al.[196]	Colorectal cancer	SW403 p53 wt WiDr p53 mut	6.5-1000μM+1 or 4Gy 2-h-incubation	Cell viability by MTT assay	Oxaliplatin-induced radiosensitization No influence of p53
Kjellstrom et al.[197]	Colorectal cancer	S1 clone of LS-180	1 + 4μM+ 0.5-4 Gy 2-h-incubation	Cell viability by MTT assay	Oxaliplatin-induced radiosensitization
Espinosa et al.[198]	Head & Neck cancer[a]	KB and Hep2, no functional p53[a]	0.0001 - 100μM+ 4-8 Gy 24-h-incubation	Clonogenic survival Cell viability	Oxaliplatin-induced radiosensitization
Rave-Frank et al.[199]	Cervical cancer Lung cancer	CaSki, no functional p53 A549 p53 wt	1.25 - 2.5 μM+ 1-6 Gy 2-h vs. 24-h-incubation	Clonogenic survival	Oxaliplatin-induced radiosensitization No influence of p53
Benzina et al.[200]	Glioblastoma	U-87 p53 wt	1.5 - 25 μM+ high LET IR 25-h-incubation	Clonogenic survival Apoptosis	Oxaliplatin-induced radiosensitization No involvement of apoptosis
Cividalli et al.[201]	Breast cancer	Spont. adenocarcinoma (CH3/TIF mice)	6-14 mg/kg single or repeated doses single dose and fractionated IR	Tumor growth delay	Synergism of oxaliplatin and IR independent from sequencing
Folkvord et al.[202]	Colorectal cancer	HT29	10 mg/kg repeated doses fractionated IR	Tumor growth	No radiosensitization; preliminary results, weak endpoint

[a] Both cell lines were originally thought to be derived from head and neck cancer, but were subsequently found, based on isoenzyme analysis, HeLa marker chromosomes, and DNA fingerprinting, to have been established via HeLa cell contamination. The cells are positive for keratin by immunoperoxidase staining. KB cells have been reported to contain human papillomavirus 18 (HPV-18) sequences (from ATCC, www.atcc.org).

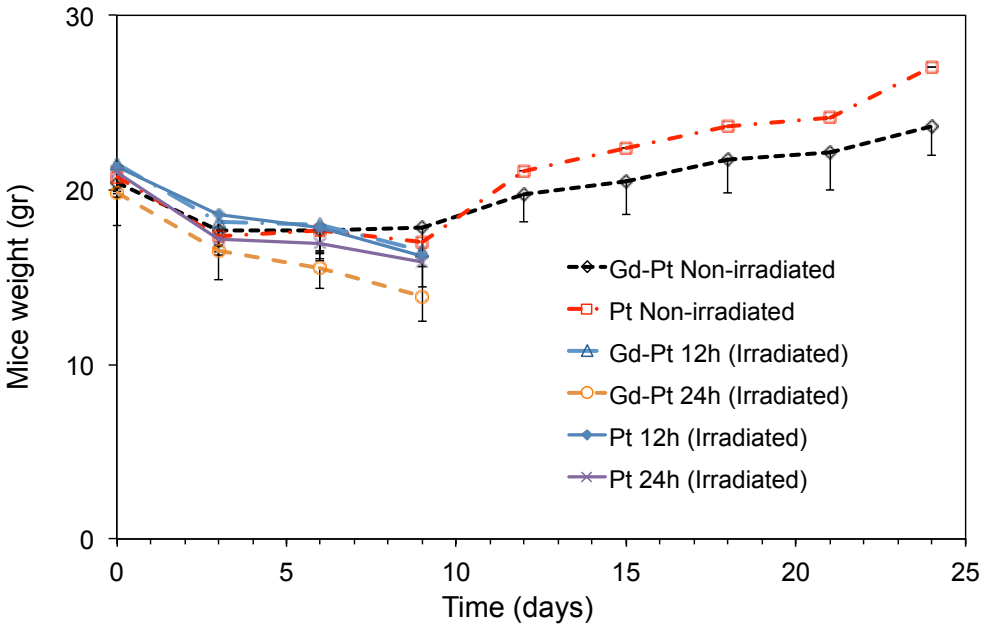

Figure 5.11: Mice weight loss after neutron irradiation for mice group injected with Gd-DTPA/DACHPt-loaded micelles and DACHPt-loaded micelles only. Data shown is average mice weight from 4-5 mice on each group with error bar indicating variance of measured data.

DNA-synthesis and repair [203]. Eventhough we could observe slight difference of tumor growth suppression compared to the non-irradiated group with significantly low gadolinium concentration, the high toxicity results suggested that the feasibility of combined radiochemotherapy for Gd-Pt nanomicelles is difficult to achieve within tolerable toxicity with current experimental setup of injected dose and neutron irradiation dose.

Chapter 6

Evaluation of Gd-DTPA/CaP nanoparticles as NCT Agent

6.1 Introduction

As continued interest on the application of nanoparticles-based drug carrier for NCT agent, in this work we carried out the feasibility evaluation of calcium phosphate (CaP) nanoparticles as Gd-DTPA delivery device for GdNCT agent.

Calcium phosphate nanoparticles have gained increasing interest in medical application because of their high biocompatibility and good biodegrability due to the fact that calcium phosphate is the inorganic mineral of human bone and teeth [204, 205], and it is also not prone to microbiological degradation like organic or polymeric carrier systems [206]. Calcium phosphate are moderately soluble at pH 7.4 and become increasingly soluble below pH 6 [207], which makes it attractive for drug delivery because CaP nanoparticles will remain intact during delivery to cells where rapid pH decrease occurs after entering endolysosome [208]. Their size can also be easily controlled by stabilizing agents such as polymers or nucleic acids [206].

Calcium phosphate-based nanoparticles can be synthesized by various methods including wet chemical routes, solid-state reactions and hydrothermal reactions at elevated temperature, biosyntetic routes, and microemulsion. The efficiency of these syntheses depends on several parameters, including calcium and phosphate ion concentrations, pH, ionic strength, temperature, and surfactant concentration and type [209]. With these advantageous characteristics of CaP nanoparticles, it is expected that we could optimize gadolinium accumulation into tumor site to achieve higher cancer cells killing effect after GdNCT treatment.

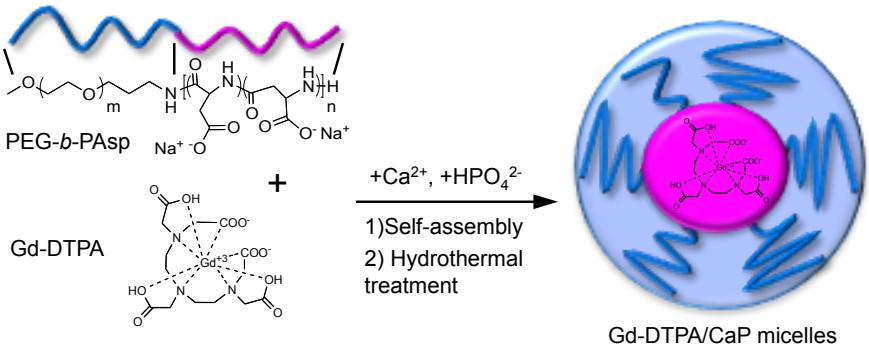

Figure 6.1: Design and synthetic procedures scheme of Gd-DTPA/CaP nanoparticles (adapted from [210]).

6.2 Materials and Methods

6.2.1 Nanomicelles Preparation and Characterization

An organic-inorganic nanoparticles of CaP core loaded with Gd-DTPA has been previously developed to enhance MRI contrast in solid tumors, where Gd-DTPA/CaP nanoparticles was prepared by mixing Gd-DTPA, PEG-b-PAsp, Ca^{2+} and $HPO_4{}^{2-}$ in buffer followed by hydrothermal synthesis at 120 Â°C for 20 min in Autoclave machine to increase Gd-DTPA/CaP nanoparticles stability in wet environments [210]. This technique has been proven to increase the colloidal stability of CaP nanoparticles in physiological condition and enhance the relaxivity of Gd-DTPA after loading in CaP nanoparticles. Preparation scheme of Gd-DTPA/CaP nanoparticles preparation is shown in Fig. 6.1.

For the characterization of Gd-DTPA/CaP nanoparticles, we performed measurement of average diameter by dynamic light scattering (DLS) using a Zetasizer Nano ZS90 (Malvern Instruments, UK), while the morphology of Gd-DTPA/CaP was confirmed using transmission electron microscope (TEM, JEM-1400, JEOL, Tokyo, Japan). To visualize the accumulation of nanoparticles in cells, we performed calcein staining during Gd-DTPA/CaP nanoparticles preparation by adding 0.1 mM calcein, and carried out purification while avoiding light. Cancer cells were seeded in 4 cm diameter dishes at a concentration of 1×10^5 cell/ml with 2 ml DMEM medium in each well. After 24 hours, the calcein labeled Gd-DTPA/CaP with the concentration of 100 μM gadolinium were added to the dishes and let to incubate for another 24 hours. The nuclei were then stained with Hoechst and evaluated with a LSM780 confocal scanning microscope (Carl Zeiss, Oberkochen, Germany).

6.2.2 Cancer cells Line and Mice Preparation

Colon carcinoma Col-26 cells used in this experiment were kindly supplied by National Cancer Center (Tokyo, Japan). The cells were maintained with DMEM supplemented with 10% fetal bovine serum and then incubated in high moisture air with 5% CO_2 at 37 C. Female BALB/c mice were obtained from Nihon SLC (Shizuoka, Japan) and used at 6-7 weeks of age. Tumor models were prepared by subcutaneous injection of 1×10^5 of Col-26 cells into right femoral of the mice. The tumor was let to grow for two weeks until the average volume reached 100 mm^3. The procedures for tumor implantation and sacrifice of the animals were carried out following the policies of the Animal Ethics Committee of the University of Tokyo.

6.2.3 Biodistribution Analysis

We performed two biodistribution experiments of *in vivo* quantitative analysis, each for single and multiple injections of Gd-DTPA/CaP nanoparticles. Intravenous injections via tail vein were performed with the dose of 1.5 mM based on Gd-DTPA. To confirm the pharmacokinetics of Gd-DTPA/CaP nanoparticles for 0.2 ml single injection, we harvested tumor, blood, and other organ samples at 12 and 24 hours following nanoparticles administration.

Three times injections of Gd-DTPA/CaP nanoparticles with 10 hours interval were then carried out in order to achieve higher gadolinium accumulation in tumor site. Tumor and blood samples were harvested at every 10 hours interval from the first injection. Samples from both experiments were analyzed using inductively coupled plasma mass spectroscopy (ICP-MS), where volume of each organ sample was measured, followed by digestion in HNO_3 left overnight, and then digested in microwave oven to ensure that all of the sample material is dissolved. The total amount of ^{157}Gd was measured using ICP-MS and the results were normalized to the tissue volume. In addition to this, previously evaluated biodistribution analysis by MRI and micro-synchrotron radiation-induced X-ray fluorescence spectrometry (μ-SR-XRF) will also be presented.

6.2.4 Neutron Irradiation

We carried out 60 minutes neutron irradiation at The Heavy Water Neutron Irradiation Facility of the Kyoto University Research Reactor (KUR-HWNIF) with OO-0000-F beam mode and 1 MW operating power. Irradiated mice were held within

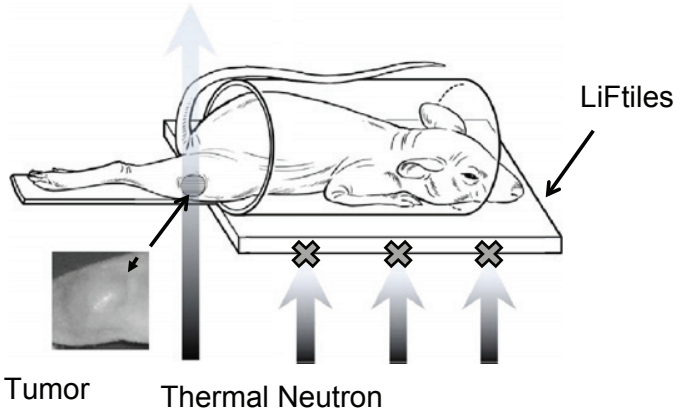

Figure 6.2: Illustration of tumor-bearing mice held in an acrylic tube prepared for neutron irradiation with subcutaneous tumor on mice leg [211].

Figure 6.3: Left: Front view of irradiation setup. Right: Backside view showing LiF shielding plate.

acrylic tube designed specifically for collimated neutron irradiation as illustrated in Fig. 6.2. Plate shielding of LiF with 5 mm thickness were placed between mice holder and neutron beam to reduce neutron irradiation into parts of mice body other than the tumor-bearing mice leg as shown in Fig. 6.3.

Neutron fluence was measured by gold foil at 2 points on the mice leg, while gamma ray dose was measured by thermoluminescent dosimeter on the same points with gold foil. For single-injected mice group, neutron irradiation was performed 24 hours following Gd-DTPA/CaP nanoparticles injection. While for the multiple-injected tumor-bearing mice, experimental procedure is described in Fig. 6.4.

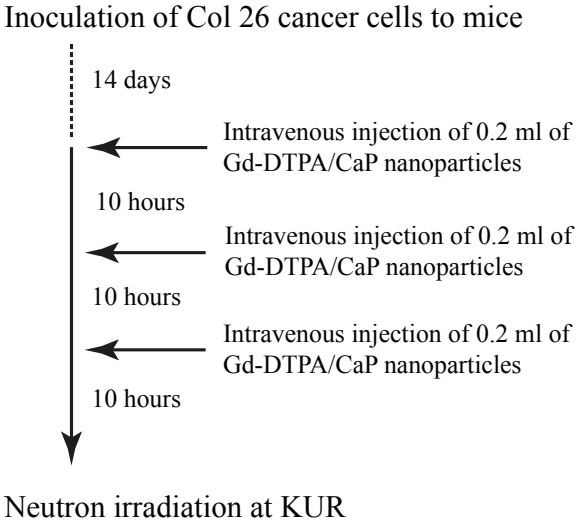

Figure 6.4: Experimental procedure for multiple injections of Gd-DTPA/CaP nanoparticles.

6.2.5 Evaluation of Antitumor Effectivity

Wit the same procedure as previous experiment, we measured mice tumor size every three days after irradiation to evaluate the antitumor activity. Tumor volume was calculated using the formula of

$$V = a \times \frac{b^2}{2} \tag{6.1}$$

, where a and b are the major and minor axes of the tumor measured by a caliper, respectively. Pathological analysis were also performed for tumor samples fixed on OCT compound and frozen at -80°C, resected on day 27th after neutron irradiation. Harvested tumor samples were sliced into 6 μm sections with a cryostat and deposited on glass slide before then stained with hematoxylin and eosin (H&E). TUNEL staining was also performed on the samples with the same slice thickness of 6 ÎŒm for evaluation of possible apoptosis occured on cancer cells by detecting the DNA fragmentation following GdNCT treatment. Negative control for both irradiated and non-irradiated groups was also prepared during the apoptotic assay.

6.3 Results and Discussions

6.3.1 Characterization of Gd-DTPA/CaP Nanoparticles

Monodispersity and spherical shape of Gd-DTPA/CaP nanoparticles were confirmed by TEM images as shown in Fig. 6.5A, with calculated volume-averaged diameter of 60 nm (Fig. 6.5B). These small size nanoparticles (<100nm) are hardly recognized by the immune system and can be easily taken up by cells. Furthermore, they are big enough to escape renal filtration, thus providing longer circulating half-life and enhanced drug accumulation in tumor tissue [212].

No agglomeration was observed from TEM images indicating the effectivity of PEGylated surface in prohibiting interaction between each of the CaP nanoparticles as previously reported [210]. Since intravenous administration of nanoparticles prone to aggregation was mentioned to result in the possibility of a pulmonary embolism, strokes, myocardial infarctions, and other microinfarctions at distant sites and organs [209], no agglomeration characteristics of Gd-DTPA/CaP nanoparticles is very advantageous in reducing the possible toxicity problems.

The surface ξ-potential value of Gd-DTPA/CaP nanoparticles is also confirmed to be around -0.5 mV, which is almost neutral and is preferable for drug delivery system. Positively charged nanoparticles are known to interact with negatively charged, phosphate-rich cell membrane and to be taken up in the reticuloendothelial system (RES) [213]. Hence, slightly negative charged or neutral carriers are more desirable to escape from the RES. Image of calcein-stained Gd-DTPA/CaP nanoparticles shown in Fig. 6.5C demonstrates accumulation of nanoparticles on the surface and inside the cancer cells, which proves the effectivity of CaP nanoparticles as carrier for Gd-DTPA. With these characteristics of Gd-DTPA/CaP nanoparticles, we could expect enhancement of gadolinium accumulation in tumor target.

6.3.2 Gadolinium Biodistribution

Gd-DTPA/CaP nanoparticles was previously proven to be capable of enhancing the MRI image contrast compared to bare Gd-DTPA as shown in Fig 6.6. Free Gd-DTPA was reported to be rapidly cleared from plasma and did not accumulate in tumor tissue, and that only trace amounts of gadolinium (nearly 0.001% dose/ml) were found in plasma 1 h after intravenous administration, while CaP nanoparticles has been previously proven to be capable of extending Gd-DTPA blood circulation time, which then increased gadolinium accumulation into tumor site [210].

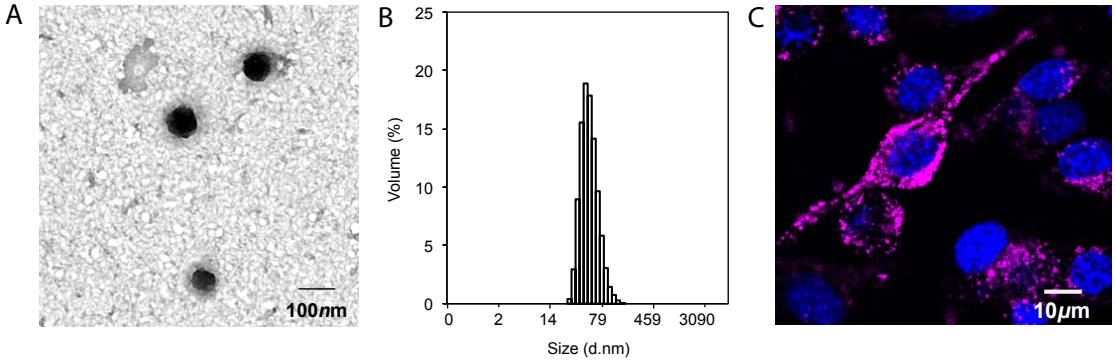

Figure 6.5: (A) TEM images of purified Gd-DTPA/CaP nanoparticles (B) Volume averaged diameter distribution calculated from TEM images. (C) Calcein-stained fluorescence images of Gd-DTPA/CaP nanoparticles accumulation on the surface and into cells.

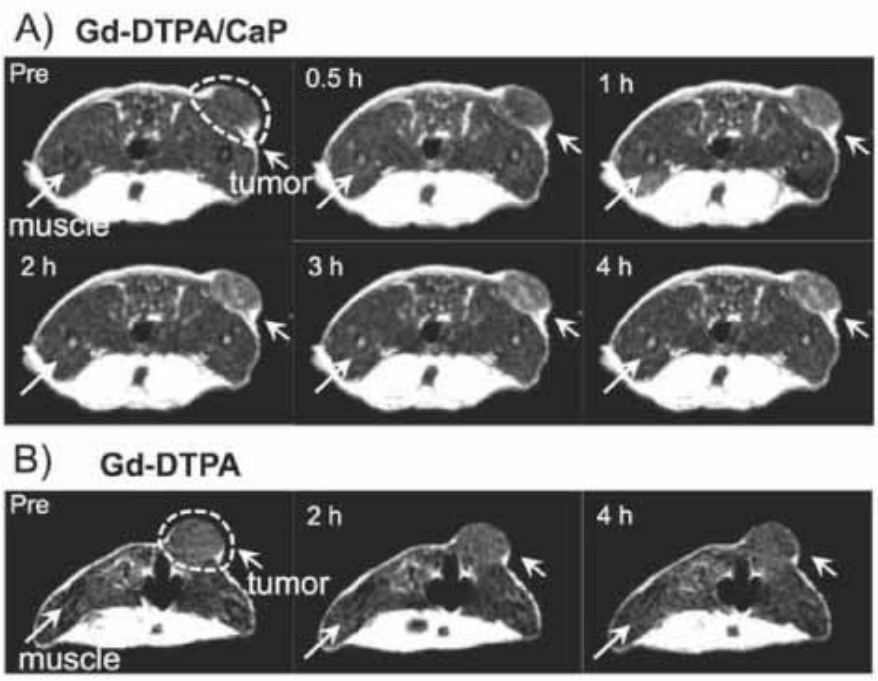

Figure 6.6: (A) MRI images of tumor-bearing mice after intravenous injection of Gd-DTPA/CaP nanoparticles (tumor site is shown by dash circle area) (B) MRI images of tumor-bearing mice after intravenous injection of bare Gd-DTPA. [210]

Table 6.1: ICP-MS measurement results of gadolinium concentration at 12 and 24 hours after Gd-DTPA/CaP nanoparticles injection. Average data is presented ± the uncertainty of ICP-MS.

	Gd concentration (μg/g or mL)	
	12 hours	24 hours
Tumor	5.85 ± 0.64	8.03 ± 0.82
Blood	14.55 ± 0.50	3.29 ± 0.40
Liver	10.71 ± 0.17	16.71 ± 0.60
Spleen	7.08 ± 0.41	10.03 ± 0.30
Kidney	2.66 ± 0.24	2.13 ± 0.06
Brain	0.16 ± 0.01	0.04 ± 0.01

Quantitative analysis from ICP-MS measurement results of gadolinium accumulation in tumor and several mice organs is shown in Table 6.1., where we could observe tumor to blood (T/B) ratio of around 2.4 at 24 hours after Gd-DTPA/CaP nanoparticles injection (Fig 6.7). This number is comparable to T/B ratio for BNCT, where the optimum ratio that could be reached is considered to be around 3-4 [90]. Small accumulation and fast clearance of gadolinium observed in brain samples is the evidence of blood brain barrier existence in normal brain because of no modification in Gd-DTPA/CaP nanoparticles for the disruption of blood brain barrier. Nevertheless, the uptake of gadolinium by liver, kidney and spleen after compound injection was still quite high, probably because of its characteristics that circulates in blood at first and then distributes into the interstitial space or is eliminated by the kidneys in the same manner with the results reported by [22] that major portion was discovered in liver and spleen as the results of predominate renal elimination. Therefore, it is necessary to ensure minimum neutron dose into organs other than tumor site to secure tolerable irradiation effect on normal tissue. However, the ratio of gadolinium concentration in tumor to those in kidney was much smaller compared to our previous result with gadoteridol-encapsulating liposome [84] (as shown in Table 6.2.), proving the effectivity of Gd-DTPA/CaP nanoparticles in escaping renal filtration with its small particle size.

Micro-distribution of Gd-DTPA/CaP in the tumors was previously reported from the analysis by using micro-synchrotron radiation-induced X-ray fluorescence spectrometry (μ-SR-XRF), which is commonly used to visualize element distribution in tumor slice. Higher intensity of Ca and Gd was found in tumor slices injected with

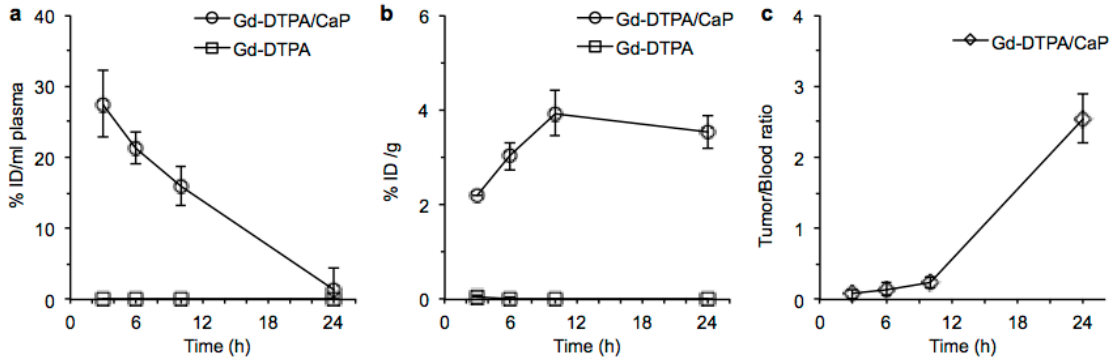

Figure 6.7: (A) Gadolinium accumulation in blood plasma. (B) Gadolinium concentration in tumor site. (C) Tumor to blood ratio of gadolinium concentration. Data shown is the average measurement with error bar indicating variance of measured data.

Table 6.2: Gadolinium concentration ratio between tumor to several mice vital organs for mice injected with Gd-DTPA/CaP nanoparticles compared to Gd-Liposome from previous work [84].

	Gd concentration ratio	
	Gd-DTPA/CaP	Gd-Liposome
Liver	1. 9	1.34
Spleen	1.13	6.18
Kidney	1.5	14

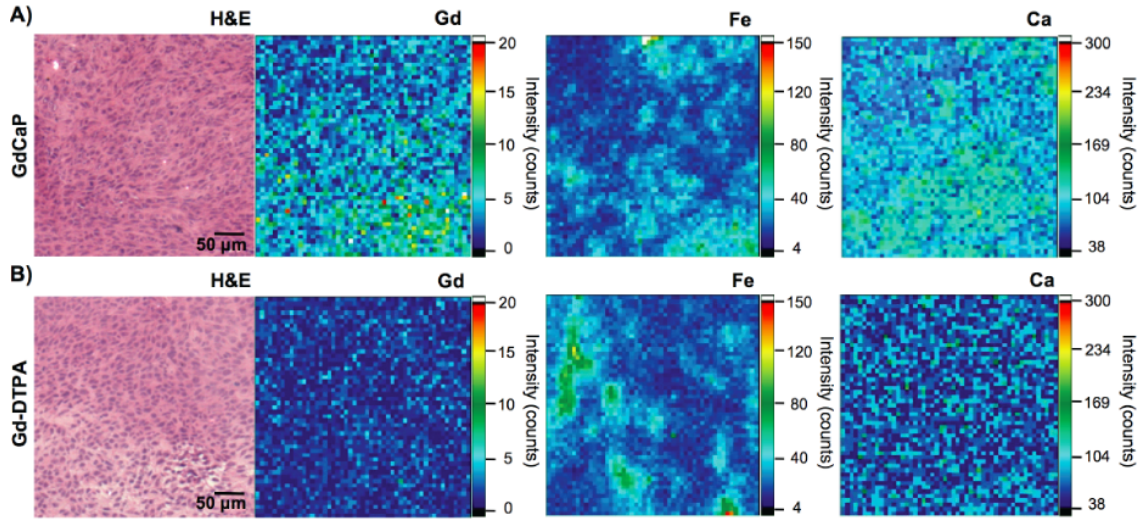

Figure 6.8: Micro-distributions of Gd-DTPA/CaP and Gd-DTPA in tumor sections scanned by μ-SR-XRF. (A)H&E staining of tumor section and Gd, Fe and Ca elements distributions in tumor slice 4 hours after intravenous injection of Gd-DTPA/CaP nanoparticles. (B) H&E staining of tumor section and Gd, Fe and Ca elements distributions in tumor slice 4 hours after intravenous injection of bare Gd-DTPA. [210]

Gd-DTPA/CaP compared to that of bare Gd-DTPA, indicating enhanced accumulation by Gd-DTPA/CaP. Moreover, the presence of the Gd and Ca atoms for Gd-DTPA/CaP was homogeneous and accumulating around and distant from the Fe-rich areas of blood vessels, suggesting effective blood circulation as well as tumor penetration of the Gd-DTPA/CaP nanoparticles as shown in Fig. 6.8 [210].

Higher gadolinium accumulation in tumor site was also successfully achieved for multiple injections of Gd-DTPA/CaP nanoparticles as shown in Fig. 6.9A, where gadolinium concentration reached the amount of more than three times higher compared to those at 10 hours after the first injection. Significant increase of gadolinium concentration in blood plasma was also observed at 30 hours after the first injection (Fig. 6.9B). This indicates the prolonged blood circulation of Gd-DTPA/CaP nanoparticles, which is important because with repeated passages of the delivery system through the tumor microvascular bed, a greater efficiency of extravasations per unit volume of the transports could be achieved.

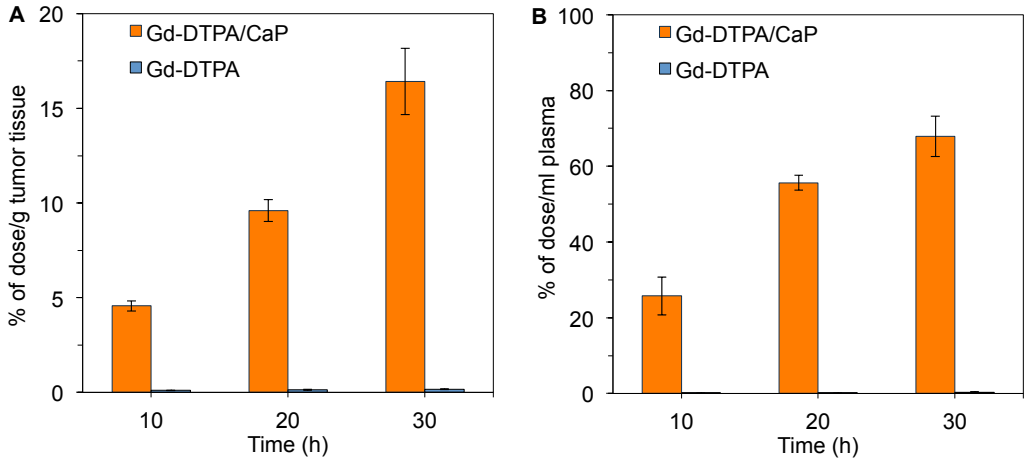

Figure 6.9: ICP-MS results for multiple injections of Gd-DTPA/CaP nanoparticles compared to bare Gd-DTPA: (A) Gadolinium concentration in tumor tissue (B) Gadolinium accumulation in blood plasma. Data shown is the average gadolinium concentration with error bar indicating the variance of measurement.

Table 6.3: Average physical dose from the measurement during neutron irradiation

	Physical dose (Gy)
Thermal neutron (∼0.5eV)	2.4×10^{-1}
Epithermal neutron (0.5eV∼10keV)	2.45×10^{-2}
Fast neutron (10keV∼)	1.8×10^{-1}
Gamma ray	4.7×10^{-1}
Total	9.1×10^{-1}
Natural gadolinium (1ppm)	2.4×10^{-3}
Gadolinium-157 (1ppm)	1.25×10^{-2}

6.3.3 Neutron Irradiation

During the 60 minutes of neutron irradiation, average neutron fluence was measured to be 1.8×10^{12} n/cm^2 for thermal neutron range and 3.2×10^{11} n/cm^2 for epithermal neutron, while physical dose from neutron and gamma ray measurement results on the surface of mice irradiation plate are shown in Table 6.3. It is defined that thermal neutron region is below 0.5 keV, the epithermal neutron region is 0.5 keV-10 keV and the fast neutron region is over 10 keV. These results are also comparable to physical dose meausured in the GdNCT experiment performed by other researchers at the same reactor facility in KUR [187].

Even though the measured physical dose for ^{157}Gd was lower compared to the dose

contribution from other components, the limitation of this value needs to be taken into account since a more pertinent equivalent dose calculation is necessary to express cancer cells killing effect after GdNCT treatment, where the Auger and Coster-Kronig electron might contribute significant biological effect in killing the cancer cells. Among GdNCR products, Auger electrons are the most biologically relevant to be comparable with high LET alpha particle and lithium ions from BNCR. They have energy range between 0 and 50 keV with an average of 4.19 keV [134], with corresponding average LET of 0.3 MeV/mm. By comparison, the average LET in BNCR is 0.2 MeV/mm for both lithium and alpha particles [4]. Contribution of Auger electrons to high-resolution neutron radiographs with gadolinium converter plate was already reported by [214], providing the evidence for the existence of Auger electrons during GdNCR.

The presence of Auger electrons after GdNCR has also been proven with the range of no more than 2.7 mg/cm2 [26]. Yasui and co-workers [87] have also reported the effectivity of gadolinium neutron capture therapy in vitro on glioblastoma multiforme cells, where they observed significant enhancement of cell killing on cells preloaded with Gd-DTPA and treated with neutron irradiation. Following observation of no necrosis with high cancer cells killing effectivity after GdNCT was reported in their experiment compared to other mice group treated with gamma, fast neutrons, and modified enhanced thermal neutron beam [88]. They mentioned the discovery of extreme autophagy in GdNCT treated group might provide the clues in understanding how Auger electron irradiation kills the cancer cells. These short-range products may enhance the therapeutic effects of gadolinium neutron capture therapy (GdNCT) and are expected to deliver high cell killing effect when incorporated into DNA [215], and with proper techniques, GdNCT might be made competitive to BNCT.

6.3.4 Evaluation of Antitumor Effectivity

In this experiment, we performed neutron irradiation on single-injected and multiple-injected nanoparticles to compare the cancer cells killing effectivity after GdNCT treatment. Effectivity of tumor growth suppression after NCT treatment for single injection group is shown in Fig 6.10. It is evident that the tumor growth of GdNCT treated group was suppressed more than three times higher compared to the non-treated group, suggesting the effectivity of GdNCT treatment. Morphological results shown in Fig 6.11 also reveals suppressed tumor volume on Gd-DTPA/CaP injected irradiated group compared to the non-irradiated and non-treated group.

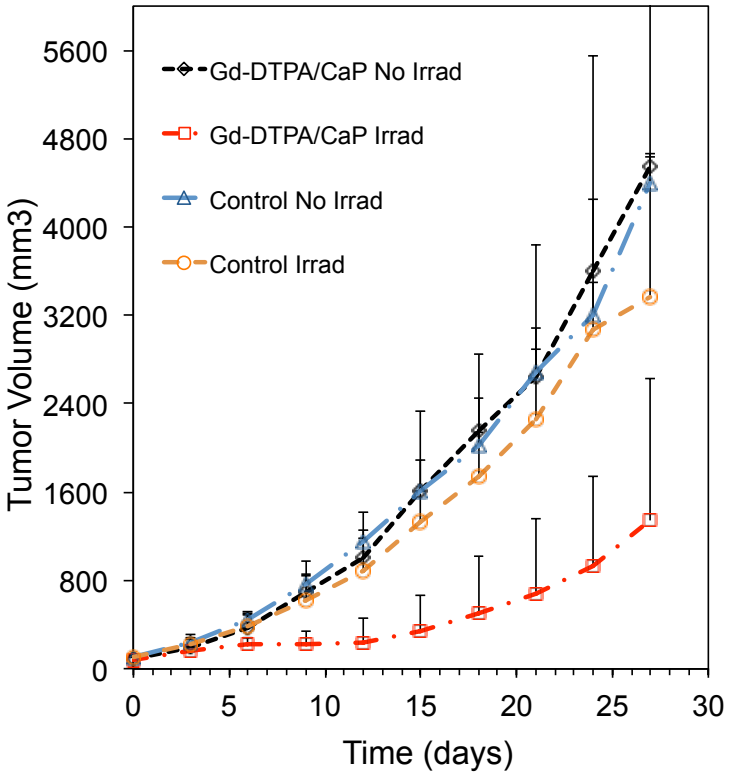

Figure 6.10: Tumor growth suppression after neutron irradiation for single-injected Gd-DTPA/CaP nanoparticles compared to non-injected group. Data shown is average tumor volume growth from 4-5 mice on each group with error bar indicating variance of measurement.

Figure 6.11: Representation of tumor-bearing mice showing the comparison of morphological observation between irradiated and non-irradiated on single injection for both Gd-DTPA/CaP nanoparticles and bare Gd-DTPA.

Tumor volume growth by time for multiple-injected group is shown in Fig 6.12, where we could observe that Gd-DTPA/CaP irradiated group revealed up to more than four times tumor growth suppression compared to non-treated group. However, the multiple-injected mice group did not reveal better tumor growth suppression even though gadolinium concentration accumulated in tumor site is much higher compared to the single-injected mice group as shown previously in Fig 6.10. There is a possibility that neutron depression occurred in this group where neutron were being absorbed and could not reach deeper site of the tumor, which might reduce the effectivity of cancer cells killing. Nevertheless, we could still observe tumor growth suppression after neutron irradiation, which suggests the possibility of cancer cells killing from secondary particles of GdNCR. No significant weight loss was observed after neutron irradiation and all mice survived until the end of observation, suggesting low toxicity of Gd-DTPA/CaP nanoparticles for GdNCT (Fig 6.13).

The low toxicity of Gd-DTPA/CaP nanoparticles is also supported by the results shown in Fig 6.14, where we observed mice dead in the group with multiple injections of bare Gd-DTPA, both fpor non-irradiated and non-irradiated group. This result indicates that the dose for three times injection of Gd-DTPA might already surpass the tolerable dose of gadolinium toxicity for tumor-bearing mice. However, encapsulating Gd-DTPA into calcium phosphate-based nanoparticles as carried out in current experiment, has lower the toxicity effect.

The therapeutic effects of GdNCT were also observed from pathological analysis results of tumor cells as shown by H&E staining results in Fig 6.15. Nucleus and cytoplasm of tumor cells treated with Gd-DTPA/CaP nanoparticles were destroyed after GdNCT treatment (cells inside the dash area), while the non-irradiated group showed normal histology with survived nuclei and abundant cytoplasm, demonstrating the characteristics of proliferative tumor cells. Similar H&E result was observed between single-injected and multiple-injected group, which agrees with the results from tumor growth suppression effect. This is also supported by TUNEL assay shown in Fig 6.16, where the number of cells undergoing stained by TUNEL, which correlates to the number of apoptosis, was higher on GdNCT treated group compared to the non-irradiated ones.

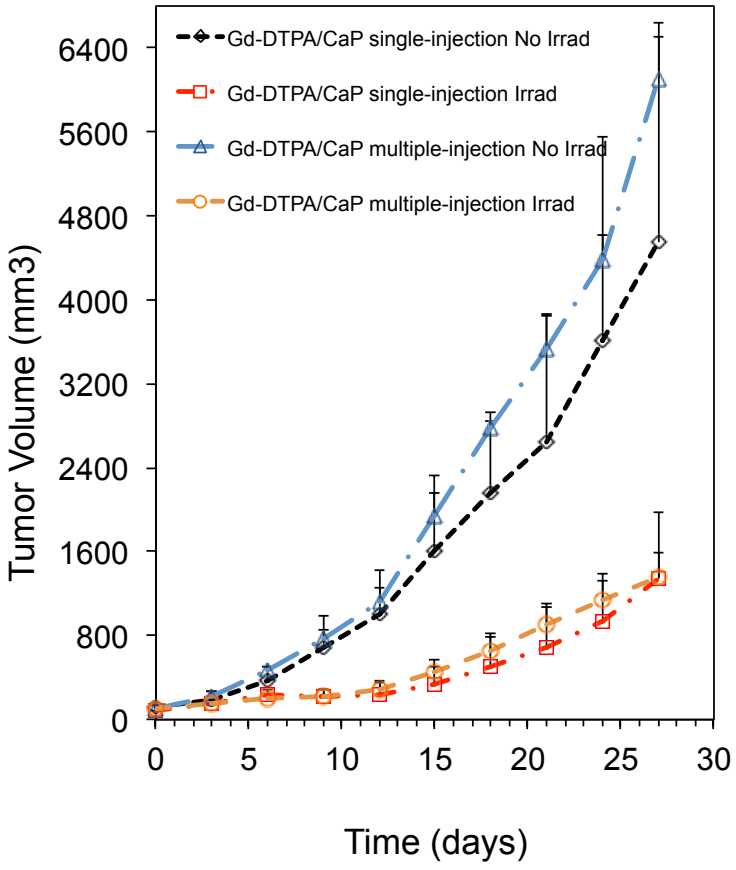

Figure 6.12: Tumor growth suppression for multiple-injected Gd-DTPA/CaP nanoparticles compared to single-injected mice for both irradiated and non-irradiated group. Data shown is average tumor volume growth from 4-5 mice on each group with error bar indicating variance of measured tumor volume.

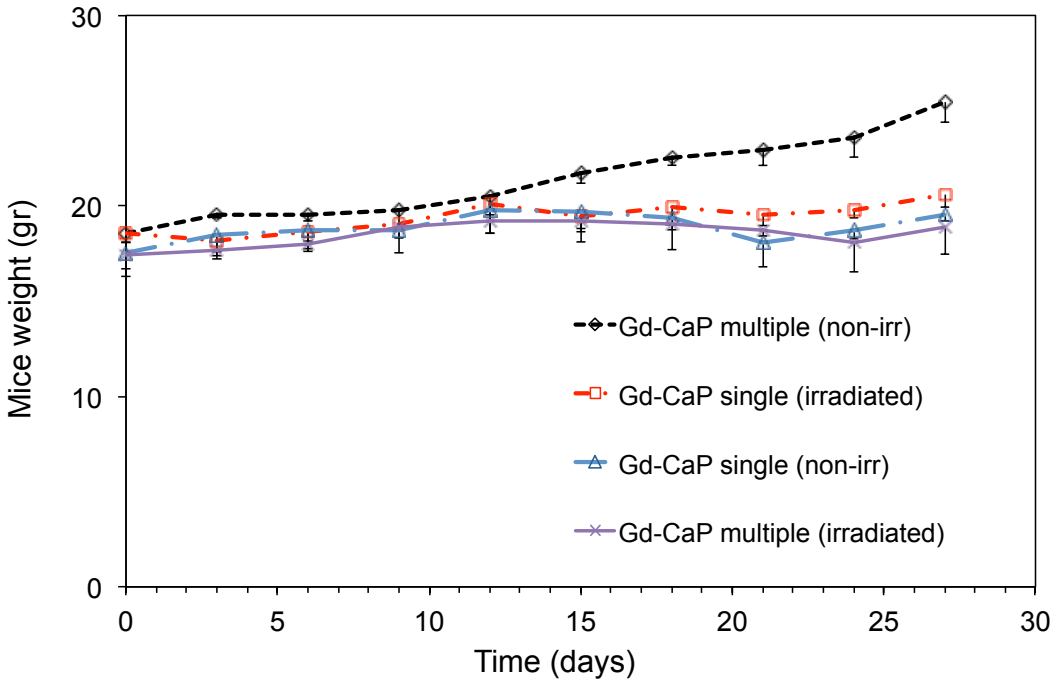

Figure 6.13: Graph of mice weight loss for single and multiple injections of Gd-DTPA/CaP nanoparticles after neutron irradiation compared to the non-irradiated group. Data shown is average mice weight from 4-5 mice on each group with error bar indicating variance of measured data.

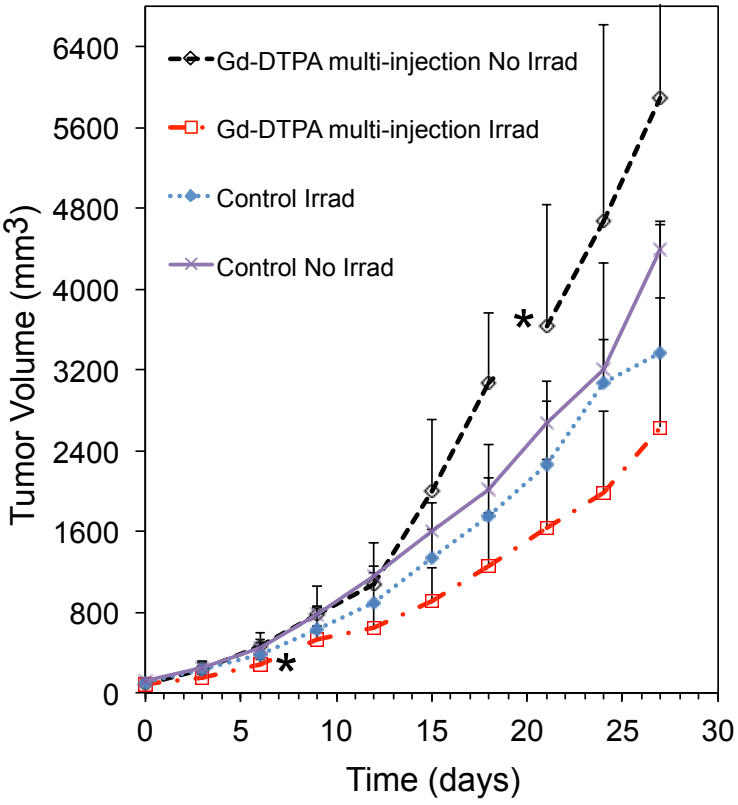

Figure 6.14: Comparison of tumor growth suppression between multiple injections of bare Gd-DTPA to control (non-injected) group. (*) mark indicates mice dead observed on multiple injected mice on both irradiated and non-irradiated group. Data shown is average tumor volume growth from 4-5 mice on each group with error bar indicating variance of measurement.

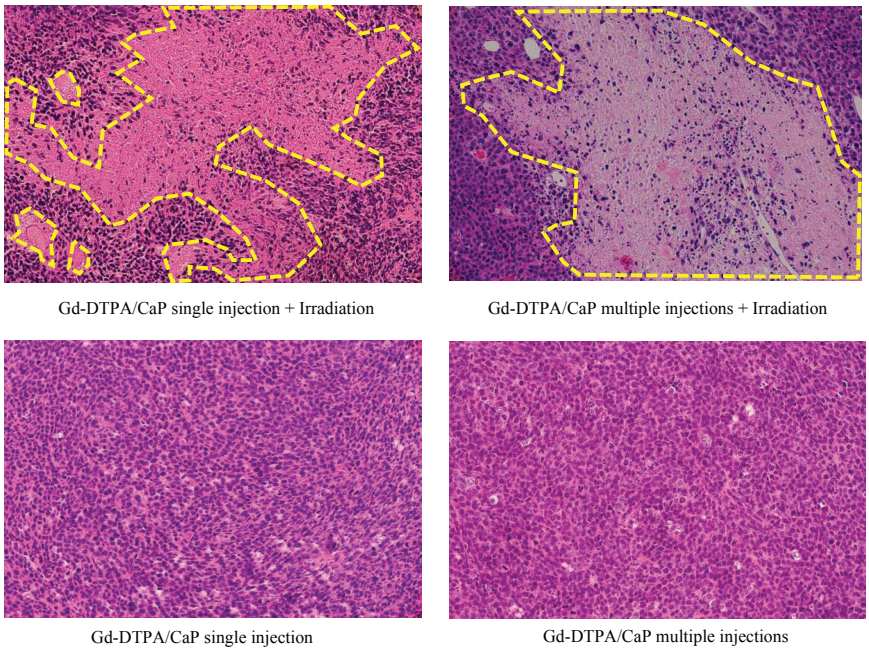

Figure 6.15: Comparison of H&E staining results for single injection and multiple injections of Gd-DTPA/CaP nanoparticles, both for irradiated and non-irradiated mouse.

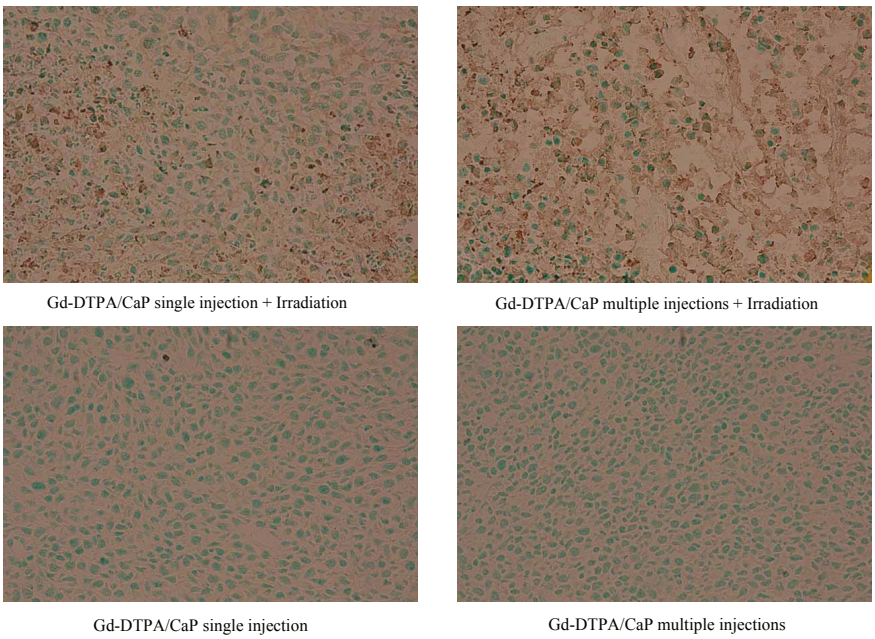

Figure 6.16: Comparison of TUNEL staining results for single injection and multiple injections of Gd-DTPA/CaP nanoparticles, both for irradiated and non-irradiated mouse.

Chapter 7

Preliminary Dosimetry of BNCT and GdNCT

7.1 Introduction

NCT is simple in theory but in reality demands a high technical quality of the involved dose contributing components. The physical parameters involved are well known but interact in a rather complex way. One factor that is necessary to consider is the production and delivery of the applied external neutron field. Thermal neutrons cannot be used directly to irradiate deeply sited target volumes since they are strongly attenuated in the tissue and more appropriate for surface tumor. Due to their better penetration, epithermal neutrons have instead been employed for neutron source in NCT as previously discussed in the neutron source subsection.

Energy release resulting from interactions of neutrons with the nuclei of a substance is usually divided into local energy release from neutron reactions, and energy release from absorption of secondary photons originating as a result of these reactions. Therefore, calculation of the absorbed dose in a target organ is determined by the sum of the doses of neutrons and secondary gamma, and the dose of primary photons of the beam [133]. Optimization of the treatment required calculation of the dose distribution at various parameter combinations to maximize the radiation dose to the target volume, while keeping the dose to normal tissues within the limits prescribed in the protocol.

As described formerly in Chapter 2, dosimetry and treatment planning system for NCT has been through extensive development especially on integrated system between NCT agent detection and dosimetry calculation for an optimized treatment

planning system. Monte Carlo method is said to be the most accurate and rigorous absorbed dose calculation method to simulate radiation transport and scoring energy deposition in heterogeneous systems such as the human body. The Monte Carlo method can accurately account for variations in density and atomic number and can handle complex geometry [216].

7.2 Materials and Methods

7.2.1 Particle and Heavy Ion Transport code System (PHITS)

We carried out dose calculation by using Particle and Heavy-Ion Transport code System (PHITS), which is a multi-purpose particle Monte Carlo transport code that has been developed under the collaboration of JAEA (Japan Atomic Energy Agency), RIST (Research Organization for Information Science and Technology), KEK (High Energy Accelerator Research Organization) and Chalmers University of Technology. PHITS is a multi-purpose particle Monte Carlo transport code, which can deal with the transport of all particles (*nucleons, nuclei, mesons, photons, and electrons*) over wide energy ranges, using several nuclear reaction models and nuclear data libraries. Various quantities such as heat deposition, track length and production yields can be deduced from the simulation, using implemented estimator functions called ”tally”. The code also has a function to draw 2D and 3D figures of the calculated results as well as the setup geometries, using a code ANGEL. Because of these features, PHITS has been widely used for various purposes such as designs of accelerator shielding, radiation therapy and space exploration [217].

In PHITS, neutrons can be transported from thermal energies up to 200 GeV. Below 20 MeV down to 0.1 meV, neutrons are described in the same manner as in the MCNP4C code based on the Evaluated Nuclear Data such as the ENDF-B/VI, JENDL-3.3, and LA150 libraries. For charged particles except for nuclei below 1 MeV, only the ionization process is considered until the charged particles are stopped. PHITS also uses Evaluated Nuclear Data for photon and electron transport in the same manner as in the MCNP4C code based on ITS version 3.0 code. The energy range of electron and photon was restricted to the energy region 1 keV - 1 GeV, but the extension of the maximum energy of these particles has been done recently by including the EGS5 code [218].

PHITS provides a variety of tallies, which score track length, flux and current of crossing surface, produced particle and residual nucleus at the collision, average

heat and distribution of deposit energy, star density, and DPA (displacements per atom). These quantities can be tallied in a cell defined by the geometry and also by the super-imposed r-z and xyz scoring meshes [218]. PHITS is also mentioned to be capable of generating multiple particles in source definition concurrently, though MCNP generates only one particle. Thus, we can make a proper beam source including both neutrons and photons at the patient position; then doses involving primary core gamma-ray dose can be evaluated effectively [219].

For the dose calculation, we used [T-Heat] tally feature in PHITS, which is mentioned to give deposit energy for optional region and deposit energy by low energy neutron, photon, and electron. By using this tally, the heat from neutrons and photons are usually obtained from Kerma factor with nuclear data. Simulation of dose distribution in this study was performed as an early stage of investigating dose contribution from various ionizing radiations including: neutron beam from nuclear reactor, gamma contamination of the neutron beam, and contribution from secondary particle produced after neutron capture reaction.

7.2.2 Simple Mouse Phantom

In this study, we designed a simple mouse phantom and performed dose calculation of neutron and gamma beam separately from the secondary particle produced after neutron capture reaction. The phantom was relatively simplistic and only consider several vital organs in which we have measured the accumulation of gadolinium during previous *in vivo* experiment and boron concentration was chosen as the minimum amount based on several clinical reports. Extreme boron and gadolinium concentration of 1000 ppm was also considered in the calculation to evaluate the possibility of neutron depression, even though it might be difficult to achieve in real application.

Geometry of the mouse phantom is shown in Fig. 7.1. Each identified organ, tissue, or structure in the phantom was assigned a tissue composition, taken from their human counterparts published in ICRU Report 46 (ICRU 46). The bulk of the remainder of the mouse was described as adipose tissue. Table 7.1 shows all of mice organs considered in current study along with their tissue compositions.

7.2.3 Cylindrical Phantom

We also performed calculation of heat deposition on a cylindrical phantom with radius of 10 cm and height 10 cm divided into 10 identical cells. Neutron beam was set to be incident directly to the cylindrical phantom's surface perpendicular to the cylinder's

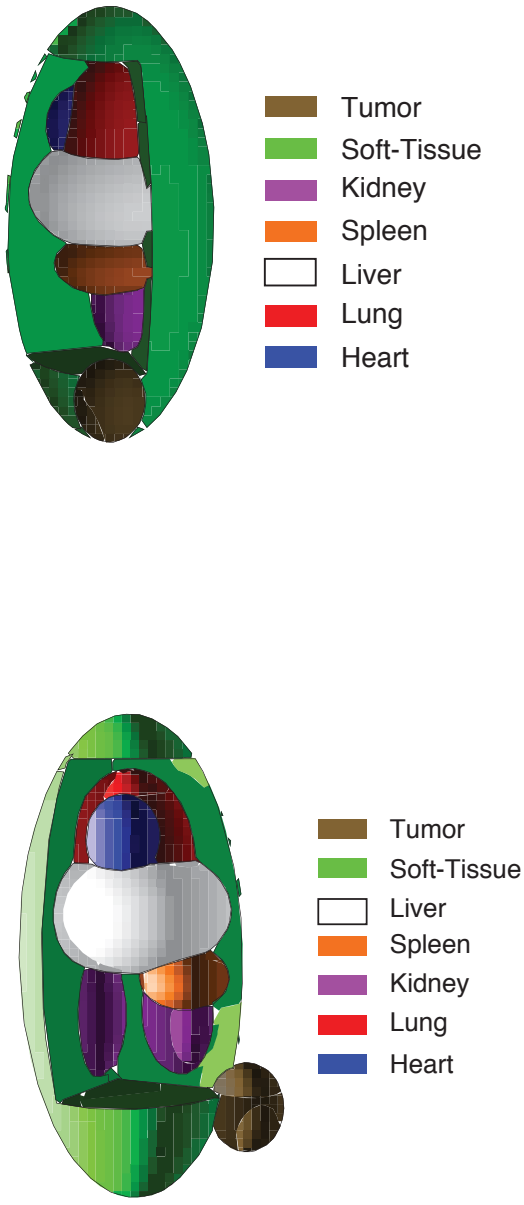

Figure 7.1: Simple geometry of mouse phantom constructed using PHITS.

Table 7.1: List of organs and tissue composition designation

Structure name	Composition designation
Lungs	ICRU 46 Lung Adult (healthy) inflated
Heart	ICRU 46 Heart Adult (healthy)
Kidney	ICRU 46 Kidney Adult
Liver	ICRU 46 Liver Adult (healthy)
Spleen	ICRU 46 Spleen Adult
Tumor	ICRU 46 GI tract Adult
Bulk of the remainder	ICRU 46 Adipose Tissue

base. Colon tissue material is assigned for the phantom by taking into account that the cancer cells in previous experiment is colon-26 cell line.

The main objective of the calculation with this cylindrical phantom is to evaluate the tendency of dose deposition by depth from neutron beam as well as the possibility of neutron depression effect when boron and gadolinium concentration is significantly higher compared to those commonly achieved for clinical trial or *in vivo* experiment. Calculation of heat deposition for comparison as well as investigation of possible combined effect between boron and gadolinium was also performed with various concentration from 20 ppm, 40 ppm and 1000 ppm compared to the heat deposition when the cylinder is filled with equally 40 ppm of boron combined with gadolinium.

7.2.4 Calculation Setup

Dose calculation performed in this study is still a preliminary investigation of NCT dose deposition with the experiment conditions for collimated neutron irradiation described in Chapter 5 and 6. This preliminary dose calculation was aimed to analyze dose deposition for collimated neutron irradiation in HWNIF of KURRI. In our experiment, neutron irradiation was carried out with OO-0000-F operation mode, a mixed neutron beam where the major neutron energy range is thermal neutron followed by epithermal and fast neutron. This operation mode is commonly used for clinical trials in treating patients and animal experiment at KUR.

Not all the geometry condition will be included in the calculation parameter since the spectrum of neutron and gamma from the nuclear reactor (as described in Chapter 4) obtained was already described as calculated from the exit of the irradiation window. The source was mentioned to be a mono-directional disc source with the radius of 12.5 cm with the energy spectrum for each neutron and photon as described

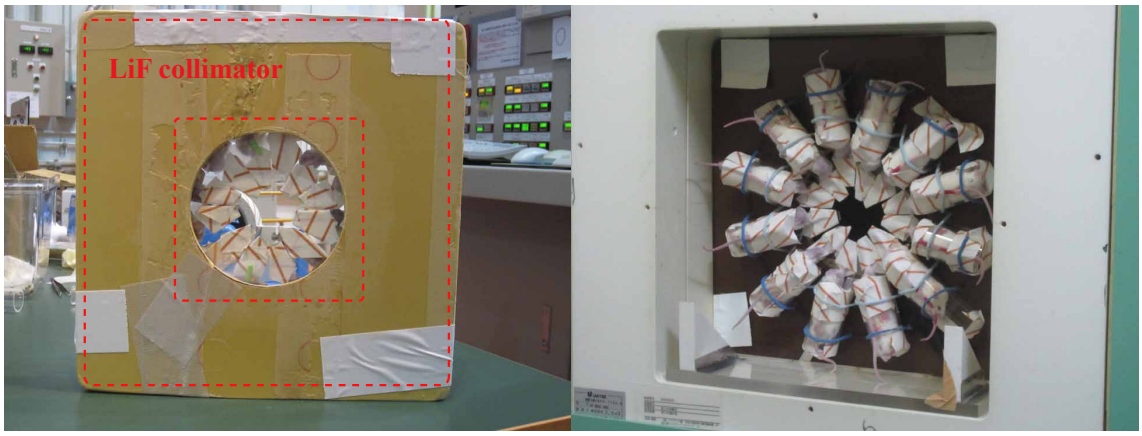

Figure 7.2: LiF shielding set-up for collimated neutron irradiation experiment.

in Chapter 4. Shielding plate made of LiF was designed to shield neutron irradiation from exposing other organs of tumor-bearing mice. Referring to the experimental set-up given in Fig. 7.2, we constructed PHITS geometry input for the LiF collimator with a circle opening in front of the tumor site as shown in Fig. 7.3.

7.3 Results and Discussions

7.3.1 Simple Mouse Phantom

Dose calculation result of deposited heat from PHITS calculation is given in Fig. 7.4. By looking at the dose distribution in mouse organs for both boron and gadolinium, we could observe higher heat deposition in tumor site on GdNCT compared to those in BNCT, possibly coming from the higher neutron cross section of gadolinium, which produces higher number of neutron capture reaction. The high heat deposition observed on LiF shielding proves its neutron absorbing effect with the largest volume compared to other cells in the calculation.

Heat deposition on tumor site for both BNCT and GdNCT is also shown to be higher compared to other mice organs indicating the effect of neutron capture reaction by such neutron absorber compound considering that the percentage of boron or gadolinium in tumor is much lower compared to the other elements composing the other organs. Similar shape was also observed on the heat deposition into other mice organs (excluding LiF shield and tumor site) for both calculation on boron and gadolinium when compared between those containing 40 ppm and 1000 ppm.

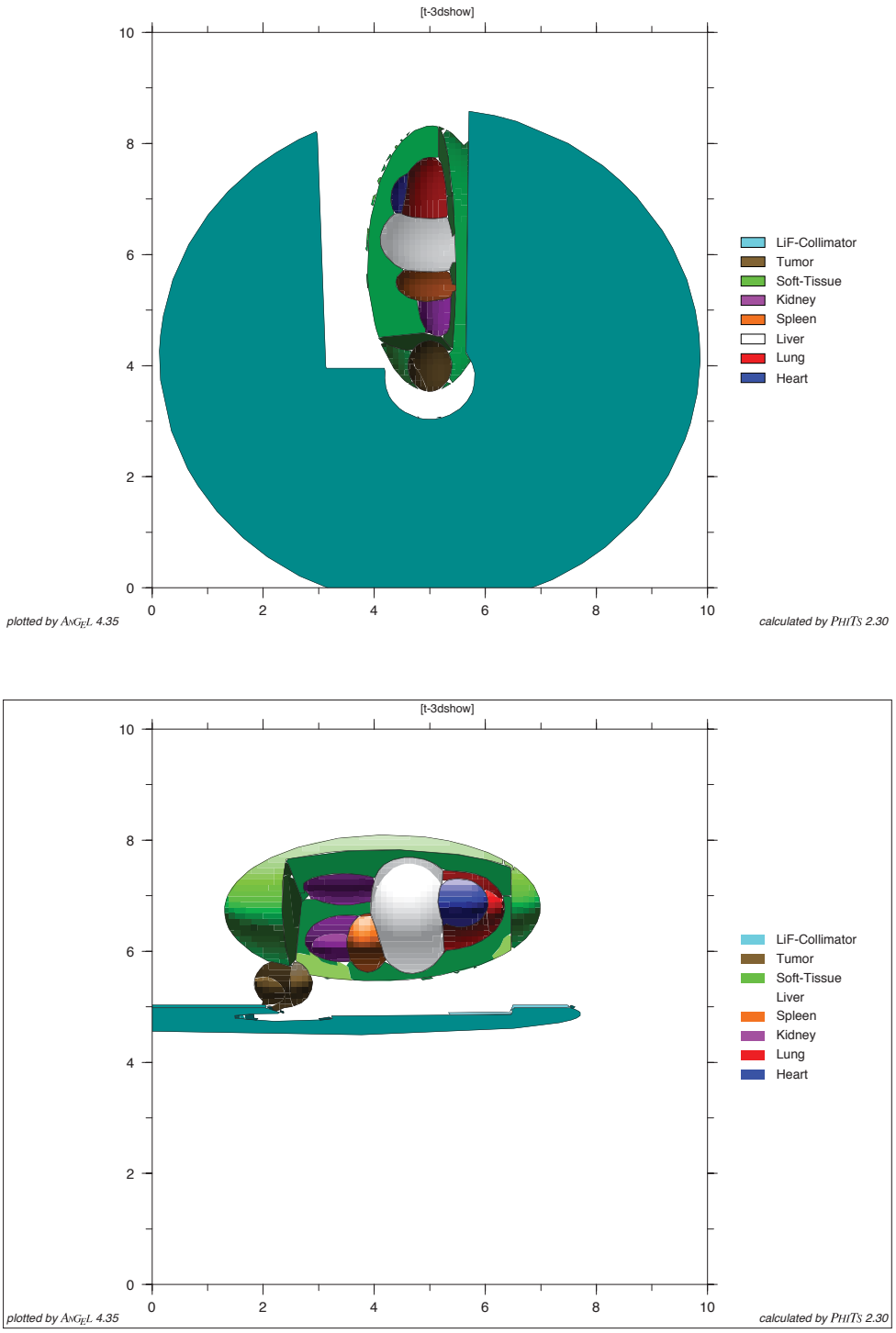

Figure 7.3: Simple geometry of mouse phantom constructed by using PHITS code. For the upper image, neutron source from the reactor is coming towards the paper direction, as for the lower image, neutron source is coming upward toward the phantom from the horizontal axis.

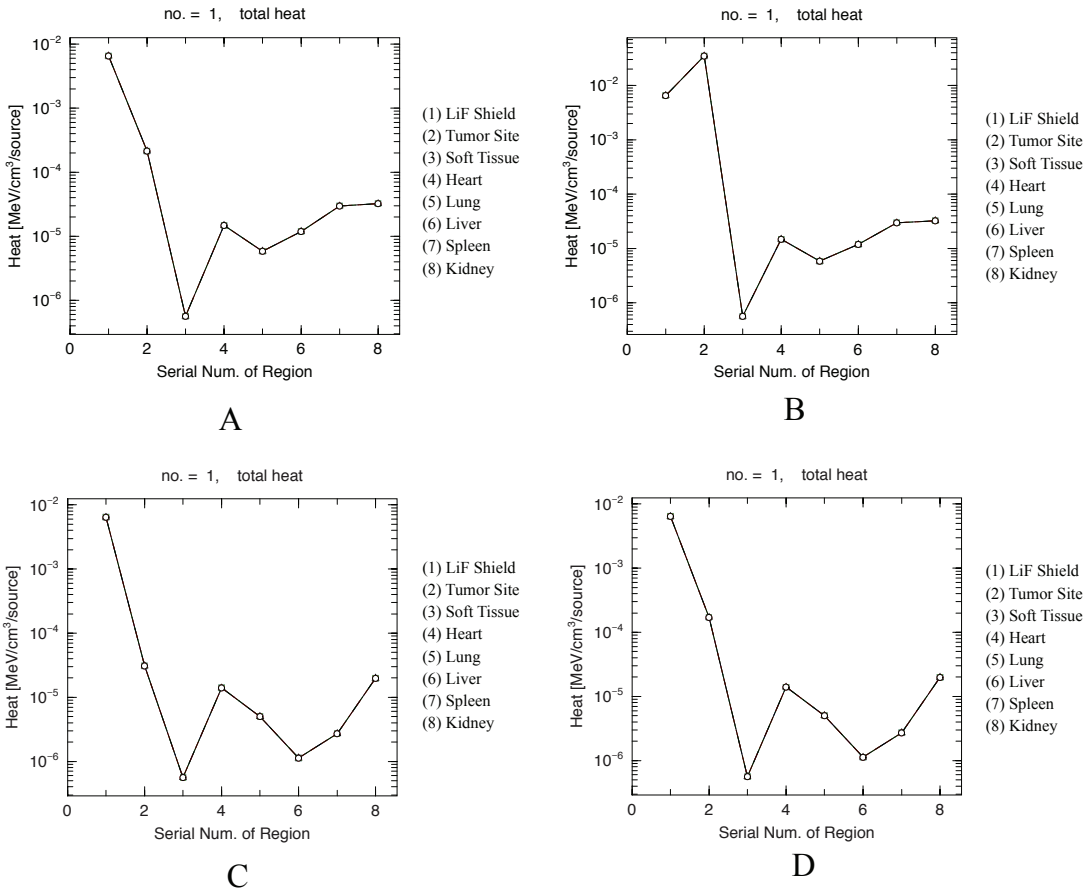

Figure 7.4: Calculated heat deposition for each region of mice organ including the LiF shielding for: (A) Boron concentration of 1000 ppm, (B) Gadolinium concentration of 1000 ppm, (C) Boron concentration of 40 ppm, (D) Gadolinium concentration of 40 ppm.

7.3.2 Cylindrical Phantom

The results of calculated neutron flux for cylindrical phantom with gadolinium concentration of 1000 ppm is given in Fig. 7.5, where we can see that it was reduced siginificantly after the second cell on the depth of 2 cm from the cylinder's surface. There could be a possibility of higher neutron depression for gadolinium from the observation of its higher decrease rate in heat deposition for both concentration being considered in the calculation as shown in n Fig. 7.6, even though the ratio is not linear compared to its ratio of neutron cross section when compared to boron.

Heat deposition tendency of boron are both similar for the concentration of 40 ppm and 1000 ppm, while it was decreased siginificantly on the second cell (2 cm depth from the cylinder's surface) for the 1000 concentration of gadolinium, suggesting the possibility of neutron depression effect, which might be caused by higher neutron cross section of gadolinium. Even though gadolinium neutron cross section is more than 60 times higher compared to boron-10 isotope, heat deposition on gadolinium was observed to be around 3 times higher compared to those deposited on the heat calculation with boron. This is comparable with the calculation previously reported by Goorley [77], in consideration that with the higher mass number of gadolinium, the same concentration of both compound translate into lower number of atom of gadolinium compared to boron.

However, it is necessary to point out that the ratio of heat deposition between gadolinium and boron from the calculation results results was observed to be increasing at the depth of 8 cm forward from the cylinder surface, suggesting the possibility of superior cells killing effect of gadolinium for deeper tumor site considering that its neutron cross section at are higher on higher neutron energy range as well compared to boron. This characteristics would also be advantageous for accelerator-based neutron source where the produced neutron spectrum are usually harder compared to those from nuclear reactor. Nevertheless, we can not come into conclusion yet before performing further advanced calculation especially the necessary to perform microdosimetry of dose deposition from very short range secondary particles such as Auger and Coster-Kronig electrons produced after GdNCR.

7.3.3 Evaluation on Possible Combined Effect of BNCT and GdNCT

To evaluate the possibility of combining boron and gadolinium as NCT agent, we performed calculation of heat deposition with various concentration from 20 ppm,

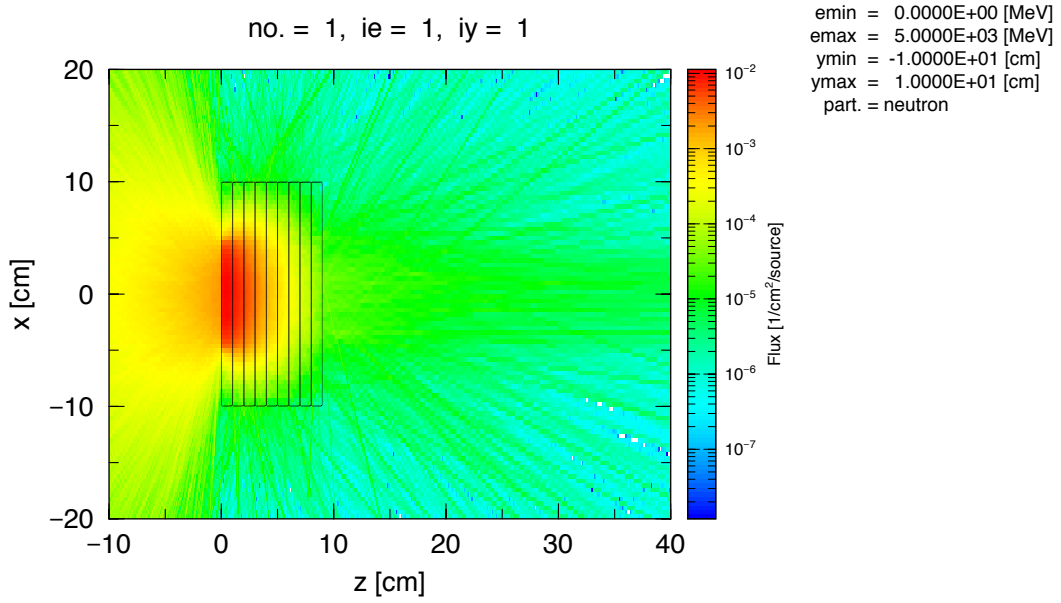

Figure 7.5: Calculated neutron flux for cylindrical phantom with gadolinium concentration of 1000 ppm.

40 ppm and 1000 ppm compared to the heat deposition when the cylinder is filled with equally 40 ppm of boron and gadolinium. From the results shown in Fig. 7.7, we can see that higher additional effect was achieved on the combination of 40 ppm boron with 1000 gadolinium, compared to the 40 ppm of gadolinium and 1000 boron. However, the calculation results in this study are still a preliminary investigation intended for further calculation. The heat deposition was calculated for total ionization effect of all secondary particles after neutron capture reaction and did not present the contribution from each ionizing radiation.

However, the depression effect on the second cell of cylinder was observed on 1000 ppm of gadolinium, indicating that combination with higher boron concentration could be a better choice for the treatment of surface tumor. Nevertheless, the ratio of 40 ppm boron + 1000 ppm Gd to the 40 ppm gadolinium + 1000 ppm boron, is increasing up to 3 times higher from 8th cell onward, indicating that combination with higher boron concentration might be preferable to treat deep-seated tumor. This result might come from the contribution of deeper penetration of epithermal neutron in the neutron beam which was still captured by gadolinium with its high neutron cross section, not only on the thermal neutron energy range.

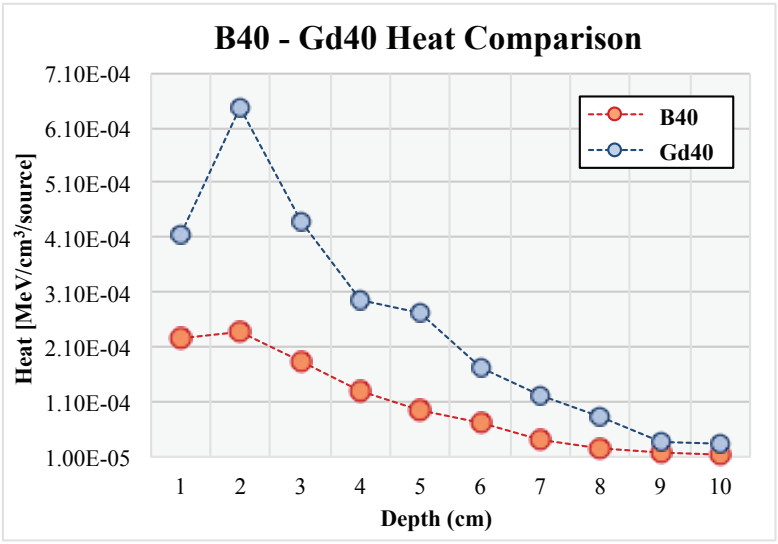

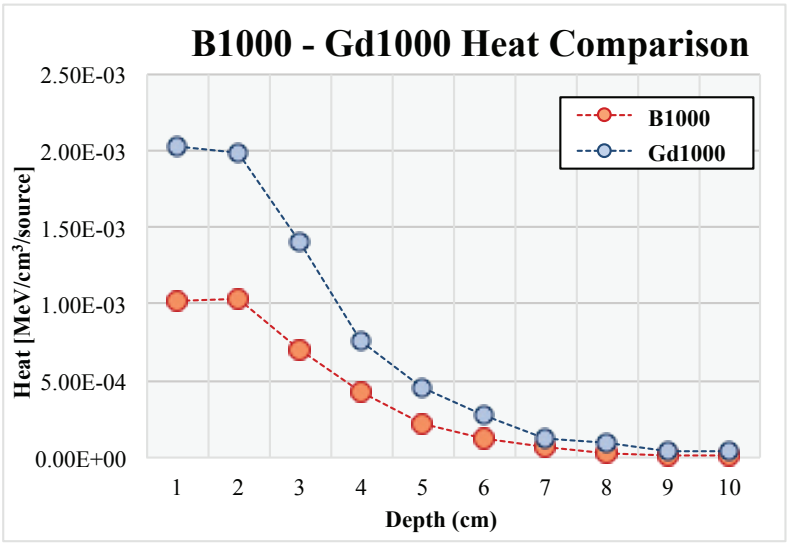

Figure 7.6: Comparison of heat deposition for 40 ppm and 1000 ppm concentration of each boron and gadolinium

On top of that, dose contribution of GdNCR short-range products such as Auger electron emission has often been neglected because it was assumed that Gd compounds remained extracellular and could not reach the cell nucleus. However, De Stasio et al., [76] has shown that Gd-DTPA not only penetrates the plasma membrane of the cells but accumulates at higher concentration in the nucleus than in the cytoplasm. Therefore, it is recommended to take into account as well the dose contribution from Auger and internal conversion electrons in the calculation for future investigation.

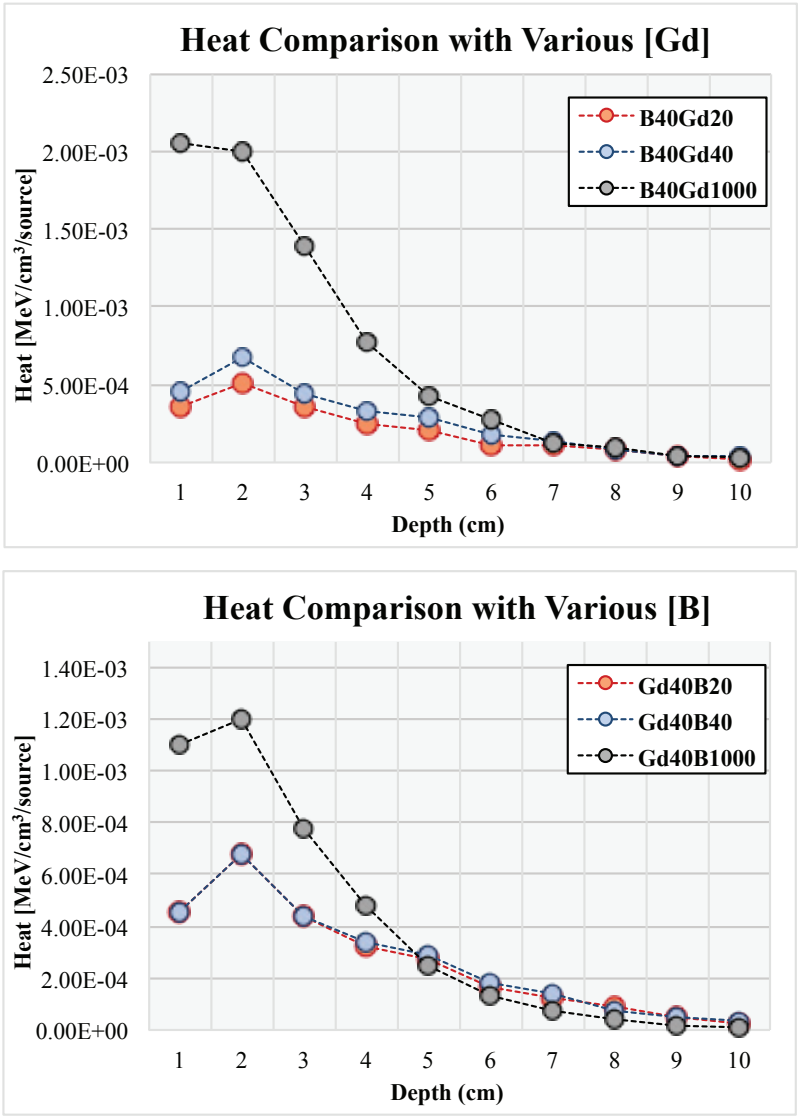

Figure 7.7: Comparison of heat deposition for 40 ppm and 1000 ppm concentration of each boron and gadolinium

Chapter 8

Closing Remarks

This thesis has considered two types of gadolinium-based drug compounds to be evaluated as GdNCT agent by performing *in vivo* experiment on colon-26-bearing-mice, irradiated by neutron source at HWNIF of KURRI in Kumatori, Osaka. Dose calculation has also been performed as an independent approach to investigate heat deposition from dose contributing elements of nuclear reactor beam along with the secondary particle produced after neutron capture reaction for both GdNCT as well as BNCT.

8.1 General Conclusion

In Chapter 5 we have presented the results of *in vivo* experiment as continued evaluation of Gd-DTPA/DACHPt-loaded nanomicelles for NCT agent. We have shown that gadolinium accumulation is more effective compared to bare Gd-DTPA from the observation of MRI contrast enhancement and ICP-MS measurement. Previous experiment at KURRI with neutron collimator, various neutron fluences, including neutron-shielded condition, still showed quite high toxicity of gadolinium-platinum nanomicelles on irradiated tumor-bearing mice. On this experiment with various neutron fluences, we observed significant prolongation of survival rate for Gd-DTPA/DACHPt-loaded nanomicelles-injected group irradiated for 17.5 minutes (1×10^{12} n/cm^2 neutron fluence). Even though only 60% survived until 27 days after neutron irradiation, this result shown that irradiation time affect deposited dose quite significantly into mouse organs that might cause mouse death.

Continued experiment of neutron irradiation on mice injected with Gd-DTPA/DACHPt-loaded micelles and DACHPt micelles only, have revealed that even with current experimental procedure, high toxicity was still observed on all irradiated mice for

both group. We have performed neutron irradiation on 12 hours and 24 hours after compound injection considering different platinum amount in blood plasma at those times. However, we still observed severe toxicity, which caused death to all irradiated mice of both Gd-DTPA/DACHPt-loaded micelles and DACHPt micelles only injected group. Our speculation is that there is a possibility of platinum photoactivation, caused by reaction between secondary particles produced after GdNCR such as gamma rays and characteristics X-ray with energy above K-edge energy of platinum, which might increase drug toxicity and induced ionizing radiation at vital organs. Moreover, as the nanomicelles compound bind gadolinium and platinum together very close, the possibility of secondary reaction to occur is higher since the effective solid angle is very large. Even though we could observe tumor growth suppression compared to the non-irradiated group, the high toxicity results suggested that the feasibility of combined radiochemotherapy for Gd-Pt nanomicelles is difficult to achieve within tolerable toxicity with current experimental setup of injected dose and neutron irradiation dose.

In Chapter 6, we have shown that Gd-DTPA/CaP nanoparticles significantly enhanced gadolinium accumulation compared to those of free Gd-DTPA proven from the results of previously reported MRI image along with the ICP-MS measurement, where the gadolinium concentration in tumor site is significantly higher for Gd-DTPA/CaP nanoparticles. Several experimental setups were performed for mice group injected with this compound and the results have demonstrated the possible effectivity of it as GdNCT agent. Tumor growth suppression was obtained up to more than four times higher compared to the non-treated group for a single injection of Gd-DTPA/CaP nanoparticles, supported by the morphological and histopathological results after neutron irradiation. H&E staining results indicated that nucleus and cytoplasm of the tumor cells were destroyed after GdNCT treatment, which agrees with the results of TUNEL staining, where the number of cells undergoing stained by TUNEL that correlates to the number of apoptosis, was higher on GdNCT treated group compared to the non-irradiated ones.

It has also been shown that Gd-DTPA/CaP nanoparticles accumulate gadolinium in tumor site more effectively after comparing the results of our previous work on gadolinium-entrapping liposome. Gd-DTPA/CaP nanoparticles' smaller particle size is proven to be capable of accumulating gadolinium in higher percentage from initial injected dose. This smaller size has also been proven to be efficient in escaping the renal filtration demonstrated by the ratio of gadolinium concentration in tumor

to kidney, which is significantly lower in Gd-DTPA/CaP nanoparticles compared to those in gadolinium-entrapped liposome from our previous work.

Higher gadolinium accumulation in tumor site was also successfully achieved for multiple injections of Gd-DTPA/CaP nanoparticles as well as significant increase of gadolinium concentration in blood plasma at 30 hours after the first injection. This indicates prolonged blood circulation of Gd-DTPA/CaP nanoparticles, which is important in optimization of drug delivery. However, the multiple-injected mice group did not reveal better tumor growth suppression even though gadolinium concentration accumulated in tumor site is much higher compared to the single-injected mice group. There is a possibility that neutron depression occurred in this group where neutron were being absorbed and could not reach deeper site of the tumor, which might reduce the effectivity of cancer cells killing. Nevertheless, we could still observe tumor growth suppression after neutron irradiation, which suggests the possibility of cancer cells killing from secondary particles of GdNCR.

Low toxicity of Gd-DTPA/CaP nanoparticles has also been proven from the observation of no significant mice weight loss during 27 days after neutron irradiation, which is also supported by the results on multiple-injected group, where we observed mice dead on multiple injections of bare Gd-DTPA while all mice injected with Gd-DTPA/CaP nanoparticles survived until the end of observation. These results let us come into conclusion that Gd-DTPA/CaP nanoparticles could be a promising delivery device for GdNCT.

Preliminary investigation of dose deposition in Chapter 7 was intended to be an early stage of independent approach before going into real calculation of dose deposition from all possible contributing elements in BNCT and GdNCT dose deposition. The calculation was designed by referring to the experimental condition of neutron irradiation for gadolinium-based compounds-injected group. Dose calculation approach performed in this study was performed on a simple mouse phantom designed based on the tumor-bearing mice irradiated at KUR along with a simple cylindrical phantom with the materials of GI tract tissue to represent colon cancer cells. For the calculation results on simple mouse phantom, higher heat deposition in tumor site was observed for GdNCT compared to those in BNCT, which might come from the higher neutron cross section of gadolinium. Heat deposition on tumor site for both BNCT and GdNCT is also shown to be higher compared to other mice organs indicating the effect of neutron capture reaction by such neutron absorber compound considering that the percentage of boron or gadolinium in tumor is much lower compared to the other elements composing the other organs.

As for the cylindrical phantom dose calculation, the possibility of higher neutron depression was indeed observed for gadolinium compound compared to that introduced to boron, demonstrating the higher capability of gadolinium in capturing thermal neutron. And for the calculation for combined effect of boron and gadolinium, we can see that higher additional effect was achieved on the combination of 40 ppm boron with 1000 gadolinium, compared to the 40 ppm of gadolinium and 1000 boron. Nevertheless, since the result of dose calculation in current study is still a preliminary investigation, we can not come into conclusion yet before performing further advanced calculation especially the necessary to perform microdosimetry of dose deposition from very short range secondary particles such as Auger and Coster-Kronig electrons produced after GdNCR.

8.2 Limitations and Suggestions

Quite severe toxicity observed in irradiated mice injected with Gd-DTPA/DACHPt-loaded nanomicelles, even with various experimental setup performed in the abovementioned evaluation indeed indicated the difficulty of this nanoparticles application in GdNCT. However, there might still be a possibility to evaluate toxicity effect by performing irradiation with only gamma-rays beam on tumor-bearing mice injected with Gd-DTPA/DACHPt-loaded nanomicelles, which is not yet carried out in current work. Similar procedure with two separate groups of Gd-DTPA/DACHPt-loaded nanomicelles and DACHPt nanomicelles only to confirm whether the toxicity effect is caused by the reaction between gadolinium or platinum with neutron or gamma only. Since platinum-based chemotherapy agent itself (such as oxaliplatin used in this work) has been previously reported to be capable of enhancing the cytotoxic effect when combined with high LET radiation (as summarized previously in Chapter 3).

Considering that current investigation of Gd-DTPA/CaP nanoparticles were performed on tumor-bearing mice by injecting cancer cells line subcutaneously, it is demonstrated effective tumor growth suppression for surface-tumor after GdNCT treatment. Further investigation on GdNCT feasibility for deep-seated tumor and detail analysis on tumor-to-skin dose ratio could be few of the parameters that could optimize GdNCT treatment for better cancer cells-killing enhancement.

The assumption of neutron depression effect on the experiment with multiple injections of Gd-DTPA/CaP nanoparticles group cannot yet be concluded from current results because there is also the possibility of inhomogeneous distribution of Gd-DTPA/CaP nanoparticles in the tumor site that the cancer cells killing effect is not

uniform. It would be recommended to perform histological analysis on several slice of the tumor sample on different site covering the surface part which is the closest to the neutron beam, the middle and the deepest part of tumor which are the furthest from neutron incident. It is expected that evaluation on the cancer cells killing effect on different position of tumor slice would give a better understanding on the effectivity of GdNCT.

Dosimetry calculation performed in this work is still limited to the estimation of NCT heat deposition from the kerma conversion factor included in PHITS. It would be recommended to conduct an advanced dose calculation study to investigate detail dosimetry including macrodosimetry and microdosimetry calculation from all possible contributing elements of ionizing radiation for optimization of both BNCT and GdNCT, especially the microdosimetry for ionization effect from the very short range secondary particles of GdNCR to investigate the possibility of their additional cancer cells killing effect. The same case applies for the evaluation of combination effect between BNCT and GdNCT.

A well-developed hospital-based of accelerator-based neutron source in near future would be more practical and patient-friendly for NCT application, which will eventually bring the possibility of its clinical approval. Developing an established detection system, especially in intercellular level for a more precise estimation of dosimetry. Investigation on the possible combination between boron and gadolinium in NCT or combination of NCT with other types of radiation therapy (e.g. proton therapy, brachytherapy and synovectomy) would be more beneficial instead of exploiting each of them as a single treatment. Interdisciplinary exchange between scientific communities along with an easy to understand socialization also plays a great role in order to obtain public acceptance for the advancement of NCT in the future.

Bibliography

[1] Louis DN, Ohgaki H, Wiestler OD, Cavenee WK, Burger PC, Jouvet A, et al. (2007) The 2007 WHO classification of tumours of the central nervous system. *Acta Neuropathol*, **114**:97-109.

[2] Ostrom QT, Gittleman H, Farah P, Ondracek A, Chen Y, Wolinsky Y, et al. (2013) CBTRUS statistical report: primary brain and central nervous system tumors diagnosed in the United States in 2006-2010. *Neuro Oncol*, **15**Suppl 2:ii1-ii56.

[3] Thakkar JP, Dolecek TA, Horbinski C, Ostrom QT, Lightner DD, Barnholtz-Sloan JS, et al., (2014) Epidemiologic and molecular prognostic review of glioblastoma. *Cancer Epidemiol. Biomarkers Prev.*, **23**(10):1985-1996.

[4] De Stasio G, Rajesh D, Casalbore P, et al., (2005) Are gadolinium contrast agents suitable for gadolinium neutron capture therapy? *Neurological Research*, **27**: 387-398

[5] Locher GL (1936) Biological Effects and therapeutic possibilities of neutrons. *American Journal of Roentgenology Radium Ther*, **36**: 1-13.

[6] Salt C, Lennox AJ, Takagaki M, Maguire JA and Hosmane NS (2004) Boron and gadolinium neutron capture therapy. *Russ. Chem. Bull., Int.Ed.*, **53**(9): 1871-88.

[7] Mughabghab SF (1984) Neutron cross sections. Academic, Orlando.

[8] Mughabghab SF (2006) Atlas of Neutron Resonances, Fifth Edition: Resonance Parameters and Thermal Cross Sections. Z=1-100. Elsevier, Amsterdam.

[9] Sears VF (1992) Neutron scattering lengths and cross sections. *Neutron News*, **3**(3):22-37.

[10] Barth RF, Soloway AH, Fairchild RG (1990) Boron neutron capture therapy of cancer. *Cancer Res.*, **50**: 1061-70.

[11] Kruger PG (1940) Some biological effects of nuclear disintegration products on neoplastic tissue. *Proceedings of the National Academy of Sciences of the United States of America*, **26**:181-192.

[12] Zahl PA, Cooper FS, Dunning JR (1940) Some in vivo effects of localized nuclear disintegration products on transplantable mouse sarcoma. *Proceedings of the National Academy of Sciences of the United States of America*, **26**(10):589-598.

[13] Zahl PA, and Cooper FS (1941) Physical and biological considerations in the use of slow neutrons for cancer therapy. *Radiology*, **37**: 673-682.

[14] Farr LE, Sweet WH, Locksley HB, Robertson JS (1954) Neutron capture therapy of gliomas using boron-10. *Trans Am Neurol Assoc*, **79**:110-113.

[15] Farr LE, Sweet WH, Robertson JS, Foster CG, Locksley HB, Sutherland DL, Mendelsohn ML, Stickley EE (1954) Neutron capture therapy with boron in the treatment of glioblastoma multiforme. *Am J Roent Ther Nucl Med*, **71**:279-293.

[16] Farr LE, Robertson JS, Stickley EE (1954) Physics and physiology of neutron capture therapy. *Proceedings of the National Academy of Sciences of the United States of America*, **40**:1087-1093.

[17] Godwin JT, Farr LE, Sweet WH, Robertson JS (1955) Pathological study of eight patients with glioblastoma multiforme treated by neutron capture therapy using boron 10. *Cancer*, **8**:601-615.

[18] Asbury AK, Ojeman RG, Nielsen SL, Sweet WH (1972) Neuropathological study of fourteen cases of malignant brain tumor treated by boron-10 slow neutron capture radiation. *J Neuropathol Exp Neurol*, **31**(2):278-303.

[19] Farr LE, Calvo WG, Haymaker WE, Lippincott SW, Yamamoto YL, Stickley EE (1961) Effect of thermal neutrons on the central nervous system (apparent tolerance of central nervous system structures in man). *Arch Neurol*, **4**:246-257.

[20] Soloway AH, Hatanaka H, Davis MA (1967) Penetration of brain and brain tumor. VII.Tumor-binding sulfhydryl boron compounds. *J Med Chem*, **10**: 714.

[21] Hatanaka H (1990) Clinical results of boron neutron capture therapy. *Basic Life Sci 54*, **15**:15-21.

[22] Weinmann HJ, Brasch RC, Press WR, Wesbey GE (1984) Characteristics of gadolinium-DTPA complex: a potential NMR contrast agent. *Am. J. Roentgenol.*, **142**: 619-624.

[23] Cacheris WP, Quay SC, and Rocklage SM (1990) The relationship between thermodynamics and the toxicity of gadolinium complexes. *Magn. Res. Imaging*, **8**: 467-481.

[24] Luigi Panza and Davide Prosperi, (2012) Boron Chemistry, In: W.A.G. Sauerwein, A. Wittig, R. Moss, H. Nakagawa (Eds.), Neutron Capture Therapy: Principles and Applications, Springer-Verlag, Heidelberg.

[25] Taylor HJ and Goldhaber M, (1935) Detection of nuclear disintegration in a photographic emulsion. *Nature*, **135**:341-348.

[26] Shih JL and Brugger RM (1992) Gadolinium as a neutron capture therapy agent. *Med. Phys.*, **19**: 733-44.

[27] Hatanaka H, (1986) Boron-neutron capture therapy for tumors. Nishimura Co. Ltd, Niigata.

[28] Mishima Y, Ichihashi M, Hatta S, et al., (1989) First human clinical trial of melanoma neutron capture. Diagnosis and therapy. *Strahlenther.Onkol.*, **165**(2-3): 251-254.

[29] Wazer DE, Zamenhof RG, Harling OK and Madoc-Jones H (1994) Boron neutron capture therapy. In: Radiation Oncology Technology and Biology, (Eds.) P. M. March and J. S. Loeffler, W. B. Saunders, Philadelphia.

[30] Ono K, Kinashi Y, Suzuki M, Takagaki M and Masunaga S (2000) The Combined Effect of Electroporation and Borocaptate in Boron Neutron Capture Therapy for Murine Solid Tumors. *Jpn. J. Cancer Res.*, **91**: 853-858.

[31] Yang W, Barth RF, Rotaru JH, et al., (2000) Boron neutron capture therapy of brain tumors: functional and neuropathologic effects of blood-brain barrier disruption and intracarotid injection of sodium borocaptate and boronophenylalanine. *Journal of Neuro-Oncology*, **48**: 179-190.

[32] Sibrian VM, Vicente MGH (2011) Boron tumor-delivery for BNCT: Recent developments and perspectives. In: Boron Science: New Technologies & Applications. (Eds.) by Hosmane NS.: CRC Press, 203-232.

[33] Kabalka GW, Wu ZZ, Yao M-L, Natarajan N (2004) The synthesis and *in vivo* biodistribution of novel boronated unnatural amino acids. *App. Rad. Isotopes*, **61**:1111-5.

[34] Kabalka GW and Yao M-L (2006) The synthesis and use of boronated amino aicds for boron neutron capture therapy. *Curr. Med. Chem. Anti-Cancer Agents*, 111-126.

[35] Kabalka GW, Yao M-L, Marepally SR, Chandra S (2009) Biological evaluation of boronated unnatural amino acids as new boron carriers. *App. Rad. Isotopes*, **67**:S374-S379.

[36] Miyatake S, Kajimoto Y, Kawabata S et. al., (2005) Modified boron neutron capture therapy for malignant gliomas performed using epithermal neutron and two boron compounds with different accumulation mechanisms: an efficacy study based on findings on neuroimages. *J Neurosurg*, **103**:1000-9.

[37] Hiroyuki Nakamura and Mitsunori Kirihata, (2012) Boron Compounds: New Candidates for Boron Carriers, In: W.A.G. Sauerwein, A. Wittig, R. Moss, H. Nakagawa (Eds.), Neutron Capture Therapy: Principles and Applications, Springer-Verlag, Heidelberg. BNCT

[38] Yamamoto T, Matsumura A, Nakai K, Shibata Y, Endo K, Sakurai F, Kishi T, Kumada H, Yamamoto K, Torii Y (2004) Current clinical results of the Tsukuba BNCT trial. *Appl Radiat Isot*, **61**(5):1089-1093.

[39] Henriksson R, Capala J, Michanek A et al (2008) Boron neutron capture therapy (BNCT) for glioblastoma multiforme: a phase II study evaluating a prolonged high dose of boronophenylalanine (BPA). *Radiother Oncol*, **88**:183-191.

[40] Joensuu H, Kankaanranta L, Seppälä T, et al., (2003) Boron neutron capture therapy of brain tumors: clinical trials at the Finnish facility using boronophenylalanine. *J Neurooncol*, **62**:123-134.

[41] Chadha M, Capala J, Coderre JA, Elowitz EH, Iwai J, Joel DD, Liu HB, Wielopolski L, Chanana AD (1998) Boron neutron-capture therapy (BNCT)

for glioblastoma multiforme (GBM) using the epithermal neutron beam at the Brookhaven National Laboratory. *Int J Radiat Oncol Biol Phys*, **40**(4):829-834.

[42] Fuwa N, Suzuki M, Sakurai Y, et al. (2008) Treatment results of boron neutron capture therapy using intra-arterial administration of boron compounds for recurrent head and neck cancer. *British Journal of Radiology*, **81**:749-52.

[43] Aihara T, Hiratsuka J, Morita N, Uno M, Sakurai Y, Maruhashi A, Ono K, Harada T. (2006) First clinical case of boron neutron capture therapy for head and neck malignancies using 18 F-BPA PET. *Head Neck*, **28**: 850-855.

[44] Kankaanranta L, Seppälä T, Koivunoro H, Saarilahti K, Atula T, Collan J, Salli E, Kortesniemi M, Uusi-Simola J, Valimaki P, et al., (2012) Boron neutron capture therapy in the treatment of locally recurred head-and-neck cancer: final analysis of a phase I/II trial. *Int J Radiat Oncol Biol Phys*, **82**:67-75.

[45] Suzuki M, Masunaga SI, Kinashi Y, Takagaki M, Sakurai Y, Kobayashi T, Ono K. The effects of boron neutron capture therapy on liver tumors and normal hepatocytes in mice. *Jpn J Cancer Res.*, **91**(10):1058-64.

[46] Pinelli T, Zonta A, Altieri S et al., (2002) Taormina: from the first idea to the application to the human liver. Research and development in neutron capture therapy. W. Sauerwein (Ed.), et al., Proceedings of the 10th International Congress on Neutron Capture Therapy, Essen, Germany, Monduzzi, Bologna, 1065-1072.

[47] Coderre JA, Glass JD, Fairchild RG, Roy U, Cohen S, Fand I. (1987) Selective targeting of boronophenylalanine to melanoma in BALB/c mice for neutron capture therapy. *Cancer Res*, **47**(23): 6377-83.

[48] Fukuda H, Hiratsuka J, Kobayashi T, Sakurai Y, Yoshino K, Karashima H, Turu K, Araki K, Mishima Y, Ichihashi M. (2003) Boron neutron capture therapy (BNCT) for malignant melanoma with special reference to absorbed doses to the normal skin and tumor. *Australas Phys Eng Sci Med.*, **26**(3): 97-103.

[49] Palmer MR, Goorley JT, Kiger WS III, Busse PM, Riley KJ, Harling OK, Zamenhof RG (2002) Treatment planning and dosimetry for the Harvard-MIT Phase I clinical trial of cranial neutron capture therapy. *Int. J. Radiat. Oncol. Biol. Phys.*, **53**:1361-1379.

[50] Diaz AZ (2003) Assessment of the results from the phase I/II boron neutron capture therapy trials at the Brookhaven National Laboratory from a clinician's point of view. *J. Neurooncol.*, **62**:101-109.

[51] Busse PM, Harling OK, Palmer MR, Kiger WS III, Kaplan J, Kaplan I, Chuang CF, Goorley JT, Riley KJ, Newton TH, et al., (2003) A critical examination of the results from the Harvard-MIT NCT program phase I clinical trial of neutron capture therapy for intracranial disease. *J. Neurooncol.*, **62**:111-121.

[52] Hatanaka H: Boron neutron capture therapy for brain tumors. (1991) In: Glioma. (Eds.) Karim A, Laws E. Berlin: Springer-Verlag; 233-249.

[53] Nakagawa Y, Hatanaka H (1997) Boron neutron capture therapy. Clinical brain tumor studies. *J. Neurooncol.*, **33**(1-2):105-115.

[54] Yamamoto T, Nakai K, Kageji T, Kumada H, Endo K, Matsuda M, Shibata Y, Matsumura A., (2009) Boron neutron capture therapy for newly diagnosed glioblastoma. *Radiother. Oncol.*, **91**:80-84.

[55] Kageji T, Mizobuchi Y, Nagahiro S, Nakagawa Y, Kumada H., (2011) Clinical results of boron neutron capture therapy (BNCT) for glioblastoma. *Appl. Radiat. Isot.*, **69**:1823-1825.

[56] Miyatake S, Kawabata S, Yokoyama K, Kuroiwa T, Michiue H, Sakurai Y, Kumada H, Suzuki M, Maruhashi A, Kirihata M, Ono K., (2009) Survival benefit of boron neutron capture therapy for recurrent malignant gliomas. *J. Neurooncol.*, **91**:199-206.

[57] Kawabata S, Miyatake S, Hiramatsu R, et al., (2011) Phase II clinical study of boron neutron capture therapy combined with X-ray radiotherapy/temozolomide in patients with newly diagnosed glioblastoma multiforme-study design and current status report. *Appl. Radiat. Isot.*, **69**:1796-1799.

[58] Kato I, Ono K, Sakurai Y, Ohmae M, Maruhashi A, Imahori Y, Kirihata M, Nakazawa M, Yura Y. (2004) Effectiveness of BNCT for recurrent head and neck malignancies. *Appl Radiat Isot*, **61**:1069-1073.

[59] Suzuki M, Sakurai Y, Nagata K, Kinashi Y, Masunaga S, Ono K, Maruhashi A, Kato I, Fuwa N, Hiratsuka J, Imahori Y (2006) Impact of intra-arterial administration of boron compounds on dose-volume histograms in boron neutron

capture therapy for recurrent head-and-neck tumors. *Int J Radiat Oncol Biol Phys*, **66**:1523-1527.

[60] Kato I, Fujita Y, Maruhashi A, Kumada H, Ohmae M, Kirihata M, Imahori Y, Suzuki M, Sakrai Y, Sumi T, et al., (2009) Effectiveness of boron neutron capture therapy for recurrent head and neck malignancies. *Appl Radiat Isot*, **67**:S37-S42.

[61] Barth RF, Vicente MG, Harling OK, et al. (2012) Current status of boron neutron capture therapy of high grade gliomas and recurrent head and neck cancer. *Radiat Oncol*, **7**:146.

[62] Kouri M, Kankaanranta L, Seppälä T, Tervo L, Rasilainen M, Minn H, et al. (2004) Undifferentiated sinonasal carcinoma may respond to single-fraction boron neutron capture therapy. *Radiother Oncol*, **72**:83-5.

[63] Auterinen I, Hiismäki P, Kotiluoto P, Rosenberg RJ, Salmenhaara S, Seppälä T, et al. (2001) Metamorphosis of a 35 years old TRIGA reactor into a modern BNCT facility. In: Proceedings of frontiers in neutron capture therapy, La Jolla, United States. p. 267-75.

[64] Auterinen I, Kotiluoto P, Hippeläinen E et. al., (2004) Design and construction of shoulder recesses into the beam aperture shields for improved patient positioning at the FiR1 BNCT facility. *Appl. Radiat. Isot.*, **61**:799-803

[65] Savolainen S, Kortesniemi M, Timonen M et al., (2013) Boron neutron capture therapy (BNCT) in Finland: Technological and physical prospects after 20 years of experiences. *Physica Medica*, **29**:233-248.

[66] Wittig A, Hideghety K, Paquis P, Heimans J: Current Clinical Results of the EORTC-Study 11961. In Research and Development in Neutron Capture Therapy. Edited by Sauerwein W, Moss R, Wittig A. Bologna: Monduzzi Editore - International Proceedings Division; 2002:1117-1122.

[67] Vos MJ, Turowski B, Zanella FE, Paquis P, Siefert A, Hideghety K, Haselsberger K, Grochulla F, Postma TJ, Wittig A, et al., (2005) Radiologic findings in patients treated with boron neutron capture therapy for glioblastoma multiforme within EORTC trial 11961. *Int. J. Radiat. Oncol. Biol. Phys.*, **61**:392-399.

[68] Burian J, Marek M, Rataj J, Flibor S, Rejchrt J, Viererbl L, Sus F. (2004) Report on the first patient group of the phase I BNCT trial at the LVR-15 reactor. *Int Congress Series*, **1259**:27-32.

[69] Capala J, Stenstam BH, Sköld K, Munck af Rosenschold P, Giusti V, Persson C, Brun A, Franzen L, Carlsson J, et al., (2003) Boron neutron capture therapy for glioblastoma multiforme: clinical studies in Sweden. *J Neurooncol*, **62**:135-144.

[70] Sköld K, Stenstam BH, Diaz AZ, Giusti V, Pellettieri L, Hopewell JW. (2010) Boron neutron capture therapy for glioblastoma multiforme: advantage of prolonged infusion of BPA-f. *Acta Neurol Scand*, **122**:58-62.

[71] Wang LW, Wang SJ, Chu PY, Ho CY, Jiang SH, Liu YW, Liu YH, Liu HM, Peir JJ, Chou FI, et al., (2011) BNCT for locally recurrent head and neck cancer: preliminary clinical experience from a phase I/II trial at Tsing Hua open-pool reactor. *Appl Radiat Isot*, **69**:1803-6.

[72] Brugger, RM, Shih, JA (1989) Evaluation of gadolinium-157 as a neutron capture therapy agent. *Strahlenther Onkol*, **165**: 153-156.

[73] Martin, RF, D'Cunha G, Pardee M et al., (1989) Induction of DNA doublestrand breaks by 157Gd neutron capture. *Pigment Cell Res.*, **2**: 330-332.

[74] Masiakowski JT, Horton JL, Peters LJ (1992) Gadolinium neutron capture therapy for brain tumors: a computer study. *Med Phys.*, **19**: 1277-1284.

[75] Cerullo N, Bufalino D, Daquino G (2009) Progress in the use of gadolinium for NCT. *Applied Radiation and Isotopoes*, **67**. S157-S160.

[76] De Stasio G, Casalbore P, Pallini et al., (2001) Gadolinium in human glioblastoma cells for gadolinium neutron capture therapy. *Cancer Res.*, **61**: 4272-7.

[77] Goorley JT (2002) Comparison of Three Gadolinium Based Approaches to Cancer Therapy (Doctor's thesis). Retrieved from http://dspace.mit.edu

[78] Kaida S, Cabral H, Kumagai M et al. (2010) Visible Drug Delivery by Supramolecular Nanocarriers Directing to Single-Platformed Diagnosis and Therapy of Pancreatic Tumor Model. *Cancer Res.*, **70**: 7031-7041.

[79] Le UM and Cui Z (2006) Long-circulating gadolinium-encapsulated liposomes for potential application in tumor neutron capture therapy. *Int J of Pharm*, **312**: 105-112.

[80] Evens AM (2004) Motexafin gadolinium: a redox-active tumor selective agent for the treatment of cancer. *Curr Opin Oncol*, **16**(6):576-80

[81] De Stasio G, Rajesh D, Ford JM, et al., (2006) Metoxafin-Gadolinium Taken Up *In vitro* by at least 90% of Glioblastoma Cell Nuclei. *Clin Cancer Res*, **12**(1):206-13.

[82] Shikata F, Tokumitsu H, Ichikawa H, Fukumori Y (2001) In vitro cellular accumulation of gadolinium incorporated into chitosan nanoparticles designed for neutron-capture therapy of cancer. *European Journal of Pharmaceutics and Biopharmaceutics*, **53**: 57-63.

[83] De Stasio G, Perfetti L, Gilbert B et al., (1999) The MEPHISTO spectromicroscope reaches 20 nm lateral resolution. Rev Sci Instrum, 70: 1740-42.

[84] Dewi N, Yanagie H, Zhu H et al., (2013) Tumor growth suppression by gadolinium-neutron capture therapy using gadolinium-entrapped liposome as gadolinium delivery agent. *Biomedicine & Pharmacotherapy*, **67**:451-7.

[85] Hofmann B, Fischer C.-O, Lawaczeck R, Platzek J, Semmler W (1999) Gadolinium neutron capture therapy (GdNCT) of melanoma cells and solid tumors with the magnetic resonance imaging contrast agent Gadobutrol. *Invest. Radiol.*, **34**:126-133.

[86] Khokhlov V.F., Yashkin P.N., Silin D.I., Djorova E.S., Lawaczeck R. (1996) Neutron capture therapy with Gd-DTPA in tumor-bearing rats, in: Y. Mishima (Ed.), *Cancer Neutron Capture Therapy, Plenum Press, New York.* 865-869.

[87] Yasui L. S., Andorf C., Schneider L., Kroc T., Lennox A., Saroja K.R. (2008) Gadolinium neutron capture in glioblastoma multiforme cells. *International Journal of Radiation Biology*, **84**: 1130-9.

[88] Yasui, L.S. and Owens K. (2012) Necrosis is not induced by gadolinium neutron capture in glioblastoma multiforme cells. *International Journal of Radiation Biology*, **88**(12): 980-90.

[89] Current Status of Neutron Capture Therapy, IAEA Tecdoc 1223. IAEA, Vienna: 175-185.

[90] Barth RF, Coderre JA, M. Vicente Graça H and Blue TE (2005) Boron Neutron Capture Therapy of Cancer: Current Status and Future Prospects. *Clin Cancer Res.*, **11**: 3987-4002.

[91] Moss R.L. (2014) Critical review, with an optimistic outlook, on Boron Neutron Capture Therapy (BNCT). *Applied Radiation and Isotopes*, **88**:2-11.

[92] Rief, H., Van Heusden, R., Perlini, G., (1993) Generating epithermal neutron beams for neutron capture therapy in TRIGA reactors. In: Advances in Neutron Capture Therapy (Eds.) Soloway, A.H., Barth, R.F., Carpenter, D.E.,

[93] Culbertson CN, Green S, Mason AJ, Picton D, Baugh G, Hugtenburg RP, et al. (2004) In-phantom characterisation studies at the Birmingham accelerator-generated epithermal neutron source (BAGINS) BNCT facility. *Appl. Radiat. Isot.*, **61**: 733-8.

[94] Yanch JC, Zhou XL, Shefer RE, Klinkowstein RE. (1992) Accelerator-based epithermal neutron beam design for neutron capture therapy. *Med Phys*, **19**:709-21.

[95] Kreiner AJ, Thatar Vento V, Levinas P, Bergueiro J, Di Paolo H, Burlon AA, et al. Development of a tandemelectrostatic-quadrupole accelerator facility for BNCT. *Appl. Radiat. Isot.*, **67**:S266-9.

[96] Kim J.K. and Kim K.O. (2009) Current research on accelerator-based boron neutron capture therapy in Korea. *Nucl. Eng. Technol.*, **41**(4):531-43.

[97] Kim K.O., Kim J.K., Kim S.Y. (2009) Optimized Therapeutic Neutron Beam for Accelerator-based BNCT by Analyzing the Neutron Angular Distribution from ^{7}Li(p,n)^{7}Be Reaction. *Applied Radiation and Isotopes*, **67**(7-8):1173-9.

[98] Lee D.J, Han C.Y., Park S.H., Kim J.K. (2004) An Accelerator-based epithermal neutron beam design for BNCT and dosimetric evaluation using a voxel head phantom. *Radiation Protection Dosimetry*, **110**(1-4):655-60.

[99] Barth RF. (2009) Boron neutron capture therapy at the crossroads: challenges and opportunities. *Appl. Radiat. Isot.*, **67**:S3-6.

[100] Wang C.K., Blue T.E., Blue J.W.. (1990) An experimental study of the moderator assembly for a low-energy proton accelerator neutron irradiation facility for BNCT. *Basic Life Sci.*, **54**: 271-80.

[101] Blue TE, Yanch JC. (2003) Accelerator-based epithermal neutron sources for boron neutron capture therapy of brain tumors. *J. Neurooncol.*, **62**:19-31.

[102] Tanaka H, Sakurai Y, Suzuki M, Masunaga S, Mitsumoto T, Fujita K, Kashino G, Kinashi Y, Liu Y, Takada M, et al., (2011) Experimental verification of beam characteristics for cyclotron-based epithermal neutron source (C-BENS). *Appl. Radiat. Isot.*, **69**:1642-1645.

[103] Kumada H., Matsumura A., Sakurai H., et al., (2014) Project for the development of the linac based NCT facility in University of Tsukuba. *Applied Radiation and Isotopes*, **88**:211-5.

[104] Kreiner, A.J., (2012). Accelerator-based BNCT. In: W.A.G. Sauerwein, A. Wittig, R. Moss, H. Nakagawa (Eds.), Neutron Capture Therapy: Principles and Applications, Springer-Verlag, Heidelberg.

[105] Nigg, D.W., (2006) Neutron sources and applications in radiotherapy - a brief history and current trends. In: Nakagawa Y., Kobayashi T., Takamatsu , Fukuda H. (Eds.), Advances in Neutron Capture Therapy Proceedings of the 12th International Congresson Neutron Capture Therapy, Japan.

[106] Kobayashi T, Kanda K. (1983) Microanalysis system of ppm order B-10 concentrations in tissue for neutron capture therapy by prompt gamma-ray spectrometry. *Nucl Instrum Methods Phys Res*, **204**: 525-31.

[107] Raaijmakers CPJ, Konijnenberg MW, Dewit L, et al., (1995) Monitoring of blood-10B concentration for boron neutron capture therapy using prompt gamma-ray analysis. *Acta Oncol*, **34**:517-23.

[108] Mukai K, NakagawaY, Matsumoto K. (1995) Prompt gamma ray spectrometry for in vivo measurement of boron-10 concentration in rabbit brain tissue. *Neurol Med Chir (Tokyo)*, **35**: 855-60.

[109] Verbakel WF, Sauerwein W, Hideghety K, Stecher-Rasmussen F. (2003) Boron concentrations in brain during boron neutron capture therapy: in vivo measurements from the phase I trial EORTC 11961 using a gamma-ray telescope. *Int J Radiat Oncol Biol Phys*, **55**:743-56.

[110] Khokhlov V.F., Zaitsev K.N., Beliayev V.N., Kulakov V.N., Lipengolts A.A., Portnov A.A. (2009) Prompt gamma neutron activation analysis of ^{10}B and Gd in biological samples at the MEPhI reactor. *Applied Radiation and Isotopes*, **67**:S251-S253.

[111] M. Ishikawa, T. Kobayashi, Y. Sakurai, K. Kanda (2001) Optimization technique for a prompt gamma-ray spect collimator system. *J Radiat Res*, **42**:387-400.

[112] IMurata I., Mukai T., Nakamura S., Miyamaru H., Kato I. (2011) Development of a thick CdTe detector for BNCT-SPECT. *Applied Radiation and Isotopes*, **69**:1706-9.

[113] Kobayashi T., Sakurai Y., Ishikawa M., (2000) A noninvasive dose estimation system for clinical BNCT based on PG-SPECT-Conceptual study and fundamental experiments using HPGe and CdTe semiconductor detectors. *Med. Phys.*, **27**:2124-32.

[114] Sakurai Y., Tanaka H., Suzuki M., Kinashi Y., Masunaga S., Maruhashi A., Ono K. (2009) A feasibility study of the post-irradiation dose estimation with SPECT technique for BNCT. *Applied Radiation and Isotopes*, **67**:S218-S221.

[115] Minsky D.M., Valda A.A., Kreiner A.J., Green S., Wojnecki C., Ghani Z., (2009) Experimental feasibility studies on a SPECT tomograph for BNCT dosimetry. *Applied Radiation and Isotopes*, **67**:S179-S182.

[116] Minsky D.M., Valda A.A., Kreiner A.J., Green S., Wojnecki C., Ghani Z. (2011) First tomographic image of neutron capture rate in a BNCT facility. *Applied Radiation and Isotopes*, **69**:1858-61.

[117] Endo K., Yamamoto T., Shibata Y. (2006) Demonstration of Inter- and Intracellular Distribution of Boron and Gadolinium Using Micro-Proton-Induced X-Ray Emission (Micro-PIXE). *Oncology Research*, **16**: 57-65.

[118] Yamamoto Y., Yamamoto T., Horiguchi Y. et al., (2014) Intra-tumor distribution of metallofullerene using micro-particle induced X-ray emission (PIXE). *Appl. Radiat. Isot.*, **88**: 114-117.

[119] Gräfe J.L., McNeill F.E., Byun S.H., Chettle D.R., Noseworthy M.D. (2010) A benchmarked MCNP model of the *in vivo* detection of gadolinium by prompt gamma neutron activation analysis. *Nuclear Instruments and Methods in Physics Research*, **B268**: 2451-2457.

[120] Gräfe J.L., McNeill F.E., Byun S.H., Chettle D.R., Noseworthy M.D. (2011) The feasibility of *in vivo* detection of gadolinium by prompt gamma neutron activation analysis following gadolinium-based contrast-enhanced MRI. *Applied Radiation and Isotopes*, **69**: 105-111.

[121] Gräfe J.L., McNeill F.E., Chettle D.R., Byun S.H. Characteristic X ray emission in gadolinium following neutron capture as an improved method of *in vivo* measurement: A comparison between feasibility experiment and Monte-Carlo simulation. *Nuclear Instruments and Methods in Physics Research*, **B281**: 21-25.

[122] Schultz D et al., (2010) The K-shell auger electron spectrum of gadolinium obtained using neutron capture in a solid state device. *J. Phys. D: Appl. Phys.*, **43**:75502-8.

[123] Evans S, Krahenbuhl U. Boron analysis in biological material: microwave digestion procedure and determination by different methods. *Fresenius Z Anal Chem*, **349**:454-9.

[124] Wittig A., Michel J., Moss R.L. (2008) Boron analysis and boron imaging in biological materials for Boron Neutron Capture Therapy (BNCT). *Critical Reviews in Oncology/Hematology*, **68**:66-90.

[125] Nigg DW (2003) Computational dosimetry and treatment planning considerations for neutron capture therapy. *J Neurooncol*, **62**:75-86.

[126] Kiger WS and Kumada H (2012).Treatment planning. W.A.G. Sauerwein, A. Wittig, R. Moss, H. Nakagawa (Eds.), Neutron Capture Therapy: Principles and Applications, Springer-Verlag, Heidelberg. BNCT.

[127] Binns PJ, Riley KJ, Harling OK, Kiger WS III, Munck af Rosenschold PM, Giusti V, Capala J, Skold K, Auterinen I, Seren T, Kotiluoto P, Uusi-Simola J, Marek M, Viererbl L, Spurny F (2005) An international dosimetry exchange for boron neutron capture therapy. Part I: Absorbed dose measurements. *Med Phys*, **32**:3729-3736.

[128] Riley KJ, Binns PJ, Harling OK, Albritton JR, Kiger WS III, Rezaei A, Skold K, Seppälä T, Savolainen S, Auterinen I, Marek M, Viererbl L, Nievaart VA, Moss RL (2008) An international dosimetry exchange for BNCT part II: computational dosimetry normalizations. *Med Phys*, **35**:5419-5425.

[129] Zamenhof RG (1997) Microdosimetry for boron neutron capture therapy: a review. *J. Neuro-Oncol.*, **33**:81-92.

[130] Gustavo A. Santa Cruz and Robert G. Zamenhof. (2009) The Microdosimetry of the 10B Reaction in Boron Neutron Capture Therapy: A New Generalized Theory. *Radiation Research*, **162**:6, 702-710.

[131] Hsu FY et al., (2009) Microdosimetry study of THOR BNCT beam using tissue equivalent proportionalc ounter. *Applied Radiation and Isotopes*, **67**:S175-S178.

[132] Mukawa T, Matsumoto T, Niita K (2011) Study on Microdosimetry for Boron Neutron Capture Therapy. *Progress in Nuclear Science and Technology* **2**:242-246.

[133] Sheino I, Khokhlov V, Kulakov V, Zaitsev K (2004) Estimation of neutron kerma in biological tissue containing boron and gadolinium compounds for neutron capture therapy. *Proccedings of the International Symposium on Boron Neutron Capture Therapy*, July 7-9, Novosibirsk, Russia: 99-110.

[134] Tim Goorley and Hooshan Nikjoo (2000) Electron and Photon Spectra for Three Gadolinium-based Cancer Therapy Approaches. *Radiation Research*, **154**:556-63.

[135] Stepanek J. (2003) Emission Spectra of Gadolinium-158. *Med. Phys.*, **30**: 41-43.

[136] Y.Sakurai, T.Kobayashi. (2002) Experimental Verification of the Nuclear Data of Gadolinium for Neutron Capture Therapy. *Journal of Nuclear Science and Technology*, **S2**:1294-1297.

[137] Enger SA et al., (2013) Dosimetry for gadolinium neutron capture therapy (GdNCT). *Radiation Measurements*, **59**:233-240.
Groshev LV, A.M.Demidov, V.N.Lutsenko, V.I.Pelekhov, Atlas of gamma spectra of the thermal neutron capture. - M: Atomizdat,1958. - 111 p.

[138] Hale G and Young P 1989 pjef22/B-10:1 5-B-10 LANL EVAL-MAR89

[139] Menapace E et al 1982 pjef-22/Gd-157:1 64-GD-157 NEA RCOM-JUN82

[140] Kadhim MA (2003) Role of genetic background in induced instability. *Oncogene*, **22**:6994-6999.

[141] Briesmeister J (1997) MCNP-a general Monte Carlo N-particle transport code, version 4B LA-12625-M Los Alamos National Laboratory

[142] Johns H and Cunningham J (1983) The Physics of Radiology (Charles C Thomas Publishing).

[143] Miller G, Hertel N, Wehring B and Horton J (1993). Gadolinium neutron capture therapy. *Nucl. Technol.*, **103**:320-330.

[144] Goodhead D. (1988). Spatial and Temporal Distribution of Energy. *Health Phys.*, **55**:231-240.

[145] Thisgaard H (2008) Accelerator based production of Auger-electron-emitting isotopes for radionuclide therapy. PhD Thesis, Faculty of the Life Sciences University of Copenhagen Denmark, RisÃž-PhD-42(EN)

[146] Matsumura, A.; Zhang, T.; Nakai, K.; Endo, K.; Kumada, H.; Yamamoto, T.; Yoshida, F.; Sakurai, Y.; Tamamoto, K.; Nose, T. (2005) Combination of Boron and Gadolinium Compounds for Neutron Capture Therapy. An *in Vitro* Study. *J. Exp. Clin. Cancer Res.*, **24**:93-98.

[147] Tokuuye K et al., (2000) Comparison of Radiation Effects of Gadolinium and Boron Neutron Capture Reactions. *Strahlenther. Onkol.*, **176**:81-83.

[148] Culbertson CN and Jevremovic T (2003) Computational assessment of improved cell-kill by gadolinium-supplemented boron neutron capture therapy. *Phys. Med. Biol.*, **48**:3943-3959.

[149] Tokumitsu H, Ichikawa H, Fukumori Y (1999) Chitosan-Gadopentetic Acid Complex Nanoparticles for Gadolinium Neutron-Capture Therapy of Cancer: Preparation by Novel Emulsion-Droplet Coalescence Technique and Characterization. *Pharmaceutical Research*, **16**(12): 1830-35.

[150] Miyamoto M, Hirano K, Ichikawa H, Fukumori Y, Akine Y, Tokuuye K (1999) Biodistribution of gadolinium incorporated in lipid-emulsions intraperitoneally administered for neutron-capture therapy with tumor-bearing hamsters. *Biol Pharm Bull*, **22**: 1331-1340.

[151] Watanabe T, Ichikawa H, Fukumori Y (2002) Tumor accumulation of gadolinium in lipid-nanoparticles intravenously injected for neutron-capture therapy of cancer. *European Journal of Pharmaceutics and Biopharmaceutics*, **54**: 119-24.

[152] Beduneau A., Saulnier P. , Hindre F. , Clavreul A. , Leroux J.C., Benoit J.P., (2007) Design of targeted lipid nanocapsules by conjugation of whole antibodies and antibody Fab' fragments. *Biomaterials*, **28**:4978-90.

[153] Deckert P.M. (2009) Current constructs and targets in clinical development for antibody-based cancer therapy. *Current Drug Targets*, **10**:158-75.

[154] Zensi A., Begley D., Pontikis C., Legros C., Mihoreanu L., Wagner S., B$^{\breve{}}$chel C., Briesen H.v., Kreuter J., (2009) Albumin nanoparticles targeted with ApoE enter the CNS by transcytosis and are delivered to neurons, *J. Control. Release*, **137**:78-86.

[155] Park K. (2012) Polysaccharide-based near-infrared fluorescence nanoprobes for cancer diagnosis. *Quant Imaging Med Surg*, **2**(2):106-113.

[156] Lammers T, Kiessling F, Hennink WE and Storm G (2012) Drug targeting to tumors: Principles, pitfalls and (pre-) clinical progress. *Journal of Controlled Release*, **161**:175-187.

[157] Kobayashi H., Watanabe R., Choyke P.L., (2014) Improving Conventional Enhanced Permeability and Retention (EPR) Effects; What Is the Appropriate Target? *Theranostics*, **4**(1):81-89.

[158] Longmire, M.R., Ogawa M, Choyke PL, Kobayashi H. (2011) Biologically optimized nanosized molecules and particles: more than just size. *Bioconjug Chem.*, **22**: 993-1000.

[159] Matsumura Y, Maeda H (1986) A new concept for macromolecular therapeutics in cancer chemotherapy: mechanism of tumoritropic accumulation of proteins and the antitumor agent SMANCS. *Cancer Res.*, **46**: 6387-6392.

[160] Van Nostrum C (2004) Polymeric micelles to deliver photosensitizers for photodynamic therapy. *Advanced Drug Delivery Reviews*, **56**:9-16.

[161] Kedar U et al., (2010) Advances in polymeric micelles for drug delivery and tumor targeting. *Nanomedicine: Nanotechnology, Biology and Medicine*, **6**(6):714-729.

[162] Gong J et al., (2012) Polymeric micelles drug delivery system in oncology. *Journal of Controlled Release*, **159**(3):312-323.

[163] Desai, M.P., Labhasetwar, V., Walter, E., Levy, R.J., Amidon, G.L., (1997) The mechanism of uptake of biodegradable microparticles in Caco-2 cells is size dependent.*Pharm. Res.*, **14**: 1568-73.

[164] Hobbs, S.K., et al., (1998) Regulation of transport pathways in tumor vessels: role of tumor type and microenvironment. *Proc. Natl. Acad. Sci. U.S.A.*, **95**: 4607-12.

[165] Harashima, H., Hiraiwa, T., Ochi, Y., Kiwada, H., (1995) Size dependent liposome degradation in blood: in vivo/in vitro correlation by kinetic modeling. *J. Drug Target*, **3**: 253-61.

[166] Litzinger, D.C., Buiting, A.M., van Rooijen, N., Huang, L., (1994) Effect of liposome size on the circulation time and intraorgan distribution of amphipathic poly(ethylene glycol)-containing liposomes*Biochim. Biophys. Acta*, **1190**: 99-107.

[167] Kreuter, J., 1995. Nanoparticles as adjuvants for vaccines. *Pharm. Biotechnol.*, **6**: 463-472.

[168] Gabizon, A., Papahadjopoulos, D., (1988). Liposome formulations with prolonged circulation time in blood and enhanced uptake by tumors. *Proc. Natl. Acad. Sci. U.S.A.*, **185**: 6949-6953.

[169] J.M. Harris, N.E. Martin, M. Modi, (2001) Pegylation - a novel process for modifying pharmacokinetics. *Clin. Pharmacokinet.*, **40**:539-51.

[170] Yamaoka T, Tabata Y, Ikada Y (1994) Distribution and tissue uptake of poly(ethylene glycol) with different molecular-weights after intravenous administration to mice. *J. Pharm. Sci.*, **83**:601-6.

[171] Yamaoka T, Tabata Y, Ikada Y (1995) Comparison of body distribution of poly(vinyl alcohol) with other water-soluble polymers after intravenous administration. *J. Pharm. Pharmacol.*, **47**:479-86.

[172] Bae YH, Park K (2011) Targeted drug delivery to tumors: Myths, reality and possibility. *J. Control. Release*, **153**: 198-205.

[173] Yanagie H, Tomita T, Kobayashi H, Fujii Y, Takahashi T, Hasumi K, Nariuchi H, Sekiguchi M (1991) Application of boronated anti-CEA immunoliposome to tumour cell growth inhibition in in vitro boron neutron capture therapy model. *Br J Cancer*. **63**(4): 522-526.

[174] Yanagie H, Tomita T, Kobayashi H, Fujii Y, Yonaka Y, Saegusa Y, Hasumi K, Eriguchi M, Kobayashi T, Ono K (1997) Inhibition of human pancreatic cancer growth in nude mice by boron neutron capture therapy.*Br J Cancer*, **75**: 660-665.

[175] Yanagie H, Kobayashi H, Takeda Y, Yoshizaki I, Nonaka Y, Naka S, Nojiri A, Shinnkawa H, Furuya Y, Niwa H, Ariki K, Yasuhara H, Eriguchi M (2002). Inhibition of growth of human breast cancer cells in culture by neutron capture using liposomes containing ^{10}B. *Biomed Pharmacother.*, **56**(2):93-9.

[176] Yanagie H, Ogata A, Sugiyama H, Eriguchi M, Takamoto S, and Takahashi H (2008) Application of drug delivery system to boron neutron capture therapy for cancer. *Expert Opin Drug Deliv*, **5**(4):427-443.

[177] Sumitani S. and Nagasaki Y (2012) Boron neutron capture therapy assisted by boron-conjugated nanoparticles. *Polymer Journal*, **44**: 522-530.

[178] Shukla S, Wu G, Chatterjee M, et al., (2003) Synthesis and Biological Evaluation of Folate Receptor-Targeted Boronated PAMAM Dendrimers as Potential Agents for Neutron Capture Therapy. *Bioconjugate Chem.*, **14**:158-167.

[179] Tachikawa S, Miyoshi T, Koganei H et al., (2014) Spermidiniumcloso-dodecaborate-encapsulating liposomes as efficient boron delivery vehicles for neutron capture therapy. *Chem.Commun.*, **50**: 12325-12328.

[180] Koganei H, Ueno M, Tachikawa S et al.,(2013) Development of High Boron Content Liposomes and Their Promising Antitumor Effect for Neutron Capture Therapy of Cancers. *Bioconjugate Chem.*, **24**:124-132.

[181] Yang W, Wu G, Barth RF, Swindall MR, Bandyopadhyaya AK, Tjarks W, Tordoff K, Moeschberger M, Sferra TJ, Binns PJ, et al., (2008) Molecular targeting and treatment of composite EGFR and EGFRvIII-positive gliomas using boronated monoclonal antibodies. *Clin Cancer Res*, **14**:883-891.

[182] Wu G, Yang W, Barth RF, Kawabata S, Swindall M, Bandyopadhyaya AK, Tjarks W, Khorsandi B, Blue TE, Ferketich AK, et al., (2007) Molecular targeting and treatment of an epidermal growth factor receptor positive glioma using boronated cetuximab. *Clin Cancer Res*, **13**:1260-1268.

[183] Yinghuai Z, Cheng Yan K, Maguire JA (2007) Recent developments in boron neutron capture therapy driven by nanotechnology. In Boron Science: New Technologies and Applications. Volume 1. Edited by Hosmane NS. CRC Press :147-163.

[184] Le UM (2008) Improving the Uptake and Retention of Gadolinium in Tumors for Potential Gadolinium-Neutron Capture Therapy (Doctor's thesis).

[185] Shikata F, Tokumitsu H, Ichikawa H, Fukumori Y. (2002) In vitro cellular accumulation of gadolinium incorporated into chitosan nanoparticles designed for neutron-capture therapy of cancer. *Eur J Pharm Biopharm*, **53**: 57-63.

[186] Tokumitsu H, Hiratsuka J, Sakurai Y, Kobayashi T, Ichikawa H, Fukumori Y (2000) Gadolinium neutron-capture therapy using novel gadopentetic acid-chitosan complex nanoparticles: in vivo growth suppression of experimental melanoma solid tumor. *Cancer Letters*, **150**: 177-182.

[187] Ichikawa H, Uneme T, Andoh T, Arita Y, Fujimoto T, Suzuki M et al., (2014). Gadolinium-loaded chitosan nanoparticles for neutron-capture therapy: Influence of micrometric properties of the nanoparticles on tumor-killing effect. *Appl Radiat Isot*: **88**: 109-13.

[188] Sakurai Y and Kobayashi T. Characteristics of the KUR Heavy Water Neutron Irradiation Facility as a neutron irradiation field with variable energy spectra. *Nuclear Instruments and Methods in Physics Research A*, **453**:569-596.

[189] Sakurai Y., Kobayashi T. (2004) Spectrum evaluation at the filter-modified neutron irradiation field for neutron capture therapy in Kyoto University Research Reactor. *Nuclear Instruments and Methods in Physics Research*, **A 531**: 585-595.

[190] Kobayashi T, Sakurai Y, Kanda K, Fujita Y, Ono K (2000) The remodeling and basic characteristics of the Heavy Water Neutron Irradiation Facility of the Kyoto University Research Reactor, mainly for neutron capture therapy. *Nuclear Technology*, **131**:354-78.

[191] Ohe Y. (2005) Chemoradiotherapy for lung cancer. *Expert Opin Pharmacother*, **6**: 2793-804.

[192] Squire LF, Novelline RA (1997). Squire's fundamentals of radiology (5th ed.). Harvard University Press. ISBN 0-674-83339-2.

[193] Hendee, William R; Morgan, Christopher J (1984). "Magnetic Resonance Imaging Part I - Physical Principles". *West J Med.*, **141** (4): 491-500. PMC 1021860. PMID 6506686

[194] Hermann R.M, Rave-Fránk M, Pradier O (2008). Combining radiation with oxaliplatin: A review of experimental results. *Cancer/Radiothěrapie*, **12**: 61-67.

[195] Koivusalo R, Krausz E, Ruotsalainen P, Helenius H, Hietanen S. (2002) Chemoradiation of cervical cancer cells: targeting human papillomavirus E6 and p53 leads to either augmented or attenuated apoptosis depending on the platinum carrier ligand. *Cancer Res.* **62**:7364-71.

[196] Magne N, Fischel JL, Formento P, Etienne MC, Dubreuil A, Marcie S, et al. (2003) Oxaliplatin-5-fluorouracil and ionizing radiation. Importance of the sequence and influence of p53 status. *Oncology*, **64**:280-7.

[197] Kjellstrom J, Kjellen E, Johnsson A. (2005) In vitro radiosensitization by oxaliplatin and 5-fluorouracil in a human colon cancer cell line. *Acta Oncologica*, **44**:687-93.

[198] Espinosa M, Martinez M, Aguilar JL, Mota A, De la Garza JG, Maldonado V, et al. (2005) Oxaliplatin activity in head and neck cancer cell lines. *Cancer Chemother Pharmacol*, **55**:301-5.

[199] Rave-Frank M, Schmidberger H, Christiansen H, Boll C, Lehmann J,Weiss E. (2007) Comparison of the combined action of oxaliplatin or cisplatin and radiation in cervical and lung cancer cells. *Int J Radiat Biol.*, **83**:41-7.

[200] Benzina S, Debomy F, Bergerat JP, Denis JM, Gueulette J, Dufour P, et al. (2007) The cytotoxicity of high-linear energy transfer radiation is reinforced by oxaliplatin in human glioblastoma. *Cancer Lett.*, **254**:54-62.

[201] Cividalli A, Ceciarelli F, Livdi E, Altavista P, Cruciani G, Marchetti P, et al. (2002) Radiosensitization by oxaliplatin in a mouse adenocarcinoma: influence of treatment schedule. *Int J Radiat Oncol Biol Phys.*, **52**:1092-8.

[202] Folkvord S, Flatmark K, Seierstad T, Hansen Ree A. (2007) In vitro and in vivo radiosensitization of colorectal carcinoma cells by oxaliplatin in combination with 5-fluoruracil. *Proceedings of the 10th international Wolfsberg Meeting on Molecular Radiation Biology/Oncology.*, **Vol 7**, Editors: Baumann M, Bodis S, Dikomey E, van der Kogel A, Overgaard J, Rodemann HP. ISBN 3-9808819-4-6.

[203] Schmidt W, Chaney SG. (1993) Role of carrier ligand in platinum resistance of human carcinoma cell lines. *Cancer Res.*, **53**:799-805.

[204] Dorozhkin SV, Epple M (2002) Biological and medical significance of calcium phosphate. *Angew Chem Int Ed Engl.*, **41**(17): 3130-46.

[205] Rey C., Combes C., Drouet C., Sfihi H., Barroug A., (2007) Physico-chmeical properties of nanocrystalline apatites: implications for biominerals and biomaterials. *Mater. Sci. Eng.*, **27**: 198-205.

[206] Epple, M. et al., (2010) Application of calcium phosphate nanoparticles in biomedicine. *J. Mater. Chem.*, **20**:18-23.

[207] Tung M.S. (1998) Calcium phosphates: structure, composition, solubility, and stability. In: Amjad Z, ed. Calcium Phosphates in Biological and Industrial Systems. Boston: Kluwer Academic Publishers: 1-19.

[208] Gerweck L.E., Seetharaman K. (1996) Cellular pH gradient in tumor versus normal tissue. *Cancer Res*, **56**:1194-8.

[209] Faraji AH and Wipf P (2009) Nanoparticles in cellular drug delivery. *Bioorg Med Chem*, **17**(8):2950-2962.

[210] Mi P. et al., (2014) Hydrothermally synthesized PEGylated calcium phosphate nanoparticles incorporating Gd-DTPA for contrast enhanced MRI diagnosis of solid tumors. *Journal of Controlled Release*, **174**: 63-71.

[211] Fujimoto T et al., (2013) Boron neutron capture therapy (BNCT) selectively destroys 1 human clear cell sarcoma in mouse model. *Appl. Radiat. Isot*, **73**:96-100.

[212] Fang Y. (1998) Transvascular Drug Delivery in Solid Tumors. Semin. *Radiat. Oncol.*, **8**: 164-75.

[213]] Ruoslahti E, Sangeeta NB, Michael JS. (2010) Targeting of drugs and nanoparticles to tumor. *The Journal of Cell Biology.*, **188**(6): 759-68.

[214] Harms A. A. and G. R. Norman (1972) The Role of Internal Conversion Electrons in Gadolinium-Exposure Neutron Imaging. J. Appl. Phys. 43(7): 3209-3212.

[215] Kassis A. I. et al., (1982) Lethality of Auger electrons from the decay of bromine-77 in the DNA of mammalian cells. *Radiat. Res.*, **90**: 362-73.

[216] Andreo P. (1991) Monte Carlo Technique in Medical Radiation Physics. *Phys. Med. Biol.*, **36**: 861-920.

[217] Sato T, Niita K, Matsuda N, Hashimoto S, Iwamoto Y, Noda S, Ogawa T, Iwase H, Nakashima H, Fukahori T, Okumura K, Kai T, Chiba S, Furuta T and Sihver L (2013) Particle and Heavy Ion Transport Code System PHITS, Version 2.52. *J. Nucl. Sci. Technol.*, **50**(9):913-923.

[218] Niita K., Iwase H., Sato T., Iwamoto Y., Matsuda N., Sakamoto Y., Nakashima H., Mancusi D., Sihver L., (2011) Recent Developments of the PHITS code. *Progress in Nuclear Science and Technology*, **1**: 1-6.

[219] Kumada H., Nakamura T., Komeda M., Matsumura A., (2009) Development of a new multi-modal Monte-Carlo radiotherapy planning system. *Applied Radiation and Isotopes*, **67**: S118-S121.

[220] Goorley JT, Kiger WS, Zamenhof RG. (2002) Reference dosimetry calculations for neutron capture therapy with comparison of analytical and voxel models. *Med. Phys.*, **29**(2):145-156.